Amine Functionalization by Initiated Chemical Vapor Deposition (iCVD) for Interfacial Adhesion and Film Cohesion

by

Jingjing Xu

Master of Philosophy, Materials Science
University of Cambridge, Cambridge, United Kingdom, 2006

Bachelor of Engineering, Polymer Science and Engineering
Beijing University of Chemical Technology, Beijing, China, 2005

Submitted to the Department of Chemical Engineering
in Partial Fulfillment of the Requirements for the Degree of

DOCTOR OF PHILOSOPHY IN CHEMICAL ENGINEERING
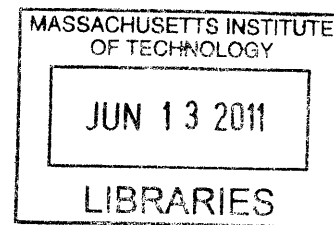
AT THE

MASSACHUSETTS INSTITUTE OF TECHNOLOGY

June 2011

Signature of Author_____
Department of Chemical Engineering
May 23, 2011

Certified by _____
Karen K. Gleason
Professor of Chemical Engineering
Thesis Supervisor

Accepted by _____
William M. Deen
Professor of Chemical Engineering
Chairman, Committee for Graduate Students

Amine Functionalization by Initiated Chemical Vapor Deposition (iCVD) for Interfacial Adhesion and Film Cohesion

by

Jingjing Xu
Submitted to the Department of Chemical Engineering
on May 23, 2011 in Partial Fulfillment of the
Requirements for the Degree of
Doctor of Philosophy in Chemical Engineering

Abstract

Amine functional polymer thin films provide a versatile platform for subsequent functionalization because of their diverse reactivity. Initiated chemical vapor deposition (iCVD) is a polymer chemical vapor deposition technique that utilizes the delivery of vapor-phase monomers to form chemically well-defined polymer films with tunable conformality and property. In this thesis work, amine functional iCVD poly(4-aminostyrene) (PAS) thin films were synthesized for the first time. The pendant amine groups enable the formation of a robust nanoadhesive with complementary epoxy functional groups. Bonded devices able to withstand >150 psi were achieved by combining polydimethylsiloxane (PDMS) and a wide variety of polymeric materials. Additionally, the all-iCVD nanoadhesive bonding process displays high resistance against hydrolytic degradation (>2 weeks). In addition to bonding, the iCVD layers remaining in the microfluidic channels provide functional groups for subsequent reaction and also act as diffusion barriers against oxygen permeation into the devices. Two applications utilizing this nanoadhesive bonding technique were introduced, including for growth of E. coli in the iCVD-bonded chips and fabrication of gas impermeable microchannels for microparticle synthesis from organic solvents. Another amine functional conformal coating has been designed, synthesized, and characterized. The novel alternating copolymer thin film synthesized from maleic anhydride and aminostyrene via iCVD extensively self-crosslinks after gentle heating. The annealed copolymer films display an elastic modulus exceeding 20 GPa, far greater than typical polymers (0.5~5 GPa). Moreover, the cross-linked films maintain their flexibility, neither cracking nor delaminating with repeated flexing. This achievement represents a significant advance in the fabrication of tough, durable, conformal, functional coatings. Furthermore, the highly crosslinked coating material has oxygen permeability lower than leading commercially available permeation barrier films, making it an attractive material for electronics or food industries. Also described is the utility of a new initiator, tert-butyl peroxybenzoate (TBPOB), for the iCVD synthesis. Using TBPOB instead of tert-butyl peroxide (TBPO), the rate of iCVD film growth increased by a factor of up to ~8 at comparable conformality and lower the filament temperature from ~250 °C to ~150 °C at a comparable deposition rate. The faster deposition rates improve the economics of the iCVD process and the ability to initiate polymerizations at a much lower filament temperature reduces heat load to substrate, which is advantageous for temperature sensitive polymeric substrates or monomers that decompose at high temperatures

Thesis Supervisor: Karen K. Gleason
Title: Alexander and I. Michael Kasser Professor of Chemical Engineering, Associate Dean of Engineering for Research

To Howard

ACKNOWLEDGEMENTS

Table of Content

List of Figures

9

List of Tables

List of Acronyms and Abbreviations

4-AS	4-aminostyrene
AFM	atomic force microscopy
ALD	atomic layer deposition
CVD	chemical vapor deposition
FTIR	fourier transform infrared spectroscopy
iCVD	initiated chemical vapor deposition
MLD	molecular layer deposition
mtorr	millitorr
NOA81	norland optical adhesive
PAS	poly(4-aminostyrene)
PASMa	poly(4-aminostyrene-*alt*-maleic anhydride)
PDMS	polydimethylsiloxane
PECVD	plasma enhanced chemical vapor deposition
PGMA	poly(glycidyl methacrylate)
$P_M/P_{M,sat}$	ratio of a species partial pressure to its saturated partial pressure at the system temperature
pCHMA	poly(cyclohexylmethacrylate)
PPFDA	poly(1H,1H,2H,2H-perfluorodecyl acrylate)
sccm	standard cubic centimeters per minute
SEM	scanning electron microscopy
TBPO	*tert*-butyl peroxide
TBPOB	*tert*-butyl peroxybenzoate
XPS	X-ray photoelectron spectroscopy

CHAPTER ONE

Introduction[*]

1.1. Background

Surface modification facilitates the incorporation of multiple functional groups and provides the ability to tune and enhance surface properties such as adhesiveness, hydrophobicity, antifouling, hardness, and roughness as well to provide a platform for further chemical modification and synthesis on the surface.

Common functional groups include carboxylic acids (-COOH), amines (-NH$_2$), epoxy (-C$_2$H$_3$O), pentafluorophenyl (-C$_6$H$_5$) and hydroxyl (-OH).[1] Carboxylic acids and amines are especially relevant to biological applications because they are the functional groups present in amino acids. Amine-functionalized surfaces have been shown to provide a versatile platform for detection of biomolecules as they readily react with the carboxylic acid groups common in these molecules. These surfaces can be functionalized either by direct attachment of specific binding groups, such as carboxylic acids, aldehydes, and epoxy groups, or through the use of various chemical linkers. Common chemical linkers include sulfosuccinimidyl-6-(biotinamido)hexanoate (sulfo-NHS-LC-biotin) which is used to bind streptavidin or avidin and 1-ethyl-3-(3-dimethylaminopropyl) carbodiimide (EDC)/ N-hydroxysulfosuccinimide (NHS) which is used to bind carboxylic acid.[2] In many cases, vapor phase treatment offers the potential for more reproducible, scalable and environmental friendly surface compared to solution methods. Additionally, many vapor methods are typically compatible with a wider range of substrates as opposed to being limited to the modification of specific types of surfaces, in contrast to the specific functionalization of gold surfaces by self-assembled monolayers. Substrates which would be damaged or swelled by solvents are often compatible with vapor phase surface modification.

1.2. Initiated Chemical Vapor Deposition (iCVD)

Figure 1-1a shows a schematic of the iCVD reactor configured for coating flat substrates. The monomer precursor and initiator flow across an array of hot filaments (Goodfellow), which is normally 1.5-3 cm above the silicon substrate on which the polymer is formed. The deposition mechanism is shown in

Figure 1-1b. Initiator is thermally decomposed in the vapor phase by a heated filament array at 200-250 °C. Active primary radicals and monomer are adsorbed onto the surface, where polymerization occurs through radical addition via initiation, propagation, and termination to form continuous polymer coatings.
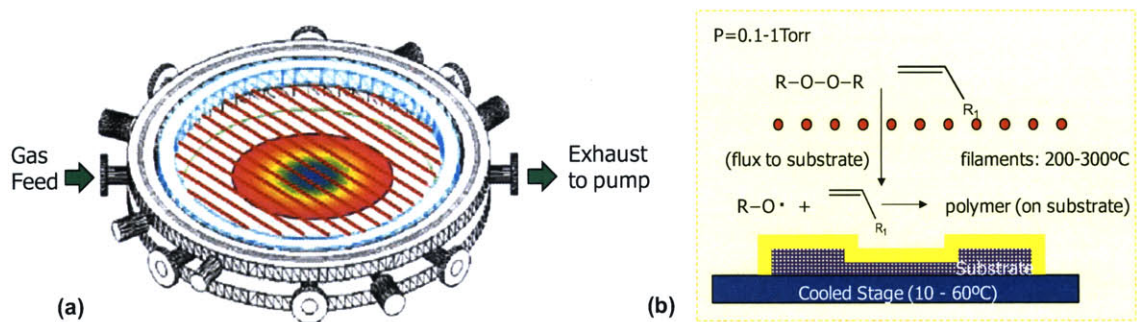
Figure 1-1. (a) iCVD reactor scheme. (b) iCVD deposition mechanism.

The substrate temperature is controlled using a recirculating liquid, which is normally water or oil. The reactor pressure is controlled using a downstream throttle valve (MKS Instruments) together with a Baratron capacitance manometer (MKS Instruments). The system is evacuated with a dry pump capable of base pressures as low as 3 mTorr. The top of the reactor consists of a glass window that enables real-time monitoring with a He-Ne laser (JDS Uniphase) whose beam is reflected off the silicon and growing film, producing an interference signal which was used to measure

the thickness of the film as a function of time. The flow rate of the monomer and initiator can be controlled by a needle valve or a MFC Flow Controller.

The iCVD technique is chemically comparable to solution phase polymerization, however, it has certain advantages over the common film formation techniques, such as spin coating, layer by layer assembly, dipping, etc. It is an all-dry process that is beneficial to environment as no solvent is involved, and this process can be used to deposit conformal coatings on complex structures due to lack of surface tension problem associated with liquid. Film thickness can easily be controlled through deposition time. This method has been used for a wide variety of vinyl monomers and already successfully created distinct free-radical polymers, alternating copolymers, and random copolymers.[3] Some of those polymers can only be formed via iCVD, such as the alternating copolymers.[4]

Depending on the kind of energy sources that activates the chemical species to induce polymerization, other kind of CVD techniques are also available, such as hot filament CVD (thermal energy), photo-initiated CVD (photochemical energy), and plasma-enhanced CVD (electrical energy). The properties of films deposited by these CVD methods are highly dependent on the energy source; retention of monomer functional groups is an important indication of these differences.[5] Among them, plasma-enhanced CVD (PECVD) has the limitation that the chemical functionality in the monomers is destructed and the films deposited are cross-linked. In this work, iCVD technique is utilized for surface functionalization.

Conformal coating can be deposited on complex structure and solvent-sensitive substrates via iCVD, which is difficult to achieve in solution phase polymerization. Furthermore, iCVD process is able to maintain some chemical

functionality in the monomers, which is of particular importance in the surface modification.

1.3. Functional Polymers by Vapor Deposition Techniques

Table 1-1 shows several examples of functionalities that have been demonstrated via different gas-phase techniques and their applications.

Ek et al. utilized atomic layer deposition (ALD), also known as atomic layer chemical deposition (ALCVD) to modify porous silica with aminopropylalkoxysilanes.[6] Aminosilanes were observed to react with silica through a site adsorption mechanism. Via gas phase deposition, hydrogen bonding between precursors and silanols of silica, and hydrolysis of alkoxy groups were avoided. In the study carried out by Adamczyk, poly(p-phenylene terephthalamide) (PPTA) thin films were deposited via molecular layer deposition (MLD), with terephthaloyl chloride (TC) and p-phenylenediamine (PD) as the bifunctional monomers.[7] Both MLD and ALD are thin film growth techniques that can be used to deposit conformal and precise ultrathin films. ALD method is for growth by alternating layers of atoms where MLD method utilizes biofunctional monomer precursors. They are based on sequential, self-limiting surface reactions. However, their growth rate is constrained by the limited number surface sites for polymer chains on the substrate.

Arroyo-Hernandez et al. used thermally activated chemical vapor deposition (TA-CVD) to obtain amine-functionalized films using 3-aminopropyltriethoxysilane (APTS) as a precursor.[8] The deposited films showed biofunctional properties due to the presence of reactive amine groups on the surface. APTS activation starts at around 600°C meaning this process is energy-intensive and thus not compatible with

temperature-sensitive substrates such as polymers. At temperatures above ~800°C, the films were observed to start cracking.

Lahann and Langer synthesized novel poly(p-xylylenes) polymers from 13 different [2.2]paracyclophanes with a variety of functionalities including amino, hydroxyl, anhydride, triflate, or trifluoroacetyl groups.[9] These polymer films provide free functional groups and could serve as interfaces for protein attachment or polymer brushes patterning. An aldehyde-functionalized poly(p-xylylene), poly[(4-formyl-p-xylylene)-co-(p-xylylene)], and its application in biomimetic surface modification was reported by Nandivada et al.[10] They also investigated a new type of biofunctional surface based on an alkyne-containing polymer, poly(4-ethynyl-p-xylylene-co-p-xylylene).[11] The reactive coating can be deposited on a variety of substrates and modified by subsequent "click chemistry",[12] which provides an opportunity in design of biofunctional surfaces for diagnostics, biosensors and biomedical device coatings. Jiang et al. synthesized poly[(p-xylylene-4-methyl-2-bromoisobutyrate)-co-(p-xylylene)] and after solventless deposition of the CVD polymer, hydrogel films could be prepared via atom transfer radical polymerization (ATRP).[13]

Surfaces with a diverse class of functional groups, such as amine,[14,15] carboxylic acid,[16] pentafluorophenyl,[17] anhydride,[18] and epoxide,[19] which enable the immobilization of biomolecules, can be synthesized utilizing plasma-enhanced chemical vapor deposition (PECVD).[20]

The plasma-polymerized ethylenediamine (PPEDA) coated slides were used for the development of DNA arrays.[14,15] Im also used PECVD to obtain an amine-functionalized surface and used it for both bonding and functionalization of a microfluidic device.[21] However, the networks of covalent bonds in the films generated using plasma are typically extremely complex due to crosslinking. Often the plasma

deposited materials are termed "polymer-like" to distinguish them from true linear polymers. While crosslinking can enhance the robustness of the resultant films, it also typically reduces the retention of functional groups. Pulsing of the plasma excitation has been widely used to reduce crosslinking and increase functional retention.[22]
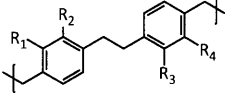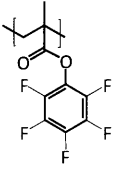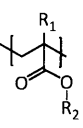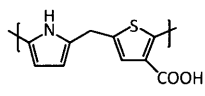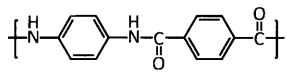
Additionally, ageing effects on plasma surfaces can limit commercial adaptation.[20]

The iCVD method, which is capable of synthesizing linear polymeric chains at high deposition rates from commercial monomers, has successfully been used to create many distinct homopolymers, random copolymers, and alternating copolymers using free radical polymerization.[4,5,23] Ultrahydrophobic, hydrophilic, chemically resistant, hydrogel and peptide-functionalized polymer surfaces have all been produced via iCVD. Table 1-1 shows other functionalities which have been successfully deposited via iCVD. The maleic anhydride functional group is attractive in biomaterial applications and has been used in functionalization of cellulose as well as various small molecule amines and alcohols.[4] Fluorinated alkyl groups are of interest because fluorocarbon films have unique optical, electrical, chemical and surface properties which make them desirable for a diverse array of optoelectronic and biomedical applications.[24] An alkyne group can be functionalized via an azide/alkyne 'click' reaction to form a triazole.[25] Furan rings can be derivatized via the rapid and selective Diels-Alder reaction which has been used to attach organic molecules to semiconductor surfaces and immobilize various biomolecules on solid substrates.[26] Baxamusa reported photoinitiated chemical vapor deposition (piCVD), a gentle synthetic method, for the preparation of ultrathin films (100 nm) of the hydrogel poly(hydroxyethyl methacrylate) (pHEMA) on a flat substrate.[27] The mild

nature of piCVD, which utilizes no plasma or solvent, makes it ideal for coating the surfaces of optodes and other sensors designed for implantation.

Oxidative chemical vapor deposition (oCVD) copolymerization of pyrrole with thiophene-3-acetic acid (TAA) led to the formation of uniform conducting polymer films with –COOH functionality.[28] A resistance-based sensing platform is developed with this copolymer and it replaced brittle poly(thiophene-3-acetic acid) (PTAA) film in sensing application.

Table 1-1. Functional polymers by vapor deposition techniques.

Method	Example functional polymer	Chemical structure	Application
CVD	functionalized poly(*p*-xylylenes)	R_1-R_4 = NH_2, CH_2OH, CHO, $COCF_3$, $COOC_6F_5$	Chemical functionalization groups including amine, carboxylic acid, anhydride, and triflate. Optically birefringent or isotropic films. Conformal chain-growth polymers from paracyclophane monomers.
Pulsed PECVD	poly(pentafluorophenyl methacrylate)		Binding of aminated ligands through nucleophilic substition. Partial retention of other pendant -R groups as for iCVD. Single-step deposition with possible surface grafting of chain-growth polymers.
iCVD	functional poly(acrylates) and methacrylates	R_1 = H or CH_3, R_2 = COC, C-C≡C, CH_2CH_2OH, H, etc.	Chemical functionalization for surface energy control and chemical binding of molecules and nanoparticles. Conformal, high-rate, deposition of chain-growth polymers with full functional retention.
oCVD	poly(pyrrole-*co*-thiophene-3-acetic acid)	COOH	Multifunctional electrically conducting films with carboxylic acid functionalization groups. Step growth through oxidative polymerization.
VDP	poly(*p*-phenylene terephthalamide)		Step-growth polymer with good molecular control, often relying on condensation addition reactions from pairs of bifunctional monomers. Similar monomers are utilized in the multi-step growth process MLD.

1.4. Application of CVD Polymers to MEMS Sealing

Biological applications of microelectromechanical systems (MEMS) are expanding to include rapid diagnostics, drug delivery, 3-D artificial organs, and integrated systems for personalized medicine.[29-32] Smaller dimensions, the ability to incorporate sensing, signaling, and actuation functions on the same substrate; and enhanced functionality are a few of the attributes desired.

MEMS fabrication generally utilizes three classes of materials. The first is made of those commonly used in microelectronics, such as silicon and glass. MEMS technology has traditionally been focused on silicon-based fabrication techniques, taking advantage of decades of fabrication technology from the semiconductor industry.[33] The second class is made up of biological materials and entities such as proteins and tissues. Over the past few years, the MEMS field has gradually extended the range of substrates used in order to broaden the potential application of MEMS devices. Polymers are of particular interest due to their unique and diverse properties.

One well-known example of a polymer substrate used in MEMS is polydimethylsiloxane (PDMS), which is patterned using soft lithography technology pioneered by George Whitesides at Harvard University.[34] However, PDMS swells significantly in the presence of organic solvents and is permeable to liquids and gases. As a result, substitute materials and surface modification techniques which provide a protective barrier that increases the chemical resistance of PDMS channels have recently gained interest.[35] Examples of polymer materials used to fabricate microfluidic devices include polyurethane[36], polycarbonate[37], polymethyl methacrylate (PMMA)[38], polystyrene[39], polyvinylchloride and polyethylene[40]. These polymers have great potential as materials suitable for biological applications because

they can be obtained at lower costs and allow greater ease in fabrication,[41] they

provide the ability to integrate functional hydrogel materials[42], and most importantly

they reduce the undesirable swelling in organic solvents when compared with PDMS.

Despite these advantages, bonding these soft polymers to each other is very

difficult and therefore researchers are restricted in their choice of substrate material.[43]

For example, oxygen plasma bonding[44,45] is widely utilized, but is applicable only to

Si-containing materials, such as PDMS and glass. Furthermore, the aggressive

oxidizing plasma will degrade cells or inactivate organic functional groups present on

the surfaces. Adhesive bonding provides high bonding strength, but non-conformal

coating can clog of small channels.[45] Thus, because conformal films can be applied to

virtually any substrate by CVD, this solventless adhesive bonding strategy is very

attractive for MEMS fabrication of miniaturized devices in a wide range of materials.

While reactive CVD coatings have been formed directly in the confined

channels assembled microfluidic,[46] extending this approach to complex channel

microgeometries is likely to be difficult. Alternately, several schemes have been

successful for applying functional and adhesive CVD polymers to the unbonded

device components.[21,47,48] Contacting the surfaces followed by annealing or UV

curing completes the bonding while the functional groups inside the channel remain

for subsequent biological binding. The CVD bonding methods are applicable to a

broad range of substrate material, enabling greater choice in the materials of

construction for MEMS fabrication.

UV irradiation of surfaces coated with iCVD poly(glycidyl methacrylate)

(PGMA) provided successful simultaneous microfluidic device sealing and channel

functionalization.[47] The sealed devices withstood modest pressures (22 psia).

Simultaneous bonding and functionalization was also achieved through the thermally activated (140 °C) reaction of the amine and aldehyde functional groups present in poly(4-formyl-p-xylylene-co-p-xylylene) and poly(4-aminomethyl-p-xylylene-co-p-xylylene) CVD polymer films.[48] This solventless adhesive bonding process (SAB) is applicable to a wide range of materials, including PDMS, poly (tetrafluoro ethylene) (PTFE), stainless steel, glass, silicon and gold. Tensile stress data showed the bonding strength is >1.21 MPa for sealed devices. However, the drawbacks for this process include the need to custom synthesize monomers, since they are not commercially available, and formation of reaction byproducts which must outgas from the seal. Thermal bonding at 70°C was achieved by contacting iCVD PGMA with plasma polymerized poly(allylamine) (PAAm) surfaces.[21] The covalent tethers form between the complementary surfaces without any gaseous byproducts and the required monomers are commercially available. Sealed devices with channel widths as small as 200 nm able to withstand ≥ 50 psia were fabricated from silicon, glass, quartz, PDMS, polystyrene, poly (ethylene terephthalate) (PET), polycarbonate (PC), and poly (tetrafluoro ethylene) (PTFE). Successful functionalization of the epoxy and amine groups remaining in the channel was achieved.

1.5. Scope of Thesis

This thesis utilizes iCVD to synthesize amine-functional homopolymer and alternating copolymer. Emphasis is placed on developing novel, functional polymer thin films and their practical applications.

CHAPTER TWO describes the synthesis of poly(4-aminostyrene) by iCVD, representing the first time that a library of iCVD functional groups has been extended to amine moieties. The pendant amine chemical functionality was confirmed by Fourier transform infrared spectroscopy (FTIR) and X-ray photoelectron spectroscopy (XPS). In addition, fluorescence microscopy and photoluminescence of quantum dot functionalized surfaces confirm that the reactive amine functional group density at the surface of iCVD PAS is ~ one order of magnitude greater than for films grown by plasma-enhanced chemical vapor deposition (PECVD). The higher amine density of the iCVD films can serve as scaffold for subsequent functionalization.

CHAPTER THREE furthers the study of amine-functional PAS as the application of a nano-adhesive layer. A novel nanoadhesive bonding technique was developed using the low-temperature (50 °C) and zero-outgassing reaction between the amine groups in iCVD PAS and the epoxy groups in iCVD poly(glycidyl methacrylate) (PGMA). Prototype microfluidic structures were fabricated and hydrolytically stable devices able to withstand high pressures were achieved by combining polydimethylsiloxane (PDMS) and a variety of other polymeric materials. This nanoadhesive bonding technique has successfully been applied to applications including growth of E. coli in the iCVD-bonded bioreactor and synthesis of microparticle in gas impermeable microchannels from organic solvents.

CHAPTER FOUR introduces the design, synthesis, and characterization of a conformal organic coating which is hard, and impermeable, yet remains flexible. First, iCVD is used to synthesis a novel alternating copolymer thin film, poly(4-aminostyrene-*alt*-maleic anhydride). Upon annealing, the functional groups of the two monomers react, resulting in extensive cross-linking. The annealed copolymer films display an elastic modulus far greater than typical polymers. Moreover, the cross-linked films maintain their flexibility, neither cracking nor delaminating with repeated flexing. This achievement represents a significant advance in the fabrication of tough, durable, conformal, functional coatings.

In CHAPTER FIVE, *tert*-butyl peroxybenzoate (TBPOB) has been used as an initiator for iCVD synthesis of poly(cyclohexyl methacrylate) (pCHMA) for the first time. TBPOB is much less volatile than *tert*-butyl peroxide (TBPO) and enables a higher surface concentration and hence results in a faster growth rate. Furthermore, with a decomposition temperature of 90 °C in solution, TBPOB holds the potential for further reducing the filament temperature of the iCVD process. Lower filament temperatures are desired for use with polymeric substrates which decompose at high temperature or which have low glass transition temperature. Lower filament temperatures are also desired for monomers that decompose at high temperature. The deposition kinetics, films composition and structure, sticking coefficient, and conformality have been compared to iCVD pCHMA films initiated by TBPO.

CHAPTER SIX provides conclusions concerning the synthesis of the amine-functional polymer films by iCVD and the utility of a new initiator. Possible amine candidates and future research possibilities for microfluidics are also included.

An appendix is also presented describing the integration of amplified fluorescent polymer (AFP) detection schemes into microfluidic systems via fluorous

interaction. Successful synthesis of poly(1H,1H,2H,2H-perfluorodecyl acrylate) (PPFDA) via iCVD has already been reported.[49] It is expected that the fluorous effects can be used to deposit fluorous amplifying fluorescent polymer (AFP) on surfaces and also to localize the fluorous-tagged ligands provided by Swager's group. This new process makes use of the novel surface functionalization schemes and nanoadhesive bonding technique developed in CHAPTER THREE.

References

(1)   Meakins, G. D. In *Oxford Chemistry Primers*; Oxford University Press: Oxford, 1996; Vol. 35.

(2)   Hermanson, G. T. *Bioconjugate techniques*; Academic Press: San Diego, 1996.

(3)   Tenhaeff, W. E.; Gleason, K. K. *Advanced Functional Materials* **2008**, *18*, 979-992.

(4)   Tenhaeff, W. E.; Gleason, K. K. *Langmuir* **2007**, *23*, 6624-6630.

(5)   Mao, Y.; Gleason, K. K. *Langmuir* **2004**, *20*, 2484-2488.

(6)   Ek, S.; Iiskola, E. I.; Niinisto, L. *Langmuir* **2003**, *19*, 3461-3471.

(7)   Adamczyk, N. M.; Dameron, A. A.; George, S. M. *Langmuir* **2008**, *24*, 2081-2089.

(8)   Arroyo-Hernandez, M.; Perez-Rigueiro, J.; Martinez-Duart, J. M.; Elsevier Science Bv: 2006, p 938-941.

(9)   Lahann, J.; Langer, R. *Macromolecules* **2002**, *35*, 4380-4386.

(10)   Nandivada, H.; Chen, H. Y.; Lahann, J. *Macromolecular Rapid Communications* **2005**, *26*, 1794-1799.

(11)   Nandivada, H.; Chen, H. Y.; Bondarenko, L.; Lahann, J. *Angewandte Chemie-International Edition* **2006**, *45*, 3360-3363.

(12)   Nebhani, L.; Barner-Kowollik, C. *Advanced Materials* **2009**, *21*, 1-27.

(13)   Jiang, X. W.; Chen, H. Y.; Galvan, G.; Yoshida, M.; Lahann, J. *Advanced Functional Materials* **2008**, *18*, 27-35.

(14)   Spanos, C. G.; Badyal, J. P. S.; Goodwin, A. J.; Merlin, P. J. *Polymer* **2005**, *46*, 8908-8912.

(15)   Jung, D.; Yeo, S.; Kim, J.; Kim, B.; Jin, B.; Ryu, D. Y. *Surface & Coatings Technology* **2006**, *200*, 2886-2891.

(16)   Hutton, S. J.; Crowther, J. M.; Badyal, J. P. S. *Chemistry of Materials* **2000**, *12*, 2282-2286.

(17)   Francesch, L.; Garreta, E.; Balcells, M.; Edelman, E. R.; Borros, S. *Plasma Processes and Polymers* **2005**, *2*, 605-611.

(18)   Schiller, S.; Hu, J.; Jenkins, A. T. A.; Timmons, R. B.; Sanchez-Estrada, F. S.; Knoll, W.; Forch, R. *Chemistry of Materials* **2002**, *14*, 235-242.

(19)   Tarducci, C.; Kinmond, E. J.; Badyal, J. P. S.; Brewer, S. A.; Willis, C. *Chemistry of Materials* **2000**, *12*, 1884-1889.

(20)   Siow, K. S.; Britcher, L.; Kumar, S.; Griesser, H. J. *Plasma Processes and Polymers* **2006**, *3*, 392-418.

(21)   Im, S. G.; Bong, K. W.; Lee, C. H.; Doyle, P. S.; Gleason, K. K. *Lab on a Chip* **2009**, *9*, 411-416.

(22)   Kuhn, G.; Retzko, I.; Lippitz, A.; Unger, W.; Friedrich, J. In *7th International Conference on Plasma Surface Engineering (PSE 2000)*; Elsevier Science Sa: Partenkirchen, Germany, 2000, p 494-500.

(23)   O'Shaughnessy, W. S.; Mari-Buye, N.; Borros, S.; Gleason, K. K. *Macromolecular Rapid Communications* **2007**, *28*, 1877-1882.

(24)   Ma, M. L.; Mao, Y.; Gupta, M.; Gleason, K. K.; Rutledge, G. C. *Macromolecules* **2005**, *38*, 9742-9748.

(25)   Im, S. G.; Kim, B. S.; Lee, L. H.; Tenhaeff, W. E.; Hammond, P. T.; Gleason, K. K. *Macromolecular Rapid Communications* **2008**, *29*, 1648-1654.

(26)   Chen, G. H.; Gupta, M.; Chan, K.; Gleason, K. K. *Macromolecular Rapid Communications* **2007**, *28*, 2205-2209.

(27)   Baxamusa, S. H.; Montero, L.; Dubach, J. M.; Clark, H. A.; Borros, S.; Gleason, K. K. *Biomacromolecules* **2008**, *9*, 2857-2862.

(28)   Vaddiraju, S.; Senecal, K.; Gleason, K. K. *Advanced Functional Materials* **2008**, *18*, 1929-1938.

(29)   Jensen, K. F. *Mrs Bulletin* **2006**, *31*, 101-107.

(30)   Arora, W. J.; Tenhaeff, W. E.; Gleason, K. K.; Barbastathis, G. *Journal of Microelectromechanical Systems* **2009**, *18*, 97-102.

(31)   Weibel, D. B.; Whitesides, G. M. *Current Opinion in Chemical Biology* **2006**, *10*, 584-591.

(32)   Bashir, R. *Advanced Drug Delivery Reviews* **2004**, *56*, 1565-1586.

(33)   Wise, K. D.; Najafi, K. *Science* **1991**, *254*, 1335-1342.

(34)   McDonald, J. C.; Whitesides, G. M. *Accounts of Chemical Research* **2002**, *35*, 491-499.

(35)   Abate, A. R.; Lee, D.; Do, T.; Holtze, C.; Weitz, D. A. *Lab on a Chip* **2008**, *8*, 516-518.

(36)   Madou, M. J.; Lu, Y. M.; Lai, S. Y.; Lee, J.; Daunert, S. *Micro Total Analysis Systems 2000, Proceedings* **2000**, 565-570.

(37)   Olsen, K. G.; Ross, D. J.; Tarlov, M. J. *Analytical Chemistry* **2002**, *74*, 1436-1441.

(38)   Wang, J.; Pumera, M.; Chatrathi, M. P.; Escarpa, A.; Konrad, R.; Griebel, A.; Dorner, W.; Lowe, H. *Electrophoresis* **2002**, *23*, 596-601.

(39)   Locascio, L. E.; Perso, C. E.; Lee, C. S. *Journal of Chromatography A* **1999**, *857*, 275-284.

(40)   Becker, H.; Locascio, L. E. *Talanta* **2002**, *56*, 267-287.

(41)   Xia, Y. N.; Whitesides, G. M. *Annual Review of Materials Science* **1998**, *28*, 153-184.

(42)   Ziaie, B.; Baldi, A.; Lei, M.; Gu, Y. D.; Siegel, R. A. *Advanced Drug Delivery Reviews* **2004**, *56*, 145-172.

(43)   Wu, H. K.; Huang, B.; Zare, R. N. *Lab on a Chip* **2005**, *5*, 1393-1398.

(44)   Gosele, U.; Tong, Q. Y. *Annual Review of Materials Science* **1998**, *28*, 215-241.

(45)   Niklaus, F.; Stemme, G.; Lu, J. Q.; Gutmann, R. J. *Journal of Applied Physics* **2006**, *99*, 28.

(46)   Chen, H. Y.; Elkasabi, Y.; Lahann, J. *Journal of the American Chemical Society* **2006**, *128*, 374-380.

(47)   Martin, T. P.; Lau, K. K. S.; Chan, K.; Mao, Y.; Gupta, M.; O'Shaughnessy, A. S.; Gleason, K. K. *Surface & Coatings Technology* **2007**, *201*, 9400-9405.

(48)   Chen, H. Y.; McClelland, A. A.; Chen, Z.; Lahann, J. *Analytical Chemistry* **2008**, *80*, 4119-4124.

CHAPTER TWO

Initiated Chemical Vapor Deposition of Amine-Functionalized Thin Films[*]

Abstract

Poly(4-aminostyrene) (PAS) thin films were synthesized via initiated chemical vapor deposition (iCVD) with tert-butyl peroxide as the initiator, representing the first time that a library of iCVD functional groups has been extended to amine moieties. The retention of the pendant amine chemical functionality was confirmed by Fourier transform infrared spectroscopy (FTIR) and X-ray photoelectron spectroscopy (XPS). Scanning electron microscope (SEM) reveals that the iCVD PAS coatings are conformal over non-planar structures. Fluorescence microscopy and photoluminescence of quantum dot functionalized surfaces confirm that the reactive amine functional group density at the surface of iCVD PAS is ~ one order of magnitude greater than for films grown by plasma-enhanced chemical vapor deposition (PECVD). The higher amine density of the iCVD films enables the formation of a robust nanoadhesive with complementary epoxy functional groups.

2.1. Introduction

Modification with specific organic groups is critical for controlling the functionality of the surface. The organic functional groups can be utilized to tune surface energy; to enable subsequent chemical attachment of desirable molecules, such as fluorescent dyes, antibodies, or cell growth factors; or to covalently bind micro- or nanoparticles to the surface. Common functional groups include amines (-NH_2), carboxylic acids (-COOH), epoxy (-C_2H_3O), hydroxyl (-OH), and aldehyde (-COH).[1] Amine-functionalized surfaces are of particular interest as they provide a versatile platform for detection of biomolecules.[2] Primary amine groups can react with a variety of functional groups including epoxy, aldehyde, carbonyl, carboxylic acid, sulfonyl chloride, and nitrous acid.[3] Surfaces with amine groups can be functionalized either by direct attachment of specific binding groups, or through the use of various chemical linkers.[1]

Some existing methods to obtain amine-functionalized surfaces include direct adsorption of polylysine,[4] amine silanization,[5-7] incorporation of polyamidoamine dendrimers,[8] and amine self-assembly.[9] Each of these approaches has one or more drawbacks such as poor stability, substrate specificity, multistep processing, and the requirement for solution phase chemistry. Gas-phase treatment, including atomic layer deposition (ALD)[10] or chemical vapor deposition (CVD)[11,12], is desired for surface modification of substrates that would swell or degrade in solvent. It is also desired for polymers that are insoluble or dissolve only in harsh, toxic or expensive solvents. A plasma-enhanced chemical vapor deposition (PECVD) method using plasma-polymerized ethylenediamine (PPEDA) was employed to coat glass slides with amine functional groups.[13] However, this approach generally suffers

34

from the drawback of poor amine functionality retention and lack of chemical selectivity because of the plasma environment.

The iCVD method has shown great promise as a surface modification technique and it has successfully been used to create many distinct homopolymers, random copolymers, and alternating copolymers using free radical polymerization.[12,14] It is chemically comparable to solution-phase polymerization, but is environmentally friendly, able to achieve good conformality and able to maintain the chemical functionality in the monomers. Amine-functionalized iCVD surfaces have not yet been reported. Selection of a monomer is challenging because many candidates have low vapor pressures as a result of hydrogen bonding between amine-groups. However, some commonly used monomers such as ethylamine and allylamine (AAm) are too volatile (vapor pressure, P_{sat} > 240 torr at 25°C) for the iCVD system and cannot be operated within the optimum process window of ~0.4 < (P/P_{sat}) < ~0.7, where P is the partial pressure of the monomer in the reactor.[15]

In this work, 4-aminostyrene (4-AS) is chosen as a precursor (vapor pressure = 0.0415 torr at 25 °C), which is compatible with the iCVD process. The conformality, surface concentration of amine functional groups, and nanoadhesive capabilities of the iCVD PAS will be compared to amine-containing films grown from PECVD utilizing the monomer AAm. The latter was chosen for comparison as it was previously demonstrated to be useful in a novel nanoadhesive bonding scheme[16] which at the same time leaves epoxy and amine functional groups inside the microchannels, providing a direct route for further functionalization.

2.2. Experimental

2.2.1. Film Preparation

All iCVD films were deposited in a custom built vacuum reactor (Sharon Vacuum), as previously described.[15,17] Thermal excitation was provided by heating a nichrome filament (80% Ni/ 20% Cr) mounted in a parallel array and the temperature was measured by a thermal couple attached to one of the filaments. The filament holder straddled the deposition stage which maintained at a set point temperature using water cooling. The vertical distance between the filament and the stage was 2 cm.

All the chemicals were used as purchased without further purification. Tert-butyl peroxide (Aldrich, 97%) initiator, at room temperature, was fed to the reactor through a mass flow controller (model 1179A, MKS) at 1 sccm. 4-Aminostyrene (4-AS) (Aldrich, 97%) monomer, heated to 85±3 °C in a glass jar, was delivered into the reactor at 0.8 sccm via a different port. Films were deposited at a filament temperature of 260 °C and a stage temperature of 50 °C. iCVD deposition conditions utilizing the monomer glycidyl methacrylate (Aldrich, 97%) were adopted from previous work reported by Mao.[18] Total pressure in the vacuum chamber was maintained at 0.35 torr and 0.22 torr for 4-AS and GMA depositions respectively.

For each polymer, nine different kinds of substrates, each ~ 8 cm^2 in area, were simultaneously coated via iCVD: (1) Si wafer, (2) polydimethylsiloxane (PDMS), (3) polycarbonate (PC), (4) glass, (5) polyethylene terephthalate (PET), (7) polyethylene (PE), (8) polyacrylate (PA), and (9) cyclic olefin copolymer (COC). All of these substrates were cleaned for 0.5-1 min with oxygen plasma (13.56 MHz, 100 W/cm^2, 100 mTorr). Film growth on the Si substrate was monitored in situ through

laser interferometry and controlled to thickness of 200-250 nm. A more accurate film thickness on the Si wafer substrates was measured post-deposition by a J.A. Woollam M-2000 spectroscopic ellipsometry at a 70 ° incidence angle using 190 wavelengths from 315 to 718 nm.

Using the plasma polymerization conditions and reactor configuration reported by Im et al.[16] Si, PDMS, PC and glass substrates were coated with PECVD polyallylamine (PAAm) to a thickness of ~ 50 nm.

2.2.2. Film Characterization

Fourier transform infrared (FTIR) measurements were performed on a Nicolet Nexus 870 ESP spectrometer in a normal transmission mode. A deuterated triglycine sulfate (DTGS) KBr detector over the range of 400-4000 cm^{-1} was utilized with a 4 cm^{-1} resolution. Films were measured immediately after deposition and measurements were averaged over 64 scans to improve the signal-to-noise ratio. All spectra were baseline corrected by subtracting a background spectrum of the Si wafer substrate. FTIR was also performed on a commercial sample of PAS (Polysciences) that was incorporated into a KBr pellet.

X-ray photoelectron spectroscopy (XPS) survey spectrum was obtained on a Kratos Axis Ultra spectrometer with a monochromatized Al Kα source. Relative sensitivity factors were calibrated by measuring poly(N-isopropylacrylamide) polymer (Aldrich) spun-cast onto Si wafer. Deposition samples and the standard were stored under vacuum overnight prior to analysis.

Both iCVD and plasma-polymerized polymers were deposited on silicon substrates patterned with trenches supplied by Analog Devices. These trenches were 7 μm deep and 0.8 μm, 1.3μm, 2.1μm, and 5μm wide respectively. Deposited trench

wafers were sputter coated with 6nm of gold (Denton Desk II) and SEM images were obtained by a JEOL JSM-6060 with acceleration voltage of 5 kV.

Fluorescence microscope images were obtained at a 100× magnification using a Zeiss Axiovert 200 inverted microscope with FITC illumination.

2.2.3. Attachment of CdSe/ZnS Quantum Dots

One milligram of commercially available CdSe/ZnS core/shell quantum dots with carboxylic acid surface groups (NN-labs, Emission=632 nm) were dispersed in water (20 mL). The solution was ultrasonicated for 30 min to ensure uniform dispersion (VWR, Model 75D). A small amount of N,N'-Dicyclohexylcarbodiimide (<1 mg) was added into the solution afterwards. To attach quantum dots, two glass substrates with iCVD deposited PAS and plasma-polymerized PAAm films were submerged in the dispersion. The jar was placed on a hotplate maintained at 60 °C for 2 hours. To remove any unreacted, loosely attached quantum dots, the samples were rinsed with deionized water for three times. After dried and put under vacuum overnight, the samples were analyzed using photoluminescence (PL).

In PL measurements, a coherent Ti-Sapphire laser with λ=395 nm, 200 fs pulse width and 100 kHz repetition rate, was used as an excitation source. Emitted photons were collected with a Hamamatsu C4780 picosecond fluorescence lifetime system consisting of a Hamamatsu C4334 Streak Camera and a C5094 spectrograph. All measurements were carried out under room temperature.

2.3. Results and Discussion

2.3.1. Film Structure Analysis

Figure 2-1 shows the FTIR spectra of 4-aminostyrene (4-AS) monomer precursor, the iCVD deposited, and the conventionally polymerized PAS films. The 4-AS spectrum (Figure 2-1a) clearly shows several signatures from vinyl bonds, as denoted by asterisks. Most clearly resolved are the C-H bond out-of-plane deformations arising from =CH and =CH$_2$ groups at 990 and 910 cm^{-1} respectively. The vinyl bonds also contribute to the sharp C=C stretching mode at 1630 cm^{-1} and to the sp^2 C-H stretching modes above ~3000 cm^{-1}. However, the phenyl groups also contribute to these later features. Film deposition through radical vinyl polymerization is verified by reduction of unsaturated carbon peaks in the spectrum of the iCVD film (Figure 2-1b) along with the increase in intensity of the sp^3 C-H stretching intensity below ~3000 cm^{-1}, indicated formation of polymer backbone containing the saturated carbon groups. As a reference standard, Figure 2-1c shows the spectrum of commercial obtained conventionally polymerized PAS bulk powder. As seen by comparing Figure 2-1b and Figure 2-1c, peak locations and areas of the iCVD deposited polymer spectrum matches well with the conventionally polymerized PAS standard.

It is important to note that PAS maintains the pendant amine functionality after polymerization, which could be used for further functionalization. The primary amino groups are indicated by signature NH$_2$ antisymmetric and symmetric stretching at 3420 and 3361 cm^{-1} respectively.[19] This amine is attached to a phenyl group having characteristic C-H stretching modes at 3020 cm^{-1}.
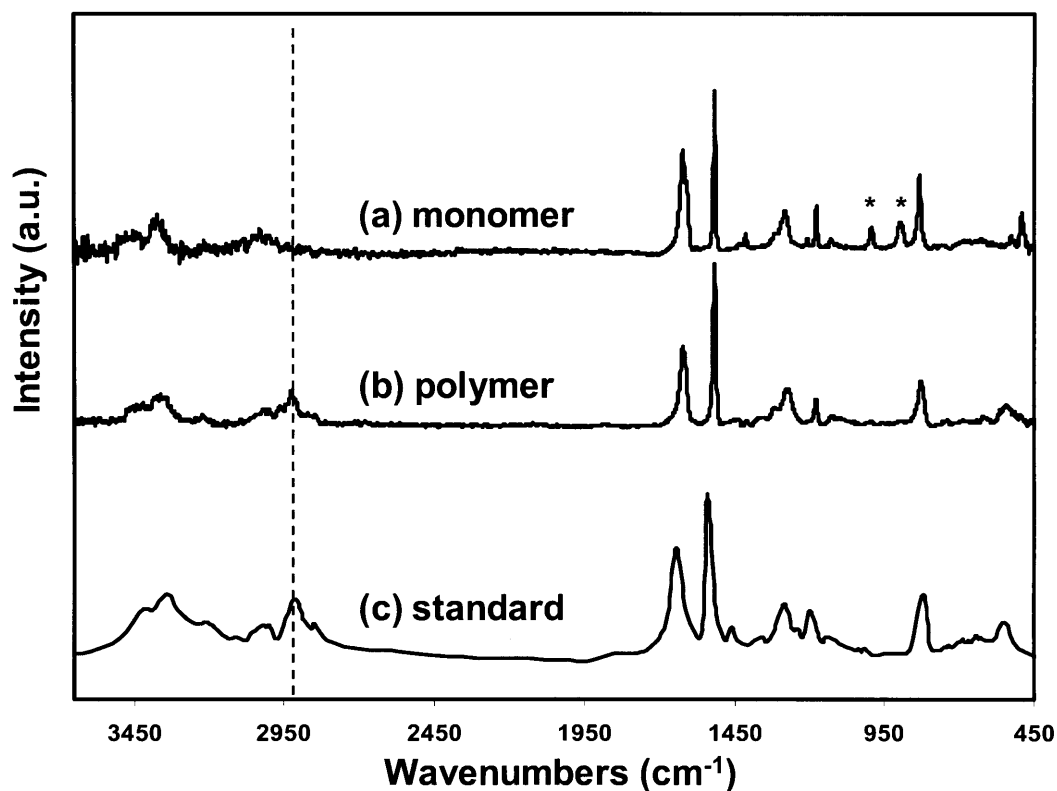
Figure 2-1. Fourier transform IR (FTIR) spectra of (a) 4-aminostyrene (4-AS) monomer, (b) iCVD deposited poly(4-aminostyrene) (PAS), and (c) PAS standard from Polysciences. Asterisks (*) represent signature vinyl bonds and dotted line refers to the sp3 C-H stretching.

Figure 2-2 shows the XPS survey scan of iCVD PAS. As expected from the chemical formula for PAS, $[C_8NH_9]_n$, carbon and nitrogen peaks are observed. In addition, a significant oxygen peak is present. Considering that the XPS sampling depth is approximately 5 nm,[20] the oxygen peak most likely indicates that water uptake or oxidation upon exposure to air has occurred at the film's surface during the 24 to 48 hrs between the completion of deposition and when XPS analysis was performed. The surface oxygen percentage is 8.8% on a hydrogen-free basis (Table 2-1). Despite the surface uptake of a species containing oxygen, the ratio of carbon:

nitrogen ratio at the surface, 8.2:1, is in reasonable agreement with the ratio based solely on the stoichiometry of PAS, 8:1.
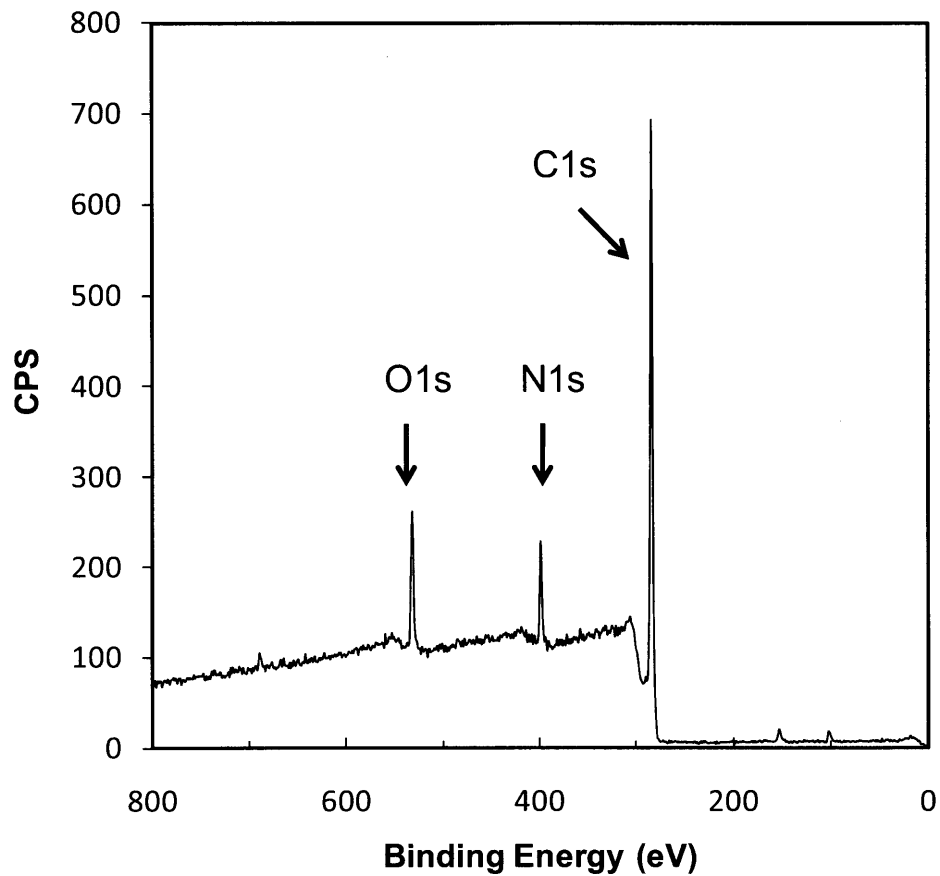
Figure 2-2. XPS survey scan for detection of the atomic concentration of oxygen, nitrogen, and carbon.

Table 2-1. Atomic concentration of carbon, nitrogen, and oxygen.

	C	N	O	C/N ratio
Binding Energy (eV)	284	399	532	
Experimental Percentage	81.3±3%	9.9±0.4%	8.8±0.3%	8.2:1
Theoretical percentage	88.9%	11.1%	0%	8:1

Both FTIR and XPS data support the hypothesis that iCVD produces the same polymeric structure as conventionally polymerized PAS and retains the pendant primary amine functional groups. This is the first time an amine functional iCVD polymer has been synthesized successfully. It not only broadens the iCVD library, but also enables many possible applications based on amine functionalization.

2.3.2. Conformal Coverage

For applications including microfluidics, medical devices, and membranes, good step coverage over non-planar or porous substrates is desired. Step coverage is defined as the ratio of the coating thickness at the bottom to that at the top of the trench. Step coverage for iCVD PAS and PECVD PAAm on trenches with different aspect ratios are shown in Figure 2-3. Clearly the conformality of the iCVD film is superior to that of PECVD layer. Even for the highest aspect ratio of 8.7, iCVD has step coverage of 90.3%, whereas for PECVD there is virtually no film in the bottom of the trench. The dashed line shows the linear best-fit for the data. This linear relationship ($R^2 > 0.99$) between logarithm of step coverage and the square of the aspect ratio agrees well with Baxamusa's results for a different iCVD polymer.[21]

0

-0.5

log(Step Coverage)

-1

-1.5

■ iCVD deposited

◇ PECVD deposited

-2

-2.5

0   20   40   60   80

(L/W)²
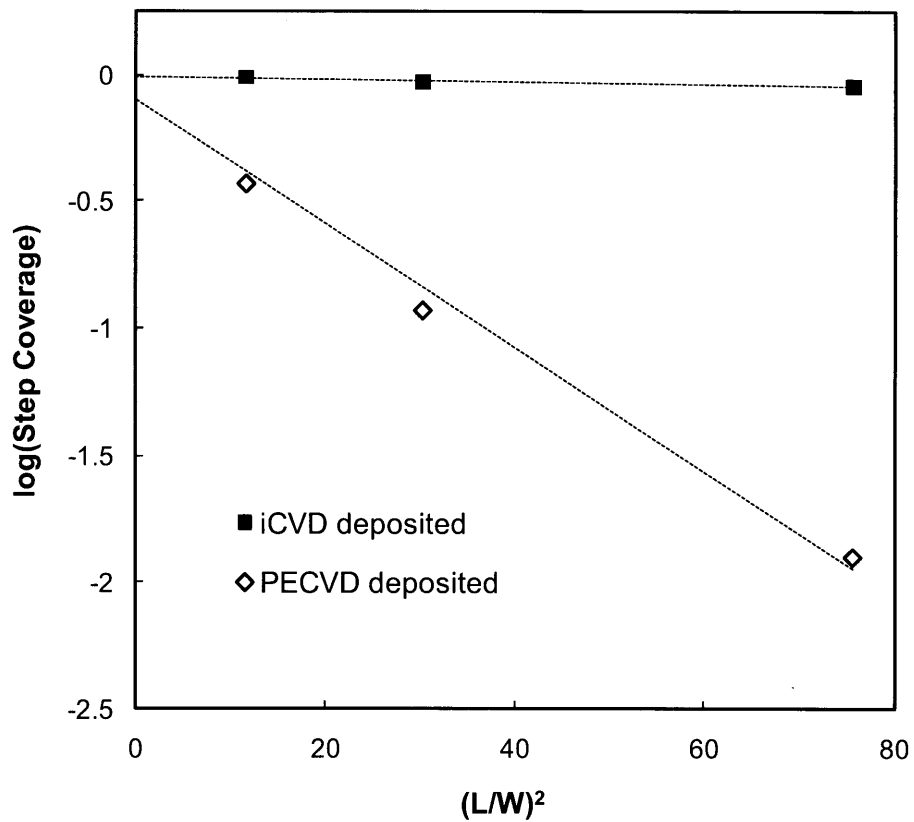
Figure 2-3. Step coverage as a function of aspect ratio square. The dashed line (R2>0.99) represents the linear best-fit line for the data and its slope is proportional to the sticking probability of the initiating radical. Here the three different aspect ratios for the trenches are 8.7, 5.5, and 3.4 respectively.
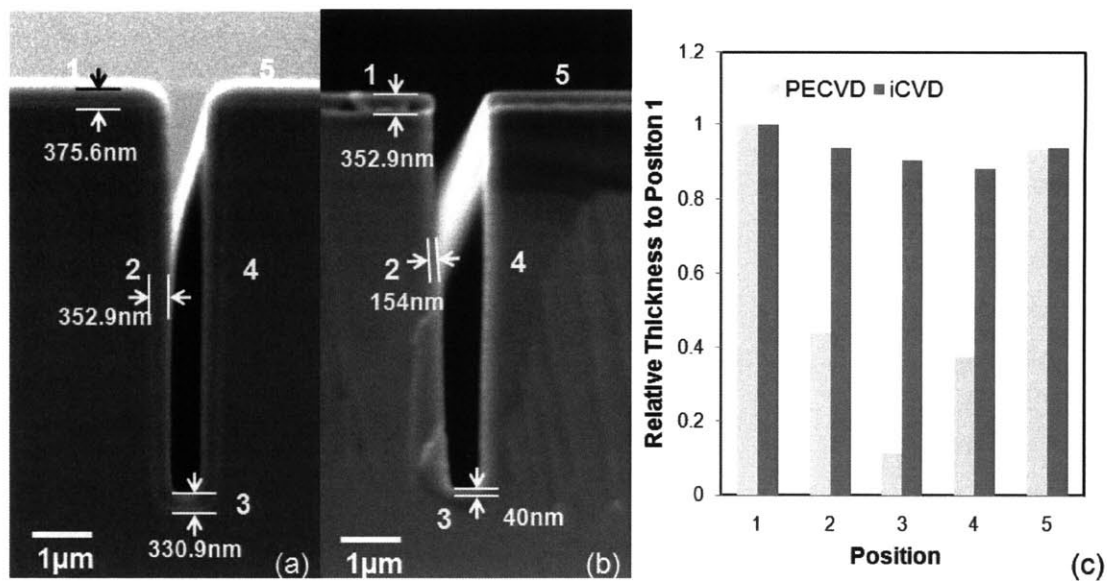
Figure 2-4. Cross-sectional SEM images films of (a) iCVD PAS, (b) PECVD PAAm, and (c) the relative thickness variation of films with respect to the trench position in (a) and (b).

Cross-sectional SEM micrographs (Figure 2-4) demonstrate the overall profiles for polymer films growing inside trenches with the aspect ratio of 5.5 by iCVD and PECVD. The PECVD film (Figure 2-4b) has little coverage on the side walls or on the bottom of the trench. In contrast, iCVD (Figure 2-4a) shows very good thickness uniformity over the entire trench feature. Figure 2-4c is the relative thickness variation of these two polymer films with respect to the positions in Figure 2-4a and Figure 2-4b.

2.3.3. Film Derivatization with CdSe/ZnS Quantum Dots

The characterization described above demonstrates that iCVD is able to deposit conformal polymers with retention of amine functionality. To address the question whether the amine functional groups maintain their reactivity, immobilization studies were carried out using CdSe/ZnS quantum dots with

44

carboxylic acid surface groups. The fluorescent microscope image in Figure 2-5b shows successful attachment of quantum dots. Three different spots on both PAS and PAAm coated samples were analyzed by photoluminescence (PL) and the results are provided in Figure 2-5a. Intensity on the iCVD PAS-coated substrate is at least one order of magnitude higher than PECVD PAAm-coated one.
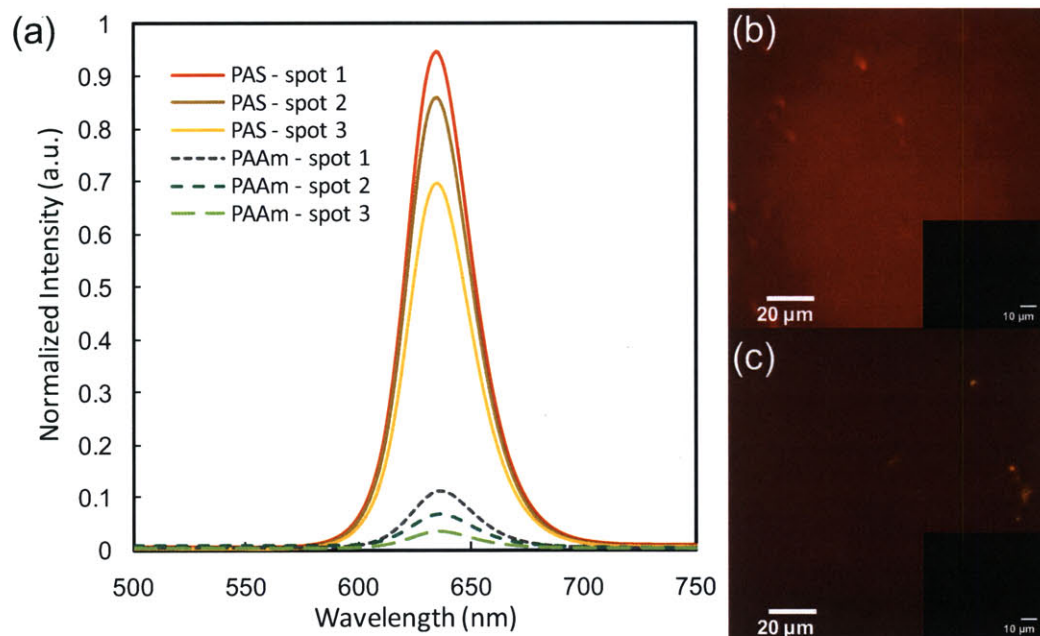
Figure 2-5. Amine functional groups density comparison between iCVD PAS and PECVD PAAm. (a) photoluminescence (PL) results. Three different spots were measured for each sample. Fluorescence micrographs of (b) iCVD PAS and (c) PECVD PAAm. The images insert in the top right of (b) and (c) represent background when there is no quantum dots attached to the surface.

Both the fluorescent microscopy and the PL results from quantum dots immobilized onto the film surfaces, indicate that iCVD PAS has a significantly higher density of reactive amine functional groups than does PECVD PAAm. The lower density of amine functionality in PECVD films most likely reflects the partial loss of chemical functionality from the monomers during plasma processing. By lowering the

input plasma power, greater retention of monomer functional groups is possible, but deposition rates also decrease. As a competition process between etching and deposition, PECVD PAAm has a low deposition rate of 2 nm/min. The iCVD film displays a much higher degree of functional retention and also has a higher deposition rate, 10 nm/min, than the PECVD film.

2.4. Conclusion

Amine functional thin films were successfully synthesized for the first time using iCVD with 4-AS as the monomer. FTIR and XPS results showed the similarity of the iCVD PAS films to the conventionally synthesized polymer. The iCVD method is advantageous over the conventional PECVD process for producing conformal coatings within complex and for retaining chemical functionality. Photoluminescence confirms that the reactive amine functional group density of iCVD PAS is ~ one order of magnitude higher than for films grown by PECVD. The accessible amine sites on the PAS surface can be served as a scaffold for further functionalization or as sites capable of nanoadhesive bonding.

Acknowledgements

References

(1)   Hermanson, G. T. *Bioconjugate techniques*; Academic Press: San Diego, 1996.

(2)   Ramanathan, T.; Fisher, F. T.; Ruoff, R. S.; Brinson, L. C. *Chemistry of Materials* **2005**, *17*, 1290-1295.

(3)   Hanson, J. R. *Functional Group Chemistry*; The Royal Society of Chemistry: Cambridge, 2001.

(4)   Dhamodharan, R.; McCarthy, T. J. *Macromolecules* **1999**, *32*, 4106-4112.

(5)   Sui, G. D.; Wang, J. Y.; Lee, C. C.; Lu, W. X.; Lee, S. P.; Leyton, J. V.; Wu, A. M.; Tseng, H. R. *Analytical Chemistry* **2006**, *78*, 5543-5551.

(6)   Kamisetty, N. K.; Pack, S. P.; Nonogawa, M.; Devarayapalli, K. C.; Kodaki, T.; Makino, K. *Analytical and Bioanalytical Chemistry* **2006**, *386*, 1649-1655.

(7)   Burleigh, M. C.; Markowitz, M. A.; Spector, M. S.; Gaber, B. P. *Chemistry of Materials* **2001**, *13*, 4760-4766.

(8)   Chan, J. C. Y.; Burugapalli, K.; Naik, H.; Kelly, J. L.; Pandit, A. *Biomacromolecules* **2008**, *9*, 528-536.

(9)   Ritchie, J. E.; Wells, C. A.; Zhou, J. P.; Zhao, J. N.; McDevitt, J. T.; Ankrum, C. R.; Jean, L.; Kanis, D. R. *Journal of the American Chemical Society* **1998**, *120*, 2733-2745.

(10)   Adarnczyk, N. M.; Dameron, A. A.; George, S. M. *Langmuir* **2008**, *24*, 2081-2089.

(11)   Lahann, J. *Polymer International* **2006**, *55*, 1361-1370.

(12)   Tenhaeff, W. E.; Gleason, K. K. *Advanced Functional Materials* **2008**, *18*, 979-992.

(13)   Jung, D.; Yeo, S.; Kim, J.; Kim, B.; Jin, B.; Ryu, D. Y. *Surface & Coatings Technology* **2006**, *200*, 2886-2891.

(14)   Baxamusa, S. H.; Im, S. G.; Gleason, K. K. *Physical Chemistry Chemical Physics* **2009**, *11*, 5227-5240.

(15)   Lau, K. K. S.; Gleason, K. K. *Macromolecules* **2006**, *39*, 3688-3694.

(16)   Im, S. G.; Bong, K. W.; Lee, C. H.; Doyle, P. S.; Gleason, K. K. *Lab on a Chip* **2009**, *9*, 411-416.

(17)   Chan, K.; Gleason, K. K. *Chemical Vapor Deposition* **2005**, *11*, 437-443.

(18)   Mao, Y.; Gleason, K. K. *Langmuir* **2004**, *20*, 2484-2488.

(19)   Daimay, L. V.; Norman, B. C.; William, G. F.; Jeanette, G. G. *The Handbook of Infrared and Raman Characteristic Frequencies of Organic Molecules*; Academic Press: New York, 1991.

(20)   Brundle, C. R.; Evans, C. A. J.; Wilson, S. *Encyclopedia of Materials Characterization: Surfaces, Interfaces and Thin Films*; Butterworth-Heinemann: Boston, 1992.

(21)   Baxamusa, S. H.; Gleason, K. K. *Chemical Vapor Deposition* **2008**, *14*, 313-318.

CHAPTER THREE

Nanoadhesive Bonding Technique
Using Amine-functional Films

Abstract

An alternative nanoadhesive bonding technique has been developed which expands the portfolio of materials that can be bonded while simultaneously leaving multifunctional coating inside the unbonded areas inside the channels to serve as a platform for further chemical functionalization or to serve as a protective layer against solvents and/or gas diffusion. The method requires only low-temperature (50 °C) and producing zero-outgassing reaction between the amine groups in poly(4-aminostyrene) (PAS) via initiated chemical vapor deposition (iCVD) and the epoxy groups in iCVD poly(glycidyl methacrylate) (PGMA). Prototype microfluidic structures were fabricated and bonded devices able to withstand >150 psia were achieved by combining polydimethylsiloxane (PDMS) and a variety of other materials including Si wafers, polycarbonate (PC), glass, polyethylene terephthalate (PET), polyethylene (PE), polyacrylate (PA), and cyclic olefin copolymer (COC). Additionally, the all-iCVD nanoadhesive bonding process displays high resistance against hydrolytic degradation (>2 weeks). Within the channels of the bonded devices, the epoxy and amine groups remain available for subsequent functionalization. This nanoadhesive bonding technique has successfully been applied to two applications. One is for growth of E. coli in the iCVD-bonded chips, which is in collaboration with Kevin Lee in Professor Rajeev Ram's group. The bonded device was hydrolytically stable for >1 week and *E. coli* grew over the entire period. Another application is to fabricate gas impermeable microchannels for microparticle synthesis from organic solvents, in collaboration with Ki Wan Bong in Professor Patrick Doyle's group. The gas permeation decreased with an increase of coating thicknesses for both applications.

3.1. Introduction

Microelectromechanical systems (MEMS) fabrication generally utilizes three classes of materials. The first is made of those commonly used in microelectronics, such as silicon and glass. MEMS technology has traditionally been focused on silicon-based fabrication techniques, taking advantage of decades of fabrication technology from the semiconductor industry.[1] The second class is made up of biological materials and entities such as proteins and tissues. Over the past few years, the MEMS field has gradually extended the range of substrates used in order to broaden the potential application of MEMS devices. Polymers are of particular interest due to their unique and diverse properties. They have great potential as materials because they can be obtained at lower costs and allow greater ease in fabrication,[2] they provide the ability to integrate functional hydrogel materials,[3] and most importantly they reduce the undesirable swelling in organic solvents when compared with polydimethylsiloxane (PDMS), a widely used substrate material in MEMS.

Despite these advantages, bonding these soft polymers to each other is very difficult and therefore researchers are restricted in their choice of substrate material.[4] Conventional sealing requires any functionalization process to be completed before the microchip can be sealed. Chen et al. applied chemical vapor deposition to previously assembled microfluidic devices and successfully deposited reactive coatings within confined microgeometries.[5] Despite this result, the process likely cannot be applied to complex microgeometries and they give no evidence that the coating inside the microchannel is conformal, which may introduce difficulties such as functional group density variations and channel clogging. Recently they developed

a solventless adhesive bonding (SAB) technique using reactive coatings, which can be applied to substrate materials other than PDMS.[6] Bonding is achieved through the reaction of the aldehyde and amine functional groups present in poly(4-formyl-p-xylylene-co-p-xylylene) and poly(4-aminomethyl-p-xylylene-co-p-xylylene). However the formation of the covalent tethers between the complementary surfaces produces a gaseous byproduct, which could result in surface defect and lower bond strength. In addition, the curing temperature for the reaction is 140°C, which is higher than the glass transition temperature of some polymeric substrates.

A novel method has recently been developed by Im et al.[7] The bonding was achieved by putting a pre-patterned surface with iCVD-deposited poly(glycidyl methacrylate) (PGMA) into contact with a flat PDMS with plasma-polymerized poly(allylamine) (PAAm), followed by curing at 70°C. The sealed device is able to withstand pressures as high as 50 psia under dry conditions. Compared with Im's work, this process applied the iCVD method to both the substrate and the cover plate, which enables good conformality inside the microchannel. Avoiding exposure of the substrates to plasma will prevent plasma damage of the substrate and also create a higher density of amine functional groups, resulting in stronger bonding. In this work, bond strength in aqueous environments was also investigated.

A nanoadhesive bonding technique has been developed via a ring-opening curing reaction between amine groups from iCVD poly(4-aminostyrene) (PAS) and epoxy groups from PGMA. It has several advantages over conventional binding techniques. Direct bonding and anodic bonding can achieve high bonding strength, but those techniques require high bonding temperatures and have the potential to damage surface functionality. However, with a process temperature of 50°C, this problem can be avoided. In addition, well-controlled thin conformal coatings can be

51

achieved via iCVD, which prevents the blockage of the microfluidic channel. This bonding process involves a relatively fast reaction rate at low temperatures and can be applied to many different types of polymer substrates, making it a general bonding method for fabrication of microfluidic devices. Furthermore, the deposited samples are stable under dry conditions and can be stored for more than 2 months prior to bonding. This process is advantageous over the conventional oxygen plasma sealing technique where immediate bonding is needed. More importantly, all four walls of the microchannel will have reactive coatings. The coatings serve as diffusion barrier layers for gas permeation and protective layers against solvent swelling. Moreover, the reactive amine and epoxy functional groups can be used for post bonding functionalization.

This nanoadhesive bonding technique has successfully been applied to two applications. One is for growth of *E. coli* in the iCVD-bonded chips, and another is to fabricate gas impermeable microchannels for microparticle synthesis from organic solvents.

3.2. Experimental

3.2.1. Bonding of Prototype Microfluidic Devices and Bond Strength Test

Linear microfluidic channels of 400 μm wide and 150 μm high were prepared in PDMS by standard soft lithographic techniques.[8] After curing at 80 °C for 2 hours, the PDMS mold with a thickness of 5 mm was peeled off the master. Fluid injection reservoirs were punched before the iCVD deposition.

Figure 3-1 shows a detailed bonding fabrication process. Oxygen plasma was applied to the substrates (0.5-1 min), both for cleaning and surface activation to enhance surface energy for better adhesion. PGMA and PAS films were deposited on

flat and patterned substrates via iCVD respectively. After placing the two substrates face-to-face, ring opening curing reaction between epoxy and amine groups, microfluidic devices with good sealing can be fabricated. Curing time was intentionally prolonged to 24 hours to ensure bond formation. It is important to note here that no additional high-pressure load is needed for the bonding process and the bonding temperature is much lower than the glass-transition temperature (T_g) of these polymeric substrates.
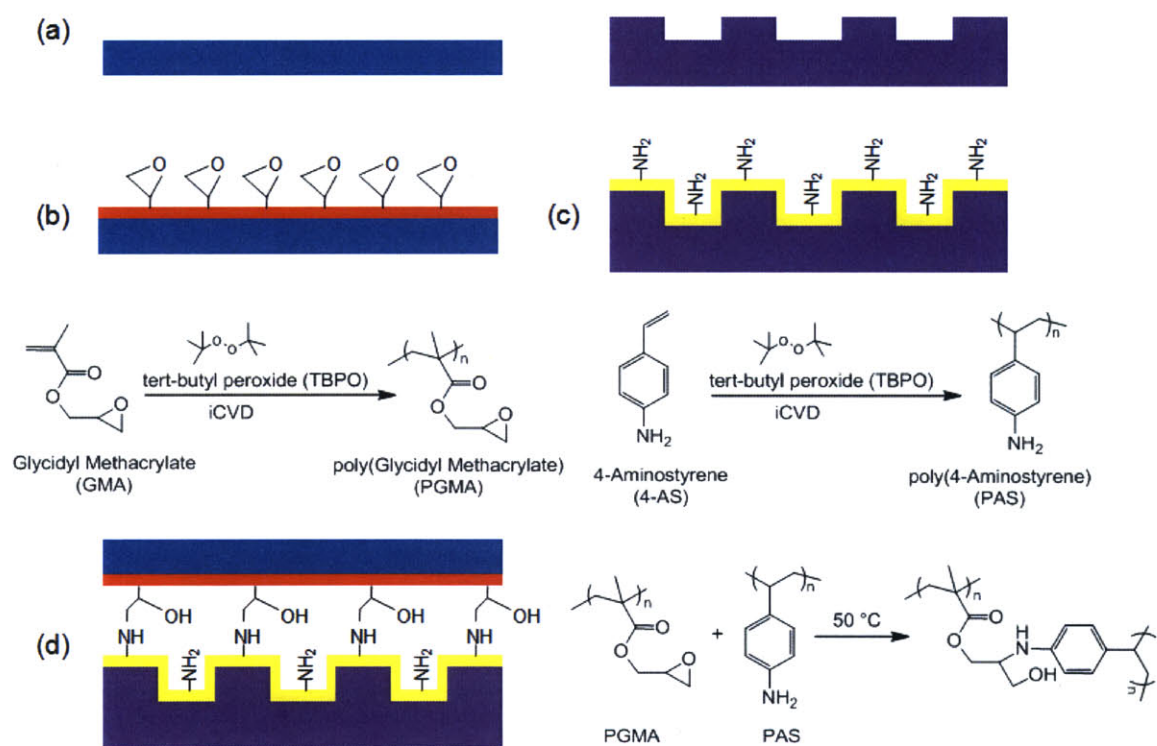
Figure 3-1. Adhesive bonding process. (a) Substrate cleaning by oxygen plasma for 0.5-1 min (b) iCVD deposition of Glycidyl Methacrylate (c) iCVD deposition 4-Aminostyrene (d) Adhesive layer curing at 50 °C for 24 hours.

Burst pressure testing was performed to measure the bond strength. Epoxy adhesives (Cotronics Corp) were used to glue the 1/16" OD capillary PEEK tubing

(IDEX Health & Science) and the inlet on the PDMS. A pressure gauge tee connected the testing device to a syringe pump.

Bonded devices with flat PDMS and pre-patterned PC substrates were used for the hydrolytic resistance test.

3.2.2. Fabrication of Bioreactors Made from Polycarbonate Plastics for Cell growth

The bioreactor chips were designed and provided by Kevin Lee in Professor Rajeev Ram's group from the electrical engineering department. The reactor must be fabricated out of a rigid clear material and an elastic membrane in order to meet the design requirement, therefore rigid polycarbonate (PC) substrates and PDMS membranes were selected as the materials. Figure 3-2 shows the illustration of the complete device, including fluid inputs, outputs, on-chip reservoirs, premixer, growth chamber, and valves.[9]
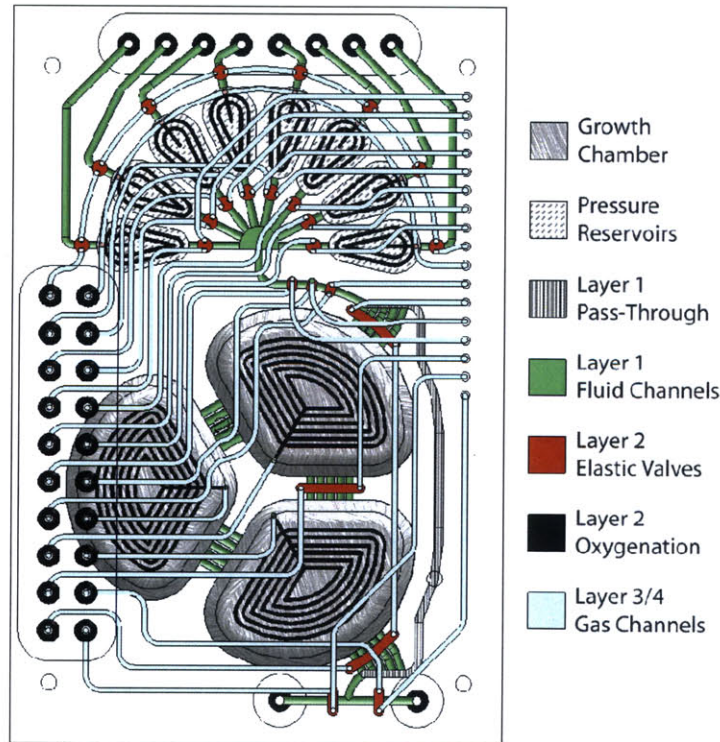
Figure 3-2. Schematic of the bioreactor design.[9]

PDMS membranes are made by spin-coating PDMS (10:1 Sylgard 184) onto flexible PC substrates. Their thicknesses are monitored in real time using an interferometer, to achieve thicknesses close to 70 μm. The membranes are then baked at 70 °C in a oven until fully cured.

PAS film was deposited on the PC chips and PGMA film was deposited on both sides of the PDMS membrane via iCVD, respectively. The PDMS membrane was placed between the PC substrates and device with good sealing was fabricated. Curing occurred at 50 °C and the curing time was intentionally prolonged to 24 hours to ensure good bond formation.

A continuous culture growth using *E. coli* FB 21591 was performed with the bonded bioreactor. Growth media consisted of LB media with an additional 5 g/L of glucose and 100 μg/mL of Kanamycin antibiotic.

3.2.3. Microparticle Synthesis in Gas Impermeable Channels

Homogenous gas impermeable microchannels were fabricated for the first time, using the developed nanoadhesive iCVD bonding technique. The fabrication process is shown in Figure 3-3. NOA81 (Norland Optical Adhesive) was casted on a SU-8 master, and then covered with a glass substrate. After cured under the UV-lamp for 10 min and unmolding, a thin film of NOA81 was mounted on the glass substrate. A blank PDMS with reservoirs was treated with oxygen plasma for 30s, and then followed by treatment with tricholorvinylsilane (Aldrich, 98%) under vacuum for 5 min. NOA 81 was casted on the SU-8 master again and then covered with the silane-treated PDMS. After UV curing for 10 min and unmolding, a thin film of NOA81with pre-patterned channels was covalently mounted on the PDMS substrates. PAS and PGMA films were deposited on the glass and PDMS substrates via iCVD,

respectively. After placing the two substrates face-to-face, ring opening curing reaction between epoxy and amine groups, microfluidic devices with good sealing can be fabricated. Again, curing time was intentionally prolonged to 24 hours to ensure bond formation.
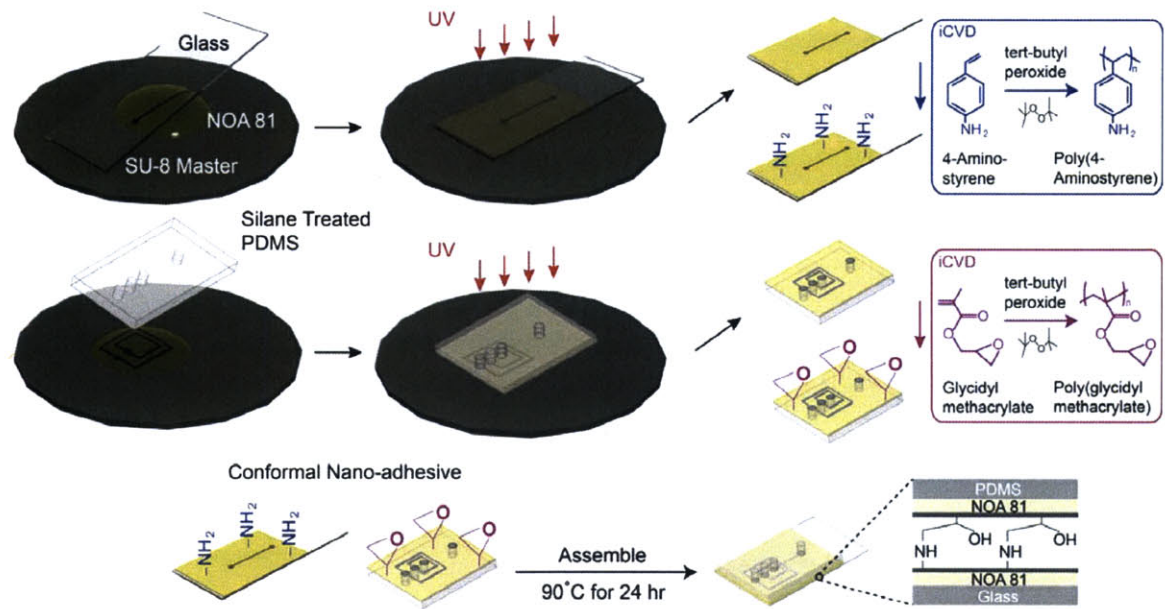
Figure 3-3. Fabrication process of gas impermeable channels.

In collaboration with Ki Wan Bong in Professor Patrick Doyle's group in the chemical engineering department, continuous-flow lithography (CFL) is used for the microparticle synthesis.[10]

3.3. Results and Discussion

3.3.1. Adhesive Bonding and Bond Strength of Sealed Microfluidic Devices

Adhesive bonding utilizing the iCVD amine functional polymer enabled strong, hydrolytically stable bonding with simultaneous formation of reactive coatings within the microfluidic channels. Si wafers, PC, glass, PET, PE, PA, and COC

polymeric substrates were successfully bonded to PDMS and the burst pressures were recorded in Table 3-1. There was no water leakage for the bonded devices under the pressure of 150 psi, when the glue used to seal the devices failed before the bond itself. This pressure exceeds the requirements for many microfluidic applications.[11,12] Furthermore, it is an addition reaction with no gaseous byproducts which must diffuse away from the bonded area. In conventional bonding reactions, water must outgas, possibly leading to leakage in the bonded substrates.

Table 3-1. Burst pressure of microfluidic devices bonded with various kinds of substrate materials.

Material	Burst Pressure
PDMS–Si	> 150 psi
PDMS–PC	> 150 psi
PDMS–glass	> 150 psi
PDMS–PET	> 150 psi
PDMS–PA	> 150 psi
PDMS–COC	> 150 psi

3.3.2. Hydrolytic Resistance

To test hydrolytic stability, blister test structure was used as shown in Figure 3-4a. PC-PDMS-PC substrates were bonded together utilizing the bonding technique mentioned above. PGMA was deposited on both sides of PDMS and PAS was deposited on the PC substrates. The well on the top PC substrate was used to store water, which would penetrate through the PDMS. In the blister test, argon flowed into the bottom PC through a needle, which was connected to polyester tubing by a universal barbed coupler (1/8", McMaster).
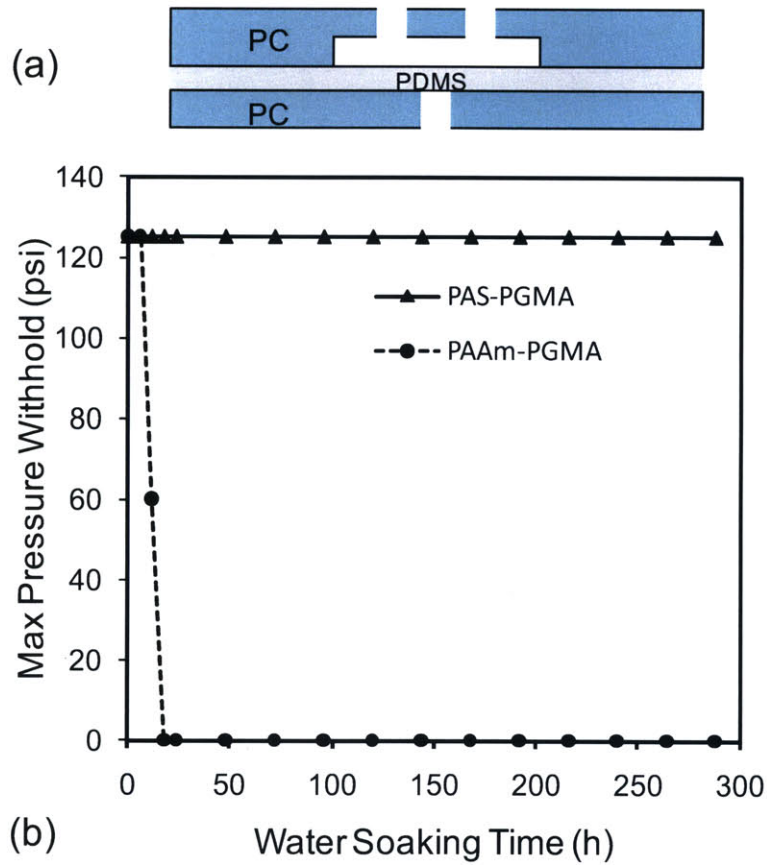
Figure 3-4. Hydrolytic resistance study. (a) Schematic of a PC-PDMS-PC structure used in the blister test (b) plot of the channel maximum pressure versus water soaking time. Dotted line shows a markedly bond strength decrease in devices utilized PAAm-PGMA chemistry. The bond starts to degrade after 6 hours and completely fails after 18 hours. The solid line represents bond strength for devices utilized PAS-PGMA chemistry. It remains almost unaffected even after 2 weeks.

The highest channel pressure reported in Figure 3-4b (125 psi) is due to the maximum operation pressure of the barbed coupler used in the blister test. As shown in the figure, devices utilized PAAm-PGMA chemistry showed bond strength degradation after 6 hours in aqueous environment and it markedly decreases with the hydrolysis time. The device completely failed after 18 hrs soaking time with water, whereas those fabricated by iCVD films remains almost unaffected even after 2 weeks. Hydrolytic resistance relates to the hydrolytic stability of individual groups presented, steric hindrance and also the hydrophilicity of backbones.[13] The stable three-dimensional molecular structure of PAS provides a good steric barrier for water molecules to access, therefore the devices utilized PAS-PGMA chemistry is much more hydrolytic stable. Hydrolytic stability is very important in microfluidic devices, especially for biological application. It usually takes days for the cell culture growth. Even for fast-dividing mammalian cells, the length of the cycle is approximately 24 hours. Bonding with long term hydrolytic stability is critical in microfluidic devices fabrication.

3.3.3. Growth of E. coli in iCVD Bonded Bioreactor

The bonded bioreactor is shown in Figure 3-5, which contains a 1 mL growth chamber, peristaltic pump, and 8 fluid inputs. Two of the three chamber sections were filled up and by deflating individual sections in sequence, the liquid was mixed simultaneously and oxygenated by the PDMS membrane from above.
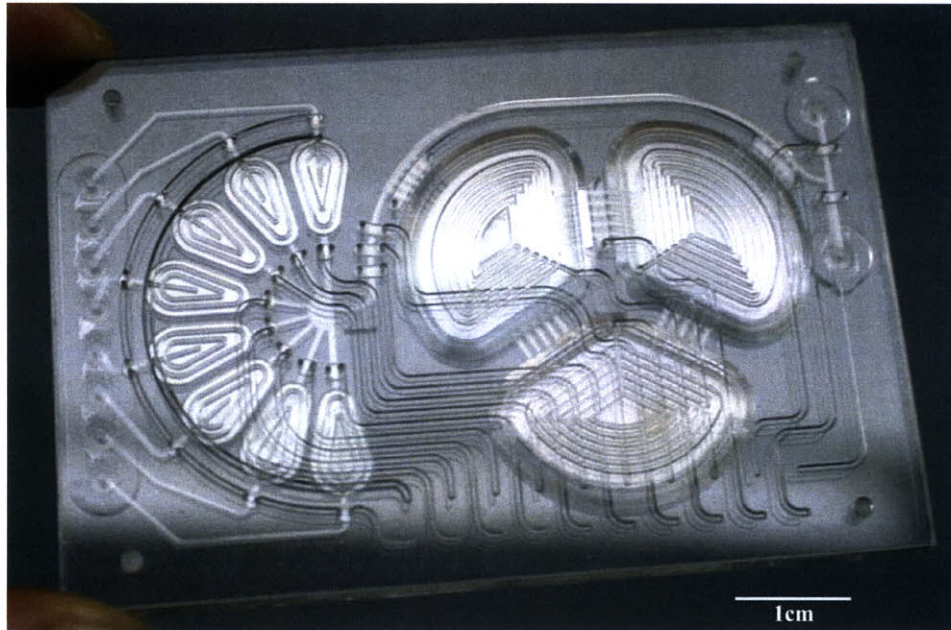
Figure 3-5. iCVD bonded chips for E. coli growth.

A continuous culture growth using *E. coli* FB 21591 was performed in the bonded bioreactor. The device was hydrolytically stable for more than one week and has been successfully used for the *E. coli* growth. The growth date is shown in Figure 3-6. The plot displays an initial lag phase due to cell adjustment to a new environment (t<2.5h), a log phase (2.5h<t<12h) and a stationary phase (t>12h) due to the loss of nutrients or accumulation of waste. As nutrients are depleted, oxygen transfer rates become insufficient and the cell growth rate starts to diminish, which leads to the stationary phase.
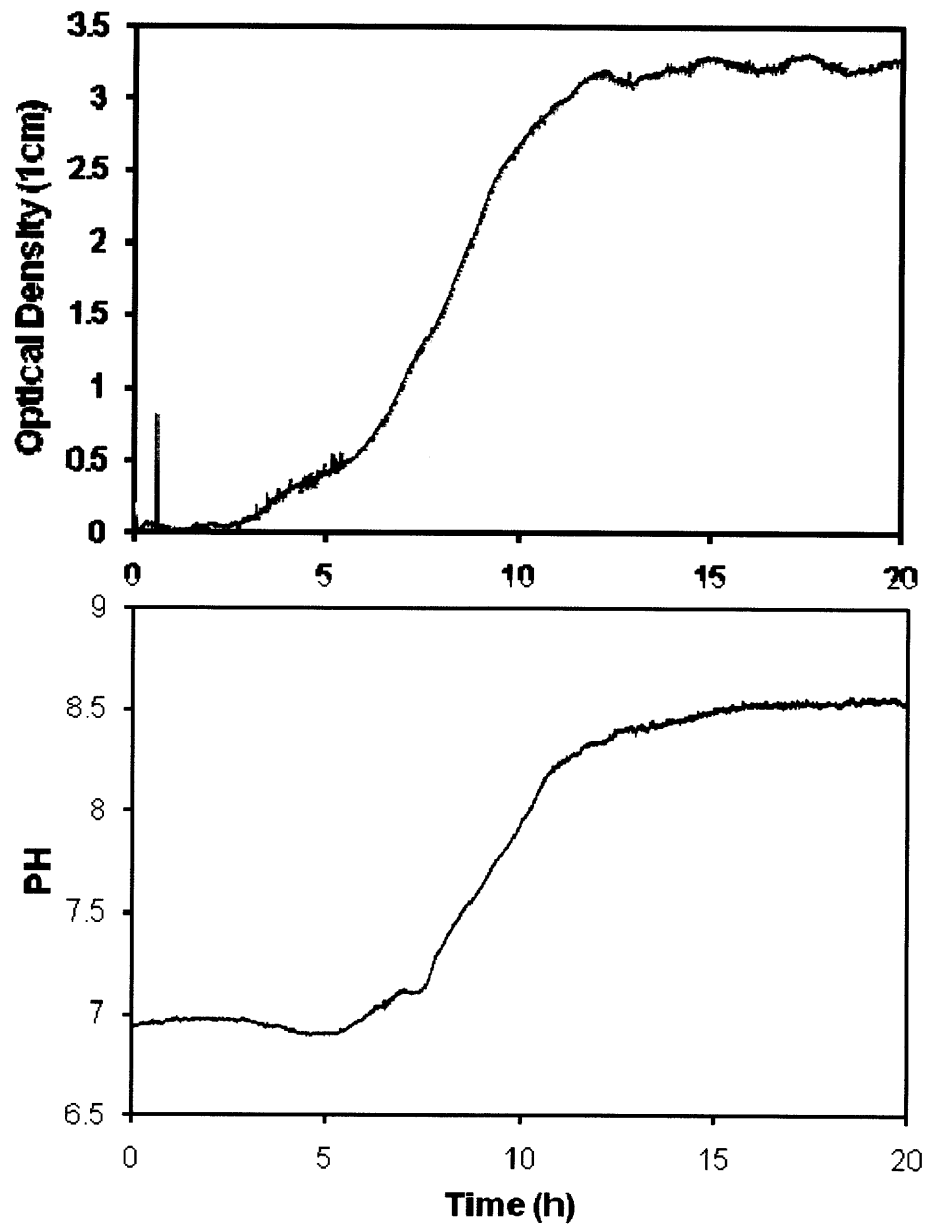
Figure 3-6. Growth curve for the culture experiment grown with E. coli FB 21591.

Oxygen concentration was measured in situ by the oxygen sensor glued inside the growth chamber. It is found that the coating thickness has an effect on the oxygen diffusion rate through the PDMS membrane (Figure 3-7). By decreasing the thickness of PGMA films on the PDMS membrane from 300 nm to 100 nm, the oxygen concentration is increased by a factor of two and has the potential to be further improved by depositing a thinner film.
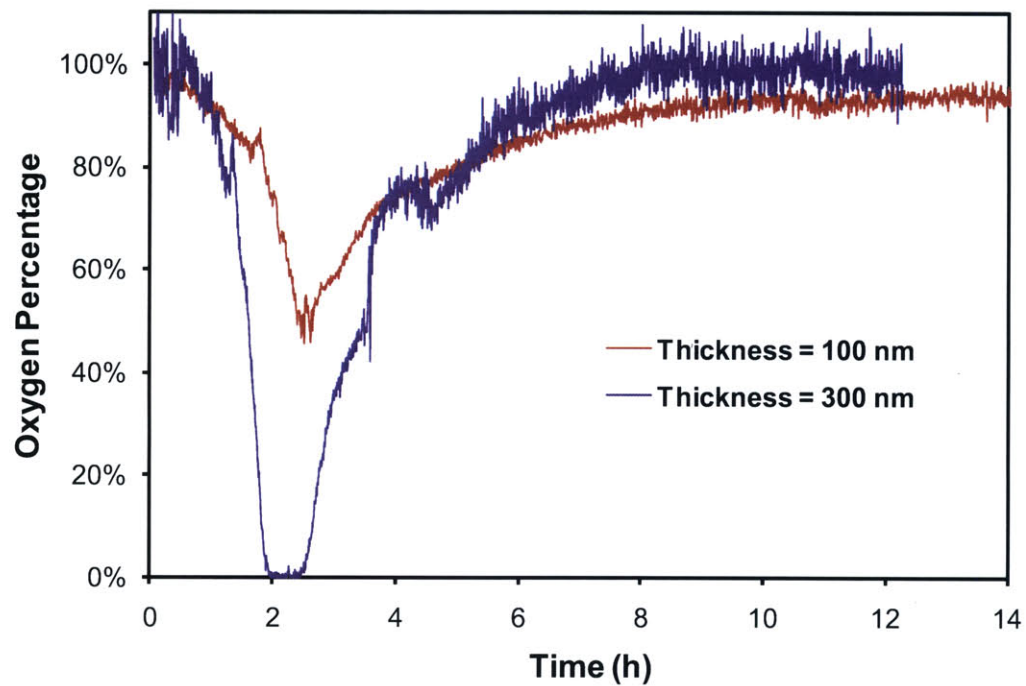
Figure 3-7. Effect of coating thickness on the oxygen concentration for the growth of E. coli FB 21591.

The oxygen permeation rates of PGMA deposited PDMS membranes were investigated (Figure 3-8). The oxygen permeation rate for a 300 nm PGMA coated PDMS is ~80% of a blank PDMS, however, with a coating thickness of 50 nm, the oxygen permeation rate is >95% of an uncoated PDMS membrane. This confirms the hypothesis that by decreasing the PGMA coating thickness on the PDMS membrane, the oxygen diffusion rate can be increased. It is important to note that the device was successfully sealed even with the PGMA coating thickness of 50 nm.
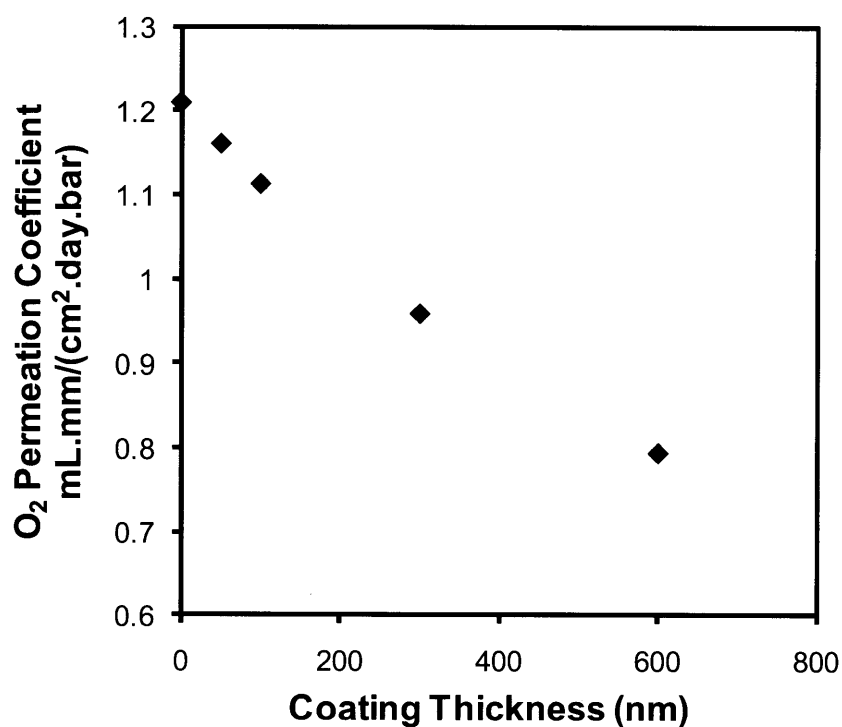
Figure 3-8. Effect of coating thickness on the oxygen permeation coefficient of poly(glycidyl methacrylate) (PGMA) deposited PDMS membranes.

3.3.4. Device fabrication for Microparticle synthesis

PDMS has been one of the most well developed polymers for microfluidics.[8] Fabrication of PDMS channels is rapid and particularly straightforward. Due to low surface free energy, its replicas can be released easily from molds. In addition, it has advantages of low cost, nontoxicity, and favorable chemical and mechanical properties. But one major drawback that limits the wider application of PDMS is its permeability to liquids and gases. Organic solvents can swell PDMS significantly and therefore the use of PDMS devices is limited to aqueous solutions. This difficulty motivated development of other materials that combine simplicity of fabrication with chemical robustness.

In Professor Doyle's group, microparticle synthesis has mainly utilized PDMS channels and therefore is limited to aqueous solutions. The UV-curable adhesive NOA81 is a promising liquid photopolymer for low-cost microfluidic chip production and is of great interest because it has better chemical resistance to organic solvents. Figure 3-9a and Figure 3-9b show the toluene resistance of PDMS and NOA81 channels. Clearly, PDMS has poor solvent resistance and shrinks dramatically after flowing through toluene for 5 min, whereas the NOA81 channels stay intact. Homogenous gas impermeable microchannels were fabricated using the developed iCVD nanoadhesive technique (Figure 3-9c). The channels display great toluene resistance, as shown in Figure 3-9d.
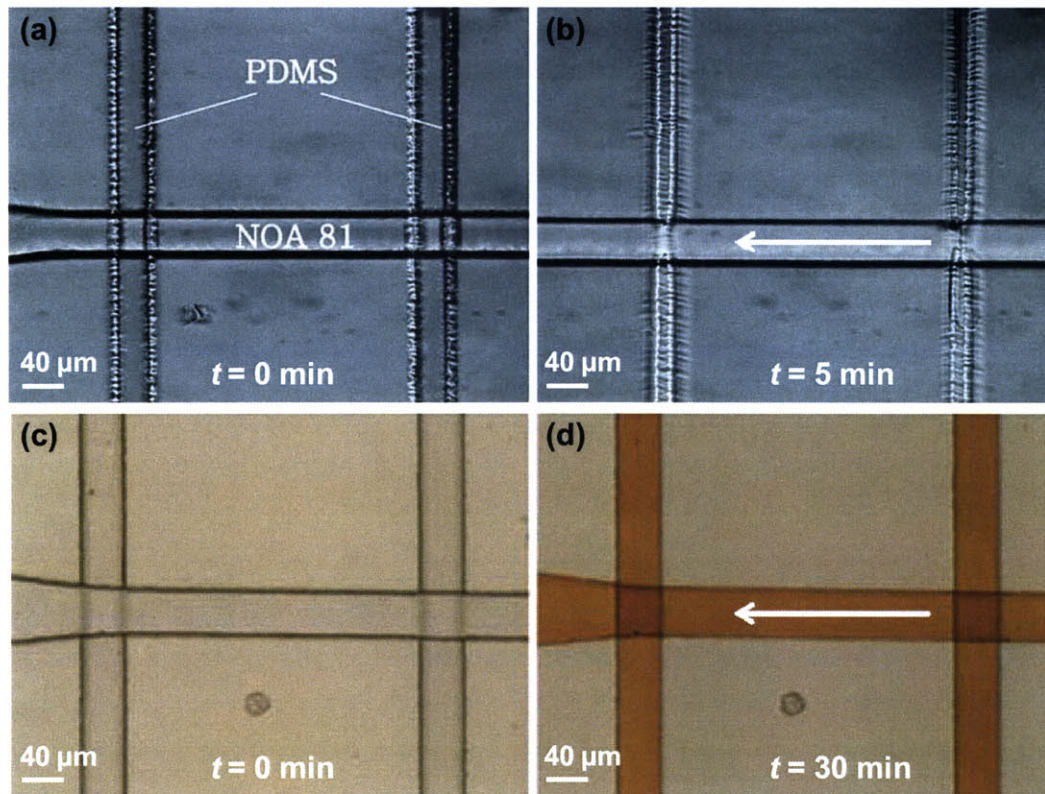
Figure 3-9. Organic solvent resistance. Bonded microfluidic devices with NOA81 and PDMS channels (a) before toluene flow and (b) after flowing toluene for 5 min. Bonded microfluidic devices with homogeneous NOA81 channels (c) before toluene flow and (d) after flowing toluene for 30 min.

In the PDMS microchannels, oxygen is able to inhibit free radical photopolymerization reactions by reacting with radical species to form chain terminating peroxide molecules[10], however, the homogenous NOA81 microchannels are impermeable to oxygen. Figure 3-10a shows a modified microparticle synthesis scheme in iCVD-bonded NOA81 microchannels.[14] Three flow streams, two of which are inert flows, pass across the NOA81 channels. Polymerization was carried out across the mid-region laminar flow to generate particles (Figure 3-10b). By varying the flow rates of the two inert flows, particle height can also be controlled (Figure 3-10c).

NOA81

inert flow

inert flow

(a)

Top   Side

50 μm   20 μm

(b)

$H_P \sim 36\ \mu m$ $H_P \sim 20\ \mu m$

50 μm

(c)
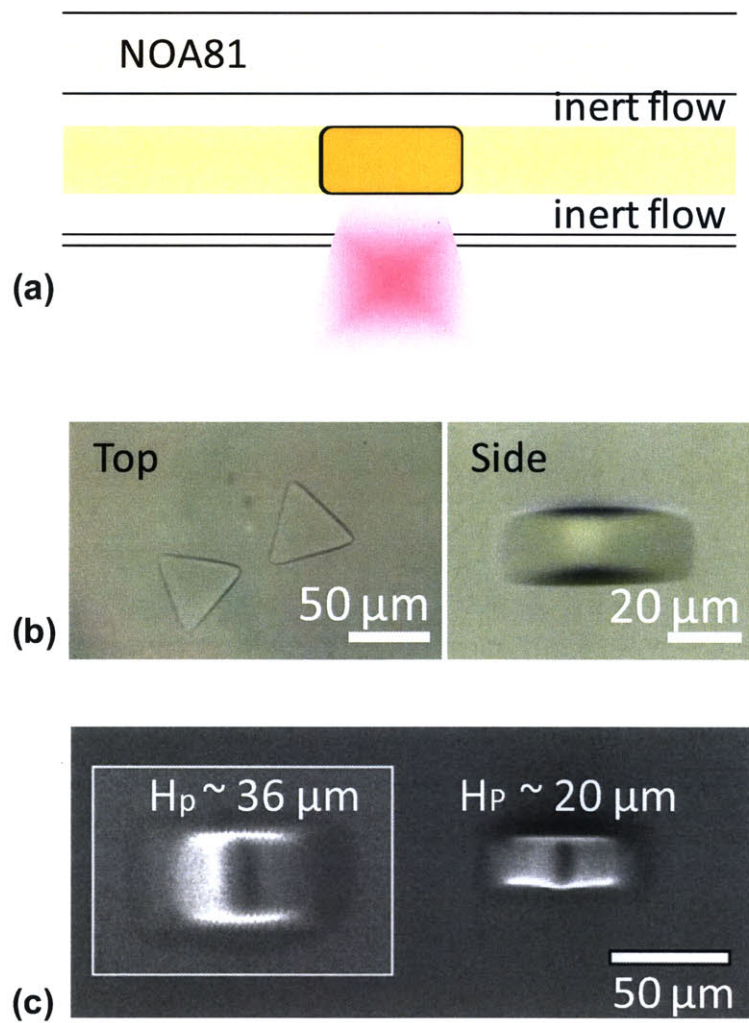
Figure 3-10. (a) Schematic of microparticle synthesis in homogeneous NOA81 microchannels using hydrodynamic focusing lithography. (b) Synthesized microparticles from top and side views. (c) Particles with controllable height synthesized in the iCVD-bonded microfluidic device.

The ability to synthesis particles in gas impermeable microchannels is of great importance because it expands the applicability of flow lithography to new types of monomers that can only be dissolved in organic solvents. One example to utilize this new microparticle synthesis method is shown in Figure 3-11. Ruthenium encapsulated microparticles have successfully been synthesized using a mixture of polyethylene glycol diacrylate (PEGDA), photoinitiator, accelerator, and Ruthenium, dissolved in toluene and methanol. The fluorescence of the Ruthenium complexes can be quenched by oxygen, which has led to their use as optode sensors for oxygen.[15]
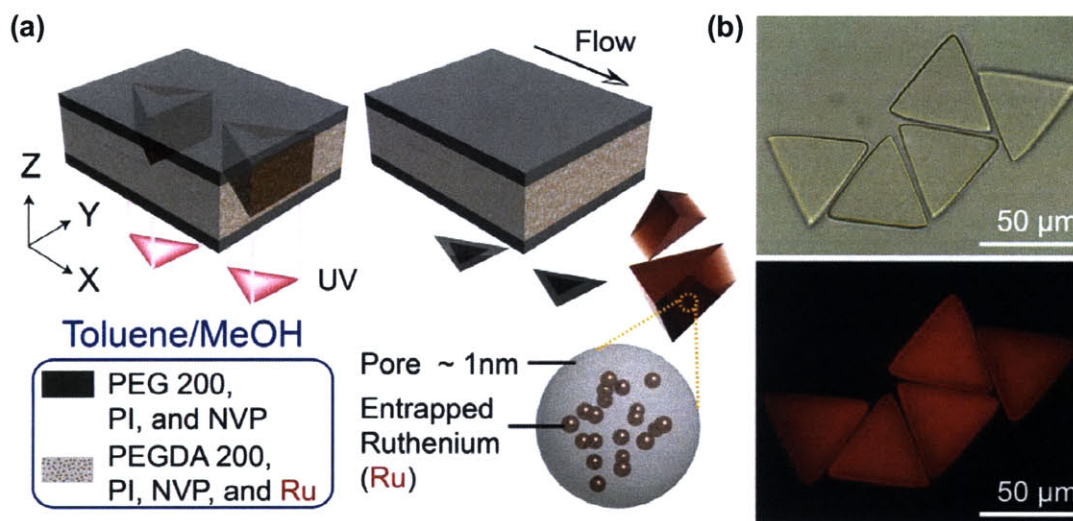
Figure 3-11. (a) Schematic of Ruthenium encapsulated microparticle synthesis from organic solvents. (b) Optical and fluorescence micrographs of synthesized Ruthenium encapsulated microparticles.

3.4. Conclusion

Si wafers, PC, glass, PET, PE, PA, and COC polymeric substrates were successfully bonded to PDMS and the fabricated devices can withstand pressure >150 psi. Sealing was achieved by contacting iCVD PGMA coated flat substrate and PAS coated pre-patterned surfaces and curing at 50 °C for 24 hours. The devices have conformal NH_2-functionalized coatings inside the microchannels, which prevent channel clogging and also enable the immobilization of biomolecules. Photoluminescence confirms that the reactive amine functional group density of iCVD PAS is ~ one order of magnitude higher than for films grown by PECVD, which results in a possibly stronger bonding. Furthermore, the device is hydrolytically stable for more than 2 weeks, whereas devices utilized PECVD PAAm-PGMA chemistry showed bond strength degradation after 6 hours in aqueous environment and complete device failure after 18 hours.

This nanoadhesive bonding technique has successfully been applied to two applications. One application is for the growth of *E. coli* in an iCVD-bonded bioreactor. The chips made of rigid polycarbonate plastics with a PDMS membrane in between. The bonded device was hydrolytically stable for >1 week and *E. coli* grew over the entire period. Oxygen permeability measurements show the coating thickness has a significant effect on the oxygen permeation rates of the PDMS membranes. However, with a coating thickness of 50 nm, the oxygen permeation rate is ~95% of an uncoated PDMS membrane, but still enables device fabrication with sufficient bond strength. Another application is to synthesize complex microparticles in gas impermeable channels from organic solvents. Homogeneous NOA81 gas impermeable channels are fabricated. They show great organic solvent resistance and

high bond strength. Microparticles have successfully been synthesized from monomers dissolved in organic solvents and their height can be controlled by varying the flow rates of two inert flows.

Acknowledgements

References

(1)   Wise, K. D.; Najafi, K. *Science* **1991**, *254*, 1335-1342.

(2)   Xia, Y. N.; Whitesides, G. M. *Annual Review of Materials Science* **1998**, *28*, 153-184.

(3)   Ziaie, B.; Baldi, A.; Lei, M.; Gu, Y. D.; Siegel, R. A. *Advanced Drug Delivery Reviews* **2004**, *56*, 145-172.

(4)   Wu, H. K.; Huang, B.; Zare, R. N. *Lab on a Chip* **2005**, *5*, 1393-1398.

(5)   Chen, H. Y.; Elkasabi, Y.; Lahann, J. *Journal of the American Chemical Society* **2006**, *128*, 374-380.

(6)   Chen, H. Y.; McClelland, A. A.; Chen, Z.; Lahann, J. *Analytical Chemistry* **2008**, *80*, 4119-4124.

(7)   Im, S. G.; Bong, K. W.; Lee, C. H.; Doyle, P. S.; Gleason, K. K. *Lab on a Chip* **2009**, *9*, 411-416.

(8)   McDonald, J. C.; Whitesides, G. M. *Accounts of Chemical Research* **2002**, *35*, 491-499.

(9)   Lee, K. S., Massachusetts Institute of Technology, 2011.

(10)   Dendukuri, D.; Pregibon, D. C.; Collins, J.; Hatton, T. A.; Doyle, P. S. *Nature Materials* **2006**, *5*, 365-369.

(11)   Lin, C. F.; Lee, G. B.; Wang, C. H.; Lee, H. H.; Liao, W. Y.; Chou, T. C. *Biosensors & Bioelectronics* **2006**, *21*, 1468-1475.

(12)   Kobayashi, J.; Mori, Y.; Okamoto, K.; Akiyama, R.; Ueno, M.; Kitamori, T.; Kobayashi, S. *Science* **2004**, *304*, 1305-1308.

(13)   Pegoretti, A.; Fambri, L.; Penati, A.; Kolarik, J. *Journal of Applied Polymer Science* **1998**, *70*, 577-586.

(14)   Bong, K. W.; Bong, K. T.; Pregibon, D. C.; Doyle, P. S. *Angewandte Chemie-International Edition* **2010**, *49*, 87-90.

(15)   Klimant, I.; Wolfbeis, O. S. *Analytical Chemistry* **1995**, *67*, 3160-3166.

CHAPTER FOUR

The Design and Synthesis of Hard and
Impermeable, yet Flexible, Conformal
Organic Coatings

Abstract

Owing to the structural constraints imposed by their covalent bonding networks, inorganic materials are typically hard and impermeable, but relatively brittle. On the other hand, organic materials are often flexible, but are relatively soft and permeable. Here we design, synthesize, and characterize a conformal organic coating which is hard and impermeable, yet remains flexible. First, initiated chemical vapor deposition (iCVD) is used to synthesize a novel alternating copolymer thin film from maleic anhydride and aminostyrene. Upon annealing at 100 °C, the functional groups of the two monomers react, resulting in extensive cross-linking. The annealed copolymer films display an elastic modulus exceeding 20 GPa, far greater than typical polymers (0.5~5 GPa). The scratch resistance improves dramatically after annealing and the scratch depth decreases from 48 nm to 6nm. Moreover, the cross-linked films maintain their flexibility, neither cracking nor delaminating with repeated flexing. This achievement represents a significant advance in the fabrication of tough, durable, conformal, functional coatings. Furthermore, the highly crosslinked coating material has oxygen permeability lower than leading commercially available permeation barrier films, making it an attractive material for electronics or food industries.

4.1. Introduction

Organic polymers and inorganic materials are typically prized for different characteristics. While, organic polymers are generally more flexible, inorganics commonly have far higher values of modulus and hardness, and also display greater scratch and abrasion resistance.[1,2] Additionally, while organic polymers often display high values of gas permeability, many different inorganics act as barriers against the transmission of species like oxygen gas and water vapor. Inorganics lack organic functional groups that provide access to a rich array of chemical modification capabilities, which is highly desirable for tuning surface energy (e.g. hydrophilic, hydrophobic), for enabling subsequent chemical attachment of molecules (e.g. chemical dyes, growth factors, antibodies), and for covalently binding micro- or nanoparticles to the surface.[3-5] Hybrid materials, which combine organic and inorganic elements, are widely used to prepare tough and durable coatings. Sol-gel process is known to be one of the practical methods for preparing organic-inorganic hybrid materials from alkoxysilanes.[6] As a wet-chemistry based method, it cannot be applied to substrates that swell or dissolve upon exposure to solvents. It also normally does not exhibit good conformality due to surface tension effects. Increasing the number of crosslinks between the inorganic and organic phases increases the young's modulus but decreases the flexibility.[7] Young's moduli (6 to 8.7 GPa) have been determined for organic-inorganic hybrid nanocomposites prepared by sol-gel condensation of bismethacrylatesilanes.[8]

Increasing Young's modulus and hardness improves durability of coatings and their capacity to protect the underlying substrate. Reducing gas permeability is of value for creating barrier layers suitable for electronics packaging, food or flat panel

display industries. For such practical applications, the substrates are often non-planar, making it highly desirable to produce protective coating layers which conform to the overall geometry and features of the substrate.[9-11] In this current work, we seek to demonstrate a new materials design paradigm to achieve conformal, all-organic coatings that retain their flexibility and functional group chemistry while simultaneously displaying properties more typically associated with inorganics, including mechanical hardness and barrier properties.

The differences in the mechanical characteristics and permeation capabilities of organic and inorganic materials arise in part from the underlying architecture of the respective covalent bonding structures. The concept of percolation of rigidity was first developed by Philips.[12] It defines a compositional transition point from an underconstrained (nonrigid) state to a constrained (rigid) one. Systems above the percolation threshold are expected to have superior modulus and hardness to the ones below the threshold, but less flexible, due to the increased structural constraints. The key parameter in this analysis is the average connectivity number, r, which is the average number of network forming bonds per network atom.[13] Higher r values reflect the additional constraints that covalent bonds impose on the possible positions and momentum vectors for each atom in the network.

To be constrained by the network structure, an atom must have two or more bonds to other atoms in the network. Consider the example of polyethylene [(-CH2-)$_n$]. The hydrogen atoms have only one bond and thus are not network atoms. In contrast, the carbon is indeed a network atom because it is bonded to two other carbon atoms. Thus, for polyethylene, $r=2$, because the only network atom is carbon and each carbon has two carbon-carbon bonds. Crosslinking the polymers chains increases r. Indeed, traditional crosslinking methods have demonstrated ability to improve the

elastic modulus of polymeric materials up into the 5 to 8 GPa range.[14] The inorganic materials are typically described by three dimensional unit cells, corresponding to r>2. For example, consider silicon dioxide (SiO2), where the silicon forms four network bonds, while both oxygen atoms participate in two network forming bonds. For the unit cell, this gives a total of 8 network forming covalent bonds by 3 network atoms, for a r=8/3=2.67.

Dohler et al. determined that for amorphous solids the percolation of rigidity occurs at r=2.4.[15] Below this value, the low degree constraints allow the material to be flexible. Above the percolation value, the constraints result in rigid structures. The percolation of rigidity analysis has been successful in explaining observed trends in the mechanical properties for hydrogenated amorphous silicon[16], crosslinked fluoropolymers[14], hybrid glasses[17], polyethylene composites[18], and organosilicate glasses[19].

In this work, we seek to use the percolation of rigidity as a design principle to guide the synthesis of an all-organic conformal coating which provides high modulus and hardness simultaneously with flexibility. As a fully cross-linked structure, the value of r should closely approach, but not exceed the percolation of rigidity value of 2.4. To achieve conformal organic coatings, we will utilize the method of initiated chemical vapor deposition (iCVD), which involves the delivery of vapor-phase monomers to form chemically well-defined polymer films with tunable conformality and properties.[20,21] The iCVD method is chemically analogous to solution phase polymerization, but possesses a number of practical advantages. It is able to deposit conformal and pinhole-free coatings on non-planar substrates with nanometer level thickness control. In addition, elimination of solvent usage makes the iCVD method compatible with a wide range of substrate materials which swell or

dissolve in solution. Furthermore, as a low-energy vapor deposition process, the iCVD process is able to maintain the functionalities from the monomers, which is crucial for subsequent functionalization.

4.2. Experimental

All iCVD films were deposited in a custom built vacuum reactor, as previously described.[22] Thermal excitation was provided by heating a nichrome filament (80% Ni/ 20% Cr) mounted in a parallel array and the temperature was measured by a thermal couple attached to one of the filaments. The filament holder straddled the deposition stage maintained at a set point temperature using water cooling. The vertical distance between the filament and the stage was 2 cm. A butterfly-type throttling valve (Type 652B, MKS) was used to maintain the pressure. All the chemicals were used as purchased without further purification. Tert-butyl peroxide (Aldrich, 97%) initiator, at room temperature, was fed to the reactor through a mass flow controller (model 1179A, MKS) at 0.85 sccm. 4-Aminostyrene (4-AS) (Aldrich, 97%) monomer, heated to 85±3 °C in a glass jar, was delivered into the reactor at controlled flow rates via a different port. Maleic Anhydride (Ma) (Aldrich, 99%) was heated to 85 °C in a glass jar and then metered into the reactor through a mass flow controller (model 1152C, MKS). Films were deposited at a filament temperature of 260 °C and a stage temperature of 50 °C. A nitrogen (ultrahigh purity, Airgas) patch flow was used to maintain the total flow rate at 6 sccm. The total pressure in the vacuum chamber was maintained at 0.9 Torr for all the depositions. iCVD deposition conditions utilizing the monomer 4-Aminostyrene (Aldrich, 97%) were adopted from previous work.[23] Film growth on the Si substrate was monitored in situ through laser interferometry and controlled to a thickness of one micron for the

mechanical property analysis and 200-250 nm for all other characterizations. A more accurate film thickness on the Si wafer substrates was measured post-deposition by a J.A. Woollam M-2000 spectroscopic ellipsometry at a 70 ° incidence angle using 190 wavelengths from 315 to 718 nm.

Fourier transform infrared (FTIR) measurements were performed on a Nicolet Nexus 870 ESP spectrometer in normal transmission mode. A deuterated triglycine sulfate (DTGS) KBr detector over the range of 400-4000 cm^{-1} was utilized with a 4 cm^{-1} resolution. Films were measured immediately after deposition and measurements were averaged over 64 scans to improve the signal-to-noise ratio. All spectra were baseline corrected by subtracting a background spectrum of the Si wafer substrate. X-ray photoelectron spectroscopy (XPS) survey spectrum was obtained on a Kratos Axis Ultra spectrometer with a monochromatized Al Kα source. Relative sensitivity factors were calibrated by measuring poly(N-isopropylacrylamide) polymer (Aldrich) spun-cast onto Si wafer. Deposition samples and the standard were stored under vacuum overnight prior to analysis.

TI-900 TriboIndenter (Hysitron) was used in the Nanoindentation and nanoscratch experiments. The indentation axis calibration was performed in air with a load increased up to 700 μN in 10 s and back to 0 μN in another 10 s. H calibration was conducted on an Aluminum sample to determine the optics-probe tip offset. The load function was adopted from previous work reported by Lee,[24] but with a maximum load of 500 μN instead of 50 μN. The moduli and hardnesses were obtained by using the software came with the triboindentor. A 5×5 grid of indents was performed on every sample, with 20 μm separation distance in the x and y direction. For each indent, 8192 data points were taken. The load function for nanoscratch consists of five segments: (*i*) X position moves to −5 μm as normal load remains at

zero, tracing across the surface at the setpoint, (*ii*) X position holds at −5 μm for 3s and the normal load is ramped up to the scratching force of 2 mN during this hold, (*iii*) the X position moves from −5 μm to +5 μm for 30 s with the normal load held constant at 2 mN, (*iv*) X position holds again and the 2 mN load is removed during this time, (*v*) the X position returns to zero, the origin, and the normal load is at zero, to prevent deformation of the surface. Eight scratches with 20 μm separation were performed on every sample. Both Nanoindentation and nanoscratch experiments were conducted on polymer film thicknesses of >1 μm to minimize any substrate impact, using a conical diamond tip (young's modulus=1140 GPa, Poisson ratio = 0.07) with the radius of 10 μm. It is generally accepted that the substrate effect is minimal at indentation depths of less than 10% of the film thickness.[25] Area function of the diamond tip was determined by performing indentation on fused silica with a known modulus of 69.6 GPa. The load of the indentation was increased from 0.1 to 10 mN by 0.1 mN increments between neighboring indents. The area function was obtained by fitting the curves that have similar displacements as those values from indentation experiments.

Permeability measurements were performed using the apparatus developed in our laboratory. The procedures have been described in previous work.[26] The permeability coefficient P was calculated with the following equation,

$$P = \frac{\Delta V}{\Delta t} \frac{L}{A\, p_1}$$

Where $\Delta V / \Delta t$ is the volumetric flow rate of the gas flow, L is the thickness of the film, A is the cross sectional area, p_1 is the upstream pressure of the permeant gas (the downstream pressure is atmospheric pressure). The permeability coefficient is expressed in Barrer, defined as 846 $cm^3 \cdot mm/(cm^2 \cdot day \cdot bar)$.

4.3. Results and Discussion

Our approach is to first to grow iCVD copolymer thin films and then to react all the pendant groups of the two different monomeric units with one another to form a massively crosslinked network. We hypothesize that an alternating copolymer will result in a higher probability for reaction between unlike pendant groups than would a random copolymer.

As our first demonstration of this principle, we have designed a new organic network structure utilizing the monomers 4-aminostyrene (4-AS) and maleic anhydride (Ma) as the precursors. Previous studies demonstrate that iCVD is able to achieve alternating copolymer thin films using Ma, an electron-accepting monomer, and styrene, an electron-donating monomer.[27] 4-AS is structurally similar to styrene but with amine functionalities that can react with anhydride groups in Ma.[28] This indicates the possibility to synthesize alternating self-crosslinking copolymer thin films in a single step with conformal coverage.

4.3.1. Deposition Rate

Figure 4-1 displays the film growth rate as a function of the partial pressures of two monomers maleic anhydride (Ma) and 4-aminostyrene (4-AS), holding all other iCVD process conditions constant. With pure MA or 4-AS only, the deposition rate is quite slow (< 6 nm/min). The simultaneous introduction of both monomers leads to deposition rates as high as 22.5 nm/min. (Figure 4-1) The improved kinetics is consistent with hypothesis that poly(4-aminostyrene-alt-maleic anhydride) (PASMa) is forming, driven by known complex formation between the electron-accepting Ma monomer, and 4-AS, an electron-donating monomer.[27] The alternating copolymer deposition rate can be varied by changing the monomer partial pressure.

79
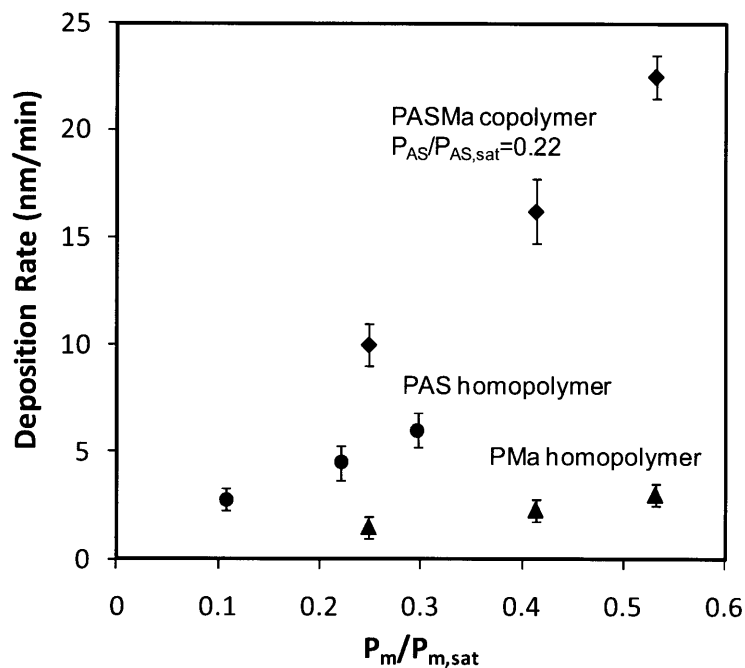
Figure 4-1. Deposition rate as a function of monomer partial pressure ratio.

4.3.2. Film Structure Analysis

Figure 4-2 shows the FTIR spectra of iCVD poly(maleic anhydride) (PMa), poly(4-aminostyrene) (PAS) homopolymer films, and the as-deposited poly(4-aminostyrene-*alt*-maleic anhydride) (PASMa) copolymer films. The incorporation of Ma and 4-AS is confirmed by the C=O stretching (1870 and 1780 cm^{-1}) and the signature NH$_2$ antisymmetric and symmetric stretching (3420 and 3361 cm^{-1}) bands, respectively.
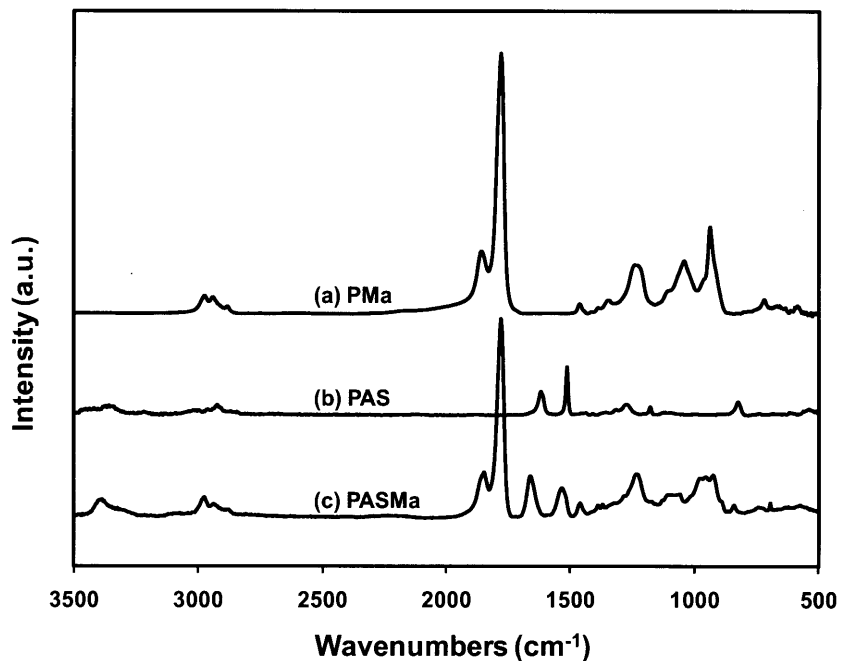
Figure 4-2. Fourier transform IR (FTIR) spectra of iCVD (a) poly(maleic anhydride) (PMa) , (b) poly(4-aminostyerene) (PAS), and (c) poly(4-aminostyerene-alt-maleic anhydride) (PASMa).

Depositions for possible combinations of three 4-AS and three Ma flow rates were performed and the flow rates are provided in Table 4-1. Compositions of iCVD-deposited copolymer films were determined by XPS survey scans. All copolymer films have Ma mole percentage of 55.1±1.3%, irrespective of the ratio of Ma/4-AS flow rates (Figure 4-3). The ratio of carbon: nitrogen at the surface is 12.3:1, also in reasonable agreement with the theoretical ratio, 12:1. The independence of film compositions from gas phase composition is expected for an alternating copolymer, as was previously observed for iCVD poly(styrene-alt-maleic anhydride).[27]

Table 4-1. Experimental flow rate settings and corresponding partial pressure ratios.

sample	flow rates (sccm)					$P_m/P_{m,sat}$	
	4-AS	Ma	TBPO	N_2	total	4-AS	Ma
AS/Ma-2/0	0.17	0	0.85	4.98	6	0.11	0
AS/Ma-4/0	0.35	0	0.85	4.8	6	0.22	0
AS/Ma-5/0	0.47	0	0.85	4.68	6	0.30	0
AS/Ma-0/2	0	2.1	0.85	3.05	6	0	0.25
AS/Ma-0/4	0	3.5	0.85	1.65	6	0	0.41
AS/Ma-0/5	0	4.5	0.85	0.65	6	0	0.53
AS/Ma-4/2	0.35	2.1	0.85	2.7	6	0.22	0.25
AS/Ma-4/4	0.35	3.5	0.85	1.3	6	0.22	0.41
AS/Ma-4/5	0.35	4.5	0.85	0.3	6	0.22	0.53
AS/Ma-2/5	0.17	4.5	0.85	0.48	6	0.11	0.53
AS/Ma-5/5	0.47	4.5	0.85	0.18	6	0.30	0.53
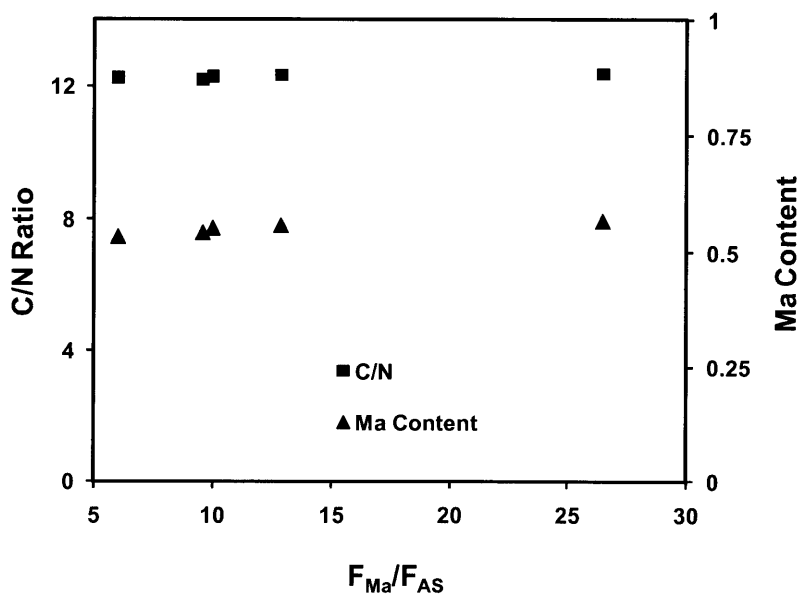
Figure 4-3. Measured maleic anhydride (Ma) contents and Carbon: Nitrogen ratios of the iCVD-deposited copolymers as a function of the ratio of Ma/AS flow rates.

Both FTIR and XPS confirm that iCVD produces an alternating copolymer from Ma and 4-AS and fully retains their pendant functional groups. This is the first time that amine-functional alternating copolymer thin films were synthesized via iCVD. This new material exhibits a self-crosslinking nature, due to the reaction between amine and anhydride functional groups. The average connectivity numbers of the as-deposited and annealed PASMa films are 2.308 and 2.385, respectively (see the supplementary information for detailed calculation), suggesting the possibility to obtain a non-rigid organic network structure simultaneously with high modulus and hardness.

4.3.3. Mechanical Property Analysis

Figure 4-4A shows that after annealing, the hardness and modulus of PASMa copolymer thin films increased by a factor of 2.7 and 1.9, respectively. This is consistent with the hypothesis that a highly cross-linked polymer network was formed. In nanoindentation testing, the annealed films also display a smaller hysteresis (Figure 4-4B), reflecting a lower viscoelasticity. The hardness and the modulus were calculated from the load-displacement curves with the following equations,[29]

$$H = \frac{P_{max}}{A(h_c)} \text{ and } E = \frac{\sqrt{\pi}}{2\sqrt{A(h_c)}} \cdot S$$

Where P_{max} is the maximum load, h_c is the contact depth and S is the contact stiffness. The area function $A(h_c)$ used in all calculations is the defined area function in the Hysitron software.
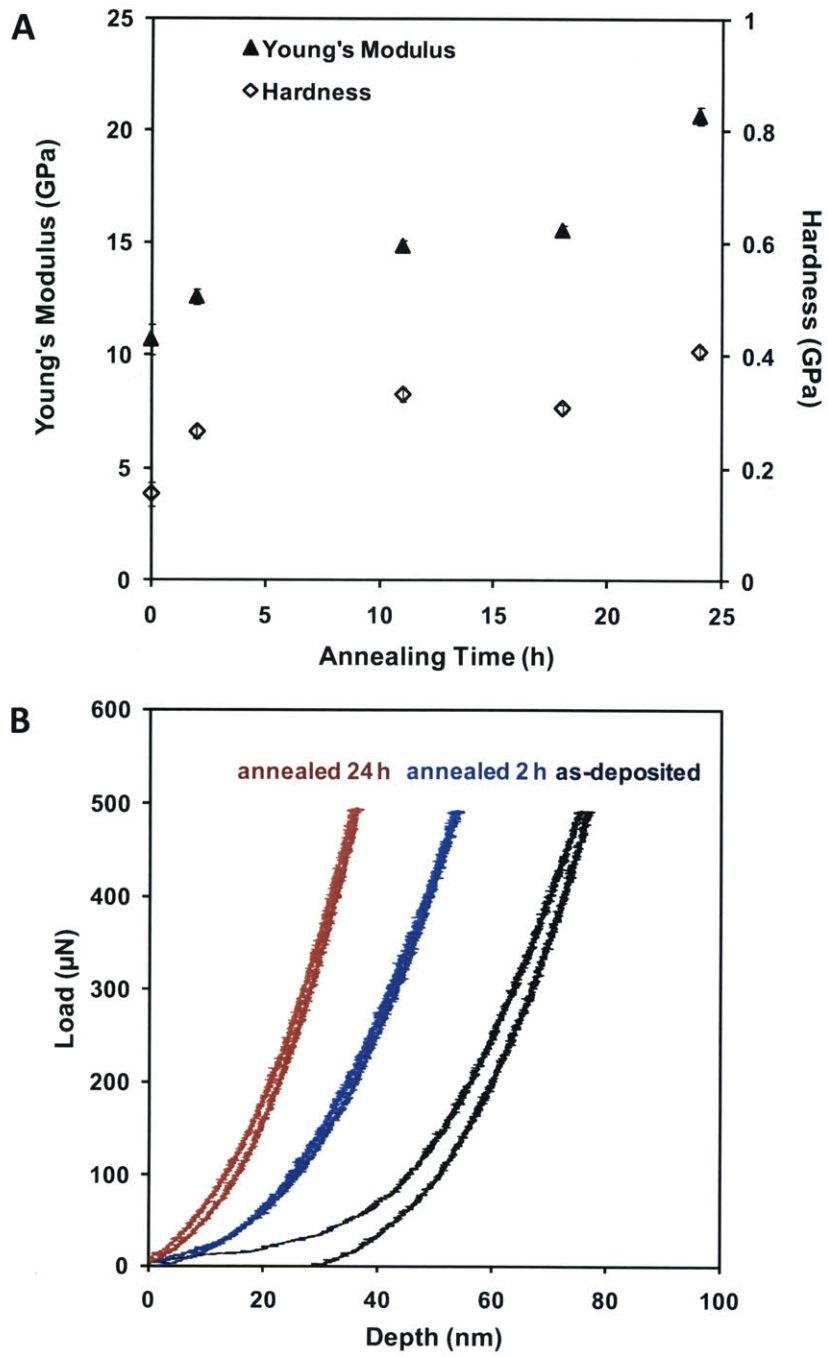
Figure 4-4. Mechanical property improvement of annealed PASMa copolymer. (A) Effect of annealing time on the Young's modulus and hardness of copolymers. (B) Load-displacement curves from nanoindentation for the as-deposited and annealed copolymers.

The copolymer films annealed for 24 hours display an elastic modulus exceeding 20 GPa, far greater than typical polymers (Figure 4-5).[30] Most polymers have modulus of 0.5~5 GPa and wood has modulus of 9~11 GPa. Even though fused silica is mechanically strong and has an elastic modulus of 69.5 GPa, it lacks organic functional groups and flexibility ($r = 2.67$).
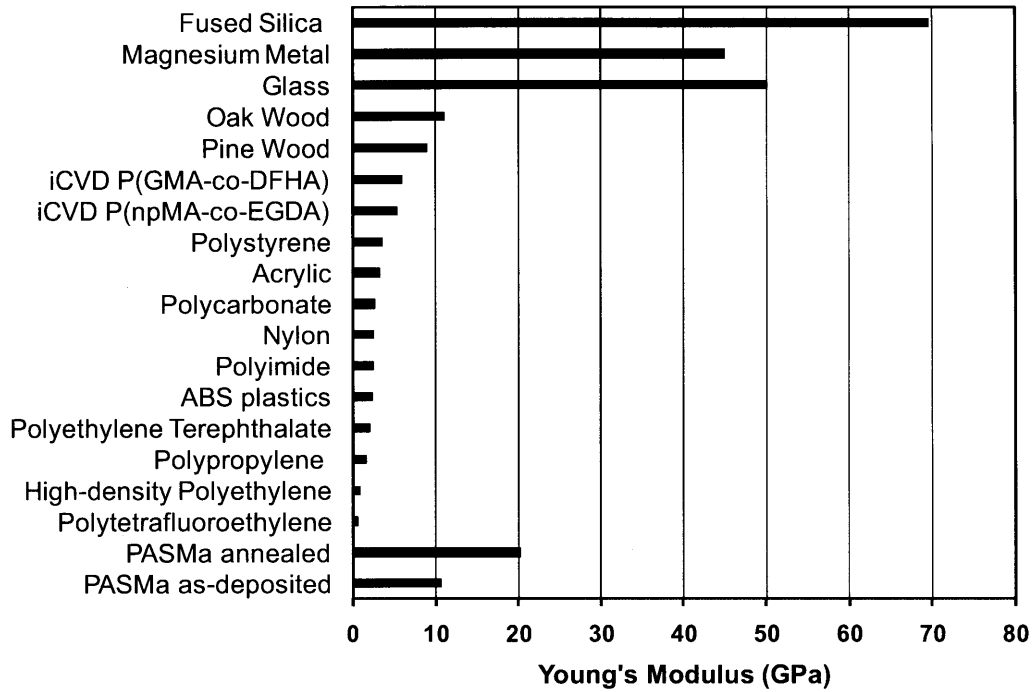
Figure 4-5. Mechanical property comparison of as-deposited and 24-hr annealed PASMa copolymer with a wide variety of organic and inorganic materials[30].

Nanoscratch experiments were performed on polystyrene (PS), as-deposited and 24-hr annealed PASMa copolymer films. AFM images (3D-MFP, Asylum Research) show that the scratch on the as-deposited PASMa films is ~48 nm in height (Figure 4-6B, E) and is much shallower than the one on the PS substrate with a height of ~130 nm (Figure 4-6A, D). However, on the PASMa film that was annealed for 24 hours, there is hardly any scratch observable on the substrate (Figure 4-6C, F). The scratch depth is <6 nm with the surface roughness of ~3nm. This achievement represents a significant advance in the fabrication of tough durable functional coatings.
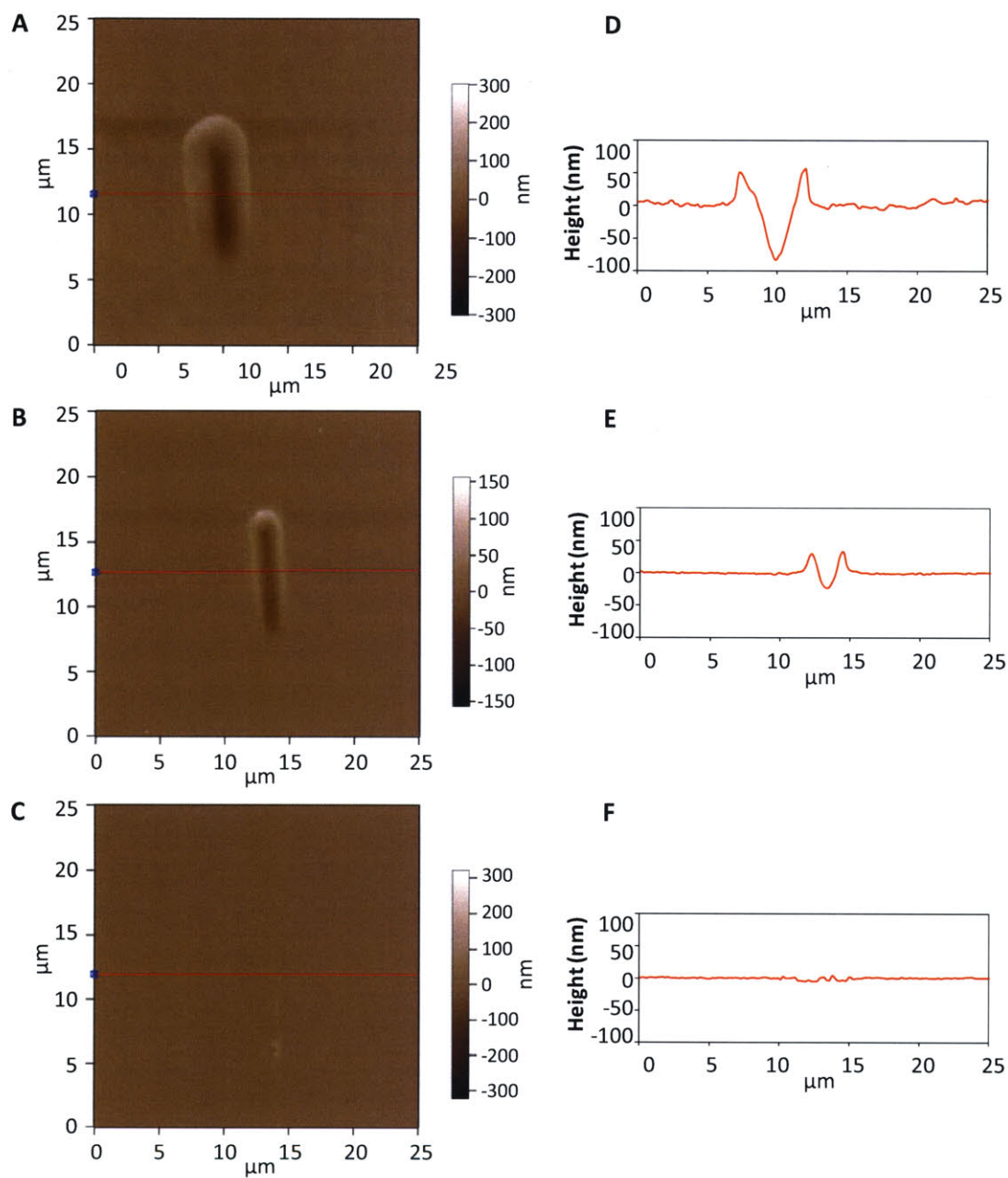
Figure 4-6. Scratch resistance. AFM images of nanoscratches on (A) polystyrene, (B) as-deposited iCVD PASMa copolymer film, and (C) 24-hr annealed PASMa copolymer film. Nanoscratch height profiles of (D) polystyrene, (E) as-deposited iCVD PASMa copolymer film, and (F) 24-hr annealed PASMa copolymer film. All the experimental conditions in the nanoscratch experiments were kept identical. The PASMa copolymer film thickness is ~ 1 micron in (B), (C), (E), (F).

The folding tests (±180°) were performed by creasing the polycarbonate (PC) substrate deposited with PASMa thin films of ~200 nm thickness. After each iteration, the PC was flattened back to 0°. We observed both the as-deposited and 24-hr annealed copolymer films to be mechanically robust to severe mechanical deformations on PC substrates (Figure 4-7). After 75 flexing cycles, the as-deposited PASMa was minimally affected, but more cracks appeared after 150 cyles. In contrast, after annealing for 24 hrs, PASMa films displayed no cracks even after 200 flexing cycles. The results indicate that the cross-linked films are mechanically strong but still maintain their flexibility, neither cracking nor delaminating with repeated flexing.
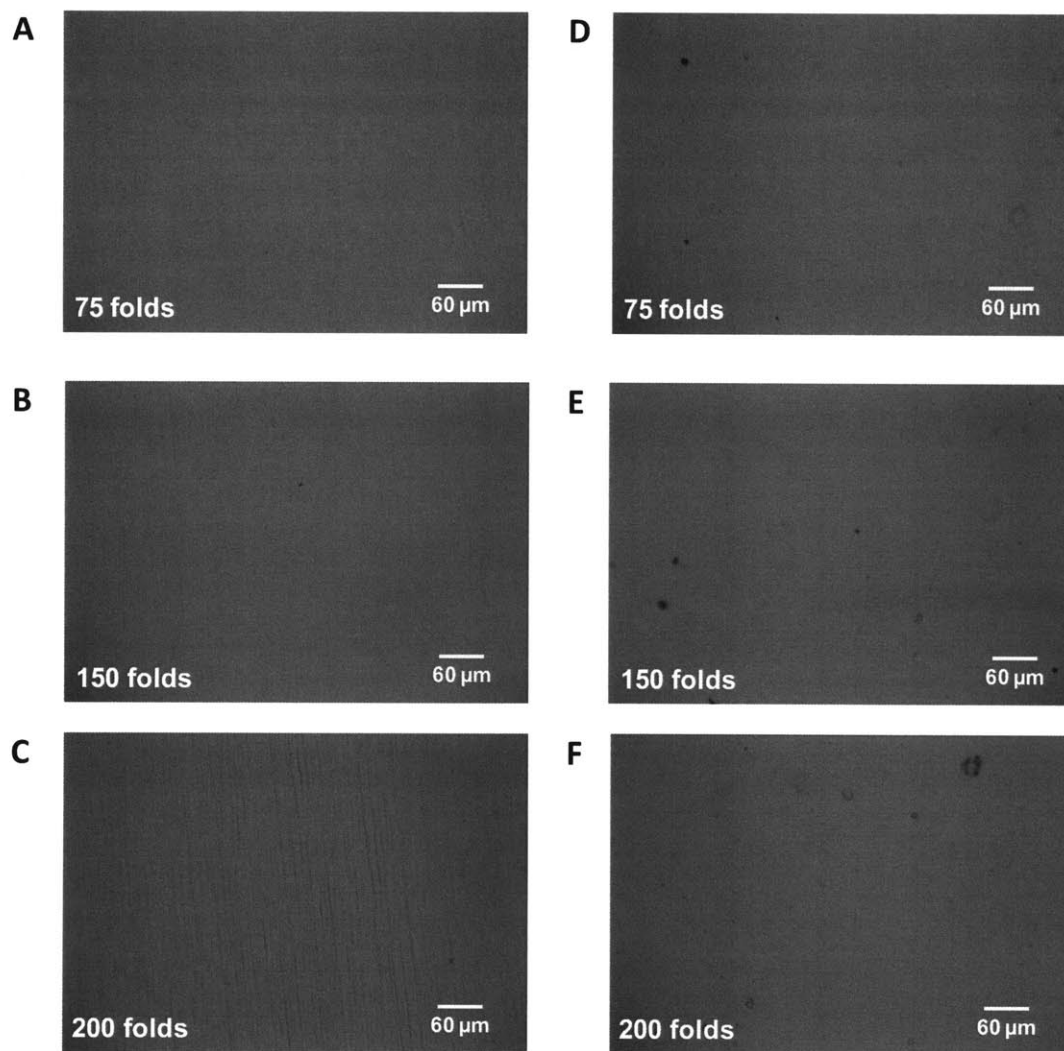
Figure 4-7. Flexibility test. Optical micrographs of as-deposited iCVD PASMa copolymer films on polycarbonate substrates after (A) 75 folds, (B) 150 folds, and (C) 200 folds. Optical micrographs of 24-hr annealed iCVD PASMa copolymer films on polycarbonate substrates after (D) 75 folds, (E) 150 folds, and (F) 200 folds. All the experimental conditions were kept identical. The PASMa copolymer film thickness is ~200nm.

4.3.4. Oxygen Permeability

The oxygen permeation rates of PASMa copolymer thin films were investigated. The measured oxygen permeability coefficient for uncoated PDMS substrate was 42 Barrers. As shown in Figure 4-8A, the permeability coefficient for a PDMS membrane (25 μm) coated with a 200 nm thick PASMa copolymer decreased to 2.3×10^{-6} Barrers, more than 7 orders of magnitude lower than the bare PDMS. It can also be seen that the permeability coefficient decreased with longer annealing time, which is as expected since more amine groups react with anhydride functionalities, increasing corss-link density and the degree of percolation of rigidity. The low oxygen permeation rates of these films are attributed to a dense structure induced by extensive crosslinking as well as the good adhesion between the organic coating layer and PDMS substrate. The 24-hr annealed PASMa thin film has an oxygen permeability of 2.3×10^{-7} Barrers, much lower than many of the fluoropolymers (Figure 4-8B).[31] It is even less permeable than the leading commercially available permeation barrier film, Kynar® PVDF, making it an attractive material for electronics packaging or food industries.
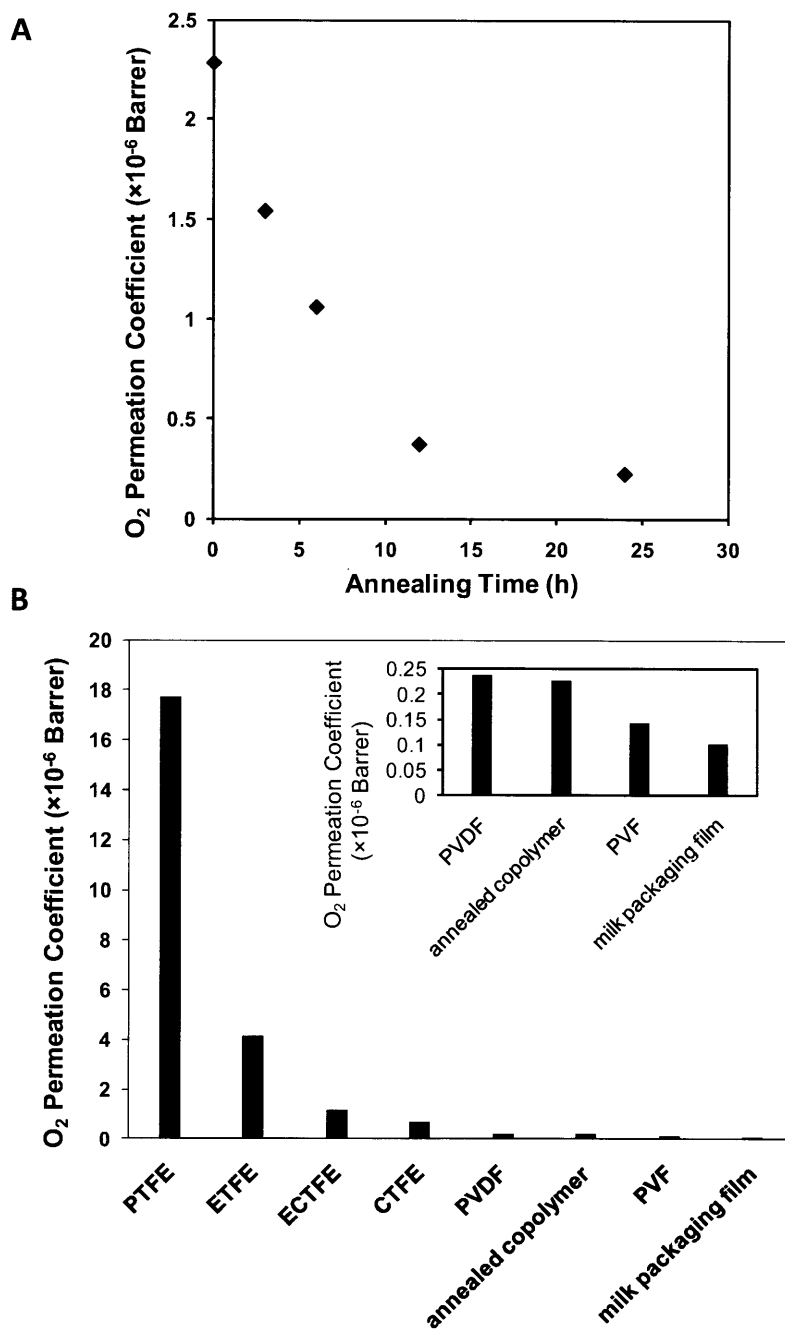
Figure 4-8. Oxygen permeability measurements. (A) The effect of annealing time on the oxygen permeation coefficient of PASMa copolymer films of 200 nm thick. (B) The oxygen permeation coefficient comparison of the 24-hr annealed PASMa copolymer film with commercially available permeation barrier films[31].

4.4. Conclusion

In summary, amine-functional alternating PASMa copolymer films were synthesized via iCVD for the first time. The retention of the pendant amine and anhydride chemical functionalities was confirmed by FTIR and XPS. The amine-rich alternating copolymer extensively self-crosslinks after gentle heating and this dramatically increases the mechanical properties of the copolymer. The annealed nanocoatings display an elastic modulus exceeding 20 GPa in nanoindentation experiments, far greater than typical polymers (0.5~5 GPa). Additionally, the cross-linked films maintain their flexibility, neither cracking nor delaminating with repeated flexing. This achievement represents a significant advance in the fabrication of tough durable functional coatings. Furthermore, the highly crosslinked coating material has oxygen permeability lower than commercially available permeation barrier coatings, making it an attractive material for electronics or food industries.

Acknowledgements

References

(1)   Berggren, M.; Nilsson, D.; Robinson, N. D. *Nature Materials* **2007**, *6*, 3-5.
(2)   van Bommel, K. J. C.; Friggeri, A.; Shinkai, S. *Angewandte Chemie-International Edition* **2003**, *42*, 980-999.
(3)   Tuteja, A.; Choi, W.; Ma, M. L.; Mabry, J. M.; Mazzella, S. A.; Rutledge, G. C.; McKinley, G. H.; Cohen, R. E. *Science* **2007**, *318*, 1618-1622.
(4)   Zammatteo, N.; Jeanmart, L.; Hamels, S.; Courtois, S.; Louette, P.; Hevesi, L.; Remacle, J. *Analytical Biochemistry* **2000**, *280*, 143-150.
(5)   Brust, M.; Bethell, D.; Kiely, C. J.; Schiffrin, D. J. *Langmuir* **1998**, *14*, 5425-5429.
(6)   Chung, J. S.; Kim, D. J.; Ahn, W. S.; Ko, J. H.; Cheong, W. J. *Korean Journal of Chemical Engineering* **2004**, *21*, 132-139.
(7)   Novak, B. M. *Advanced Materials* **1993**, *5*, 422-433.
(8)   Muh, E.; Frey, H.; Klee, J. E.; Mulhaupt, R. *Advanced Functional Materials* **2001**, *11*, 425-429.
(9)   Cheyns, D.; Vasseur, K.; Rolin, C.; Genoe, J.; Poortmans, J.; Heremans, P. *Nanotechnology* **2008**, *19*, 6.
(10)   Binh-Khiem, N.; Matsumoto, K.; Shimoyama, I. *Applied Physics Letters* **2008**, *93*, 3.
(11)   Hozumi, A.; Takai, O. *Applied Surface Science* **1996**, *103*, 431-441.
(12)   Phillips, J. C. *Journal of Non-Crystalline Solids* **1979**, *34*, 153-181.
(13)   Burkey, D. D.; Gleason, K. K. *Journal of Applied Physics* **2003**, *93*, 5143-5150.
(14)   Mao, Y.; Gleason, K. K. *Macromolecules* **2006**, *39*, 3895-3900.
(15)   Dohler, G. H.; Dandoloff, R.; Bilz, H. *Journal of Non-Crystalline Solids* **1980**, *42*, 87-95.
(16)   Janotta, A.; Janssen, R.; Schmidt, M.; Graf, T.; Stutzmann, M.; Gorgens, L.; Bergmaier, A.; Dollinger, G.; Hammerl, C.; Schreiber, S.; Stritzker, B. *Physical Review B* **2004**, *69*.
(17)   Oliver, M. S.; Dubois, G.; Sherwood, M.; Gage, D. M.; Dauskardt, R. H. *Advanced Functional Materials*, *20*, 2884-2892.
(18)   Verbeek, C. J. R. *Journal of Thermoplastic Composite Materials* **2007**, *20*, 137-149.
(19)   Ross, A. D.; Gleason, K. K. *Journal of Vacuum Science & Technology A* **2005**, *23*, 465-469.
(20)   Tenhaeff, W. E.; Gleason, K. K. *Advanced Functional Materials* **2008**, *18*, 979-992.
(21)   Asatekin, A.; Barr, M. C.; Baxamusa, S. H.; Lau, K. K. S.; Tenhaeff, W.; Xu, J. J.; Gleason, K. K. *Materials Today* **2010**, *13*, 26-33.
(22)   Baxamusa, S. H.; Montero, L.; Dubach, J. M.; Clark, H. A.; Borros, S.; Gleason, K. K. *Biomacromolecules* **2008**, *9*, 2857-2862.
(23)   Xu, J. J.; Gleason, K. K. *Chemistry of Materials* **2010**, *22*, 1732-1738.
(24)   Lee, L. H.; Gleason, K. K. *Journal of the Electrochemical Society* **2008**, *155*, G78-G86.
(25)   Oliver, W. C.; Pharr, G. M. *Journal of Materials Research* **1992**, *7*, 1564-1583.
(26)   Asatekin, A.; Gleason, K. K. *Nano Letters* **2011**, *11*, 677-686.

(27)   Tenhaeff, W. E.; Gleason, K. K. *Langmuir* **2007**, *23*, 6624-6630.

(28)   Padwa, A. R.; Sasaki, Y.; Wolske, K. A.; Macosko, C. W. *Journal of Polymer Science Part a-Polymer Chemistry* **1995**, *33*, 2165-2174.

(29)   Li, X. D.; Bhushan, B. *Materials Characterization* **2002**, *48*, 11-36.

(30)   ToolBox, E., p Retrieved March 2011, from http://www.engineeringtoolbox.com/young-modulus-d_417.html.

(31)   Fitz, H. *Kunststoffe-German Plastics* **1980**, *70*, 27-33.

CHAPTER FIVE

Low-temperature iCVD Process Using
Tert-Butyl Peroxybenzoate as an
Initiator*

Abstract

Conformal poly(cyclohexyl methacrylate) (pCHMA) thin films were synthesized via initiated chemical vapor deposition (iCVD), with *tert*-butyl peroxybenzoate (TBPOB) as the initiator, representing the first time that TBPOB has been used as an initiator for iCVD synthesis. Using TBPOB instead of *tert*-butyl peroxide (TBPO), the rate of iCVD film growth increased by a factor of up to ~8 at comparable conformality and lower the filament temperature from ~250 °C to ~150 °C at a comparable deposition rate. The conformal deposition of functional thin films is desired for applications including microfluidics, medical devices and membranes. Lower filament temperatures reduce the heat load to the deposition surface and thus are advantageous for polymeric substrates that are temperature sensitive or monomers that decompose at high temperatures. Fourier transform infrared spectroscopy (FTIR) and X-ray photoelectron spectroscopy (XPS) results demonstrate the similarity of the TBPOB- to the TBPO-initiated pCHMA main chains. However, the aromatic group in TBPOB provided a unique spectral signature of the polymer chain endgroup in the FTIR and the peak intensity increased with increase of filament temperature. Scanning electron micrographs (SEMs) revealed that the pCHMA coatings are conformal over non-planar structures, however, at identical process conditions TBPO-initiated films showed a slightly better conformality due to the lower sticking coefficient of TBPO. At a monomer partial pressure of 0.45, TBPOB has a sticking coefficient value of 0.1188, which is ~ three times as high as that of TBPO (0.0413). The step coverage is insensitive to filament temperature if the surface concentration of the monomer is fixed.

5.1. Introduction

Conformal films over non-planar or porous substrates have attracted increasing interest for applications including micro-electro-mechanical systems (MEMS), medical devices, membranes, and electronic packaging.[1-4] A variety of vapor phase surface modification techniques enable the deposition of thin films with good conformality,[5-7] which is difficult to achieve with solution polymerization techniques due to the surface tension effects. Polymers are a desirable class of materials because of their low cost, ease in fabrication, and wide array of chemical and physical functionalities. Their organic functional groups can be utilized to tune surface energy, to enable subsequent chemical attachment of desirable molecules, or to covalently bind micro- or nanoparticles to the surface. Initiated chemical vapor deposition (iCVD) is a polymer chemical vapor deposition technique that utilizes the delivery of vapor-phase monomers to form chemically well-defined polymer films with tunable conformality and properties. Using this technology, a number of functional and biocompatible polymer films have been synthesized and used for applications in microfluidic devices, sensors, and membranes.[8-10] The iCVD method is chemically analogous to solution phase polymerization, but possesses a number of practical advantages. It is able to deposit conformal and pinhole-free coatings on non-planar substrates with nanometer level thickness control.[11-13] In addition, elimination of solvent usage makes the iCVD method compatible with a wide range of substrate materials which swell or dissolve in solution. Furthermore, as a low-energy vapor deposition process, the iCVD process is able to maintain the functionalities from the monomers, which is crucial for subsequent functionalization.[6,14]

A variety of initiator systems can be used to bring about the polymerization. Radicals can be produced by thermal, photochemical, and redox methods.[15] The thermal, homolytic dissociation of initiators is the most widely used mode of generating radicals to initiate polymerization. There are two methods which use thermal initiators with vapor phase monomers. One is to apply non-volatile initiators to the surface and then exposes the treated surface to monomer vapors, known as vapor-phase assisted surface polymerization (VASP).[16] In order to be introduced into the vacuum chamber as a vapor, the initiator for iCVD must exhibit reasonable volatility. The initiation of chains occurs continuously throughout the iCVD process, allowing films of arbitrary thickness to be achieved.[17] Additionally the substrate need not be heated to cause the initiator to decompose. To date, iCVD polymerization has utilized primarily thermal initiators, including *tert*-butyl peroxide (TBPO),[9,18,19] *tert*-amyl peroxide,[20] perfluorooctane sulfonyl fluoride,[21] and triethylamine.[22] These molecules contain labile bonds that allow for decomposition of the initiator with a minimal energy input. Indeed, the required filament temperatures are in the range of only ~200–300 °C for the TBPO initiator. Hence, the initiators can selectively form free radicals at conditions under which the monomeric species are stable allowing complete functional group retention in the deposited polymer chains. Additionally, photoinitiators, such as 2,2'-azobis(2-methylpropane)[23] and benzophenone,[24] can also be used to initiate CVD polymerization by UV irradiation.

Although the reactions of benzoyl peroxide have been studied in great detail by various researchers during the past decades,[25-27] its low vapor pressure makes it difficult to deliver into the vacuum chamber. In this work, *tert*-butyl peroxybenzoate (TBPOB) has been tested in the iCVD system for the first time and used as an initiator to deposit conformal poly(cyclohexyl methacrylate) (pCHMA) thin films on non-

planar substrates. TBPOB, a peroxyester, is a strong free radical source. It is used as a polymerization initiator, catalyst and vulcanizing agent, crosslinking agent, and a chemical intermediate.[28] It is much less volatile than TBPO and may enable a higher surface concentration and hence result in a faster growth rate. TBPOB contains the same weak peroxy (O–O) bond as the TBPO molecule. The TBPO initiated chains will have endgroups derived from the t-butoxy radical. While t-butoxy dervived endgroups will also be present in the TBPOB initiated films, additionally there will be endgroups derived from the oxybenzoate radical. The aromatic group in TBPOB provides a unique spectral signature in the FTIR and may allow quantification of the formation of endgroups from the oxybenzoate. Furthermore, with a decomposition temperature of 90 °C in solution, TBPOB holds the potential for further reducing the filament temperature of the iCVD process. Lower filament temperatures are desired for use with polymeric substrates which decompose at high temperature or which have low glass transition temperature. Lower filament temperatures are also desired for monomers that decompose at high temperature.

To use TBPOB as an initiator for iCVD system is challenging because its vapor pressure is only 0.00337 Torr at room temperature, which is much lower than TBPO (27.3 Torr at 25 °C). TBPOB cannot be heated to achieve a higher flow rate because it becomes dangerous during decomposition reaction under high temperature.[28] The self-accelerating decomposition temperature (SADT) is approximately 65.8 °C. In this work, a bubbler is used to deliver the TBPOB with nitrogen as the patch flow. Conformal poly(cyclohexyl methacrylate) (pCHMA) thin films were synthesized via iCVD, with TBPOB as the initiator, representing the first time that TBPOB has been used as an initiator for iCVD system. The deposition

kinetics, films composition and structure, sticking coefficient, and conformality will be compared to iCVD pCHMA films initiated by TBPO.

5.2. Experimental

5.2.1. Deposition Setup

Experiments were performed in a custom built vacuum reactor (Sharon Vacuum) with a radius of 12 cm, as previously described.[12] The ChromAlloy filaments (Goodfellow) were mounted in a parallel array to provide the thermal excitation, heated by a DC power supply (Sorensen). The filament temperature was measured by a K type thermocouple (Omega Engineering) attached to one of the filaments. The vertical distance between the filament and the deposition stage was 1.5 cm. The stage was back-cooled by a recirculating chiller/heater (NESLAB), which served as the purpose of maintaining the substrate temperature constant to prevent the heating of the sample due to the heated filaments. The chiller/heater to the substrate platen was set to 30 °C for all the depositions.

A stainless steel bubbler (Strem Chemicals, Inc.) was used to delivery *tert*-butyl peroxybenzoate, with nitrogen as the gas carrier. All the chemical species were used as purchased without further purification and their structures are shown in Figure 5-1. *tert*-Butyl peroxide (Aldrich, 97%) initiator at room temperature, was fed into the reactor through a mass flow controller (model 1479, MKS Instruments) at 0.6 sccm. Cyclohexyl methacrylate (CHMA) (Aldrich, 95%) monomer, heated to 80 °C in a glass jar, was delivered into the reactor at 4.6 sccm via a needle valve. The flow rate of nitrogen patch flow was set to 1 sccm for both TBPO and TBPOB initiated depositions. Total pressure in the vacuum chamber was maintained at 0.17 Torr.

tert-butyl peroxide
(TBPO)

tert-butyl peroxybenzoate
(TBPOB)

cyclohexyl methacrylate
(CHMA)
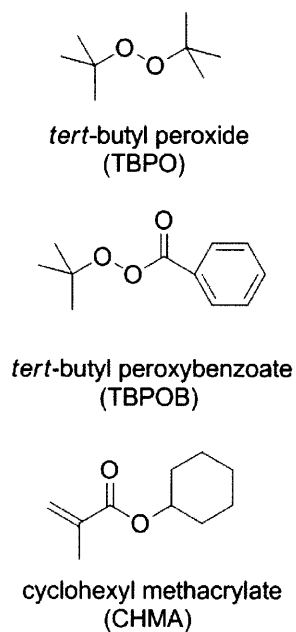
Figure 5-1. Initiators and monomer used in this work.

5.2.2. Film Characterization

The deposition process was monitored *in situ* by interferometry with a 633 nm He–Ne laser (JDS Uniphase). The film thickness measurements were performed on a variable angle spectroscopic ellipsometry (VASE) (J. A. Woollam M-2000). All samples were measured at an incidence angle of 70° and with a wavelength range of 315–700 nm. A Cauchy–Urbach model was used to fit the data by a nonlinear least-squares minimization algorithm. Film thickness was obtained upon convergence of the algorithm.

Fourier transform infrared (FTIR) measurements were performed on a Nicolet Nexus 870 ESP spectrometer in a normal transmission mode. A deuterated triglycine sulfate (DTGS) KBr detector over the range of 400-4000 cm^{-1} was utilized with a 4 cm^{-1} resolution. Films were measured immediately after deposition, and measurements were averaged over 64 scans to improve the signal-to-noise ratio. All

spectra were baseline-corrected by subtracting a background spectrum of the Si wafer substrate. The intensity of the FTIR spectra for films deposited at different filament temperatures was normalized using the peak at 1714.6 cm^{-1} (C=O stretching) as the reference point.

An X-ray photoelectron spectroscopy (XPS) survey spectrum was obtained on a Kratos Axis Ultra spectrometer with a monochromatized Al Kα source. Relative sensitivity factors were calibrated by measuring poly(cyclohexyl methacrylate) polymer (Aldrich) spun-cast onto a Si wafer. Deposition samples and the standard were stored under vacuum overnight prior to analysis.

Both TBPO- and TBPOB-initiated pCHMA films were deposited on silicon substrates patterned with trenches supplied by Analog Devices. These trenches were 7 μm deep and 0.8 μm, 1.3 μm, 2.1 μm, and 5 μm wide, respectively. Deposited trench wafers were sputter-coated with 6 nm of gold (Denton Desk II), and SEM images were obtained by a JEOL JSM-6060 with acceleration voltage of 5 kV.

5.3. Results and Discussion

5.3.1. Deposition Kinetics

Figure 5-2 shows the deposition rate as a function of filament temperature, using TBPO and TBPOB as initiators for iCVD pCHMA, respectively. The deposition rate increases as the filament temperature increases for both initiators. As the filament temperature increases further, the deposition rate plateaus, indicating the kinetics transitions to a mass transfer regime where the deposition rates are less dependent on the filament temperature.[12] Polymerization of the CHMA films using TBPO as the initiator could be achieved with filament temperatures > 250 °C, whereas TBPOB permits deposition at filament temperature as low as 150 °C.

Furthermore, in the mass transfer regime, the maximum deposition initiated by TBPOB is approximately twice that observed with ones initiated by TBPO. The faster deposition rates are important in situations where thick films are required. High rates also improve the economics of the iCVD process. The ability to initiate polymerizations at a much lower filament temperature reduces heat load to substrate.[29] Thus, TBPOB has the great potential for situations where temperature sensitive substrates are used. It is also superior to TBPO when using monomer precursors which decompose at high temperatures, thus expanding the applicability of iCVD to new types of polymers.
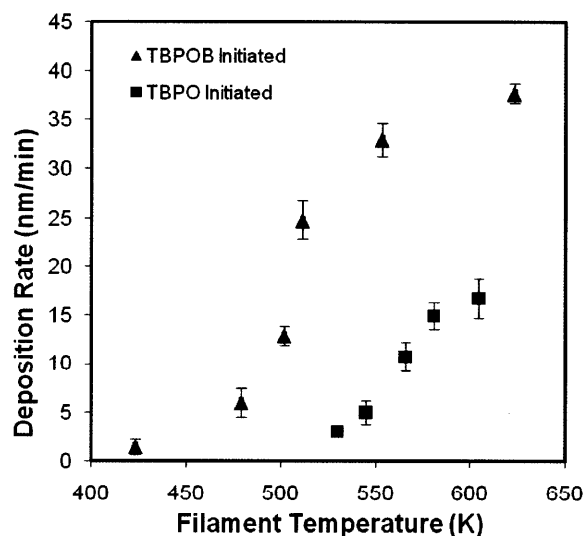
Figure 5-2. Deposition rate as a function of filament temperature, with TBPOB and TBPO as initiators. Flow rates of monomer and initiator precursors, substrate temperature and monomer partial pressure are identical for the two sets of experiments.

The apparent activation energies in low temperature regime before the plateau is reached are calculated as 82.8 and 72.6 kJ/mol for TBPO and TBPOB, respectively (Figure 5-3). The higher value for TBPO is consistent with data from the solution synthesis using cumene as the solvent, where TBPO has a higher reported

activation energy (153.46 kJ/mol) than TBPOB (134 kJ/mol).[30] However, both values from the solution synthesis are much greater than that derived directly from Figure 5-3. For TBPO, this apparent discrepancy was resolved by studying the temperature of the gas in the region between the filaments and the substrate by Ozaydin-Ince.[12] While solution synthesis takes place a single uniform temperature, in iCVD there is a temperature gradient between the filament and the substrate. Accounting for this temperature gradient, resulted in the calculation of an apparent activation energy of 166 kJ/mol for TBPO decomposition in the iCVD, which is approximately double of the value extracted directly from the Arrhenius plot using only the filament temperature. Thus, the value calculated accounting for the temperature gradient is consistent with the cleavage of the O–O cleavage of the bond in the initiator.
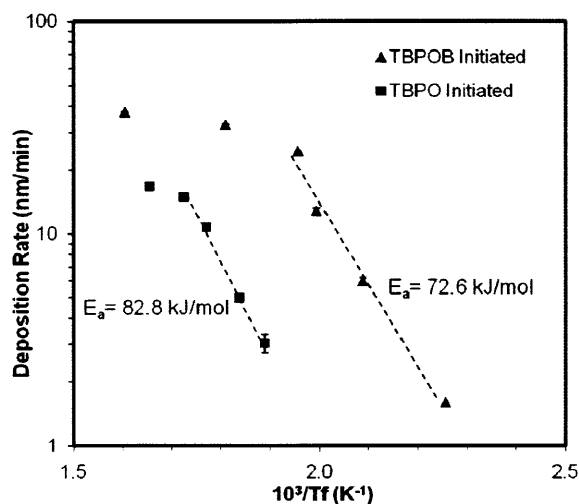
Figure 5-3. Deposition rates as a function of inverse filament temperature. Apparent activation energies of 82.8 kJ/mol and 72.6 kJ/mol are calculated in the low temperature regime for TBPO- and TBPOB-initiated reactions, respectively.

5.3.2. Confirmation of Polymerization by FTIR

Figure 5-4 shows the FTIR spectra of CHMA monomer precursor, the iCVD deposited pCHMA films using TBPO and TBPOB as the initiators. Successful vinyl polymerization is confirmed by the reduction of unsaturated carbon peaks, as denoted by asterisks in Figure 5-4a. Most clearly resolved is the sharp C=C stretching mode at 1630 cm^{-1}. The spectra for both types of iCVD films (Figure 5-4b and Figure 5-4c) contain peaks that are characteristic of CHMA: the CH_2 antisymmetrical and symmetrical cyclohexyl vibrations (2939.2 cm^{-1} and 2861.4 cm^{-1}), C=O stretching (centered at 1714.6 cm^{-1}), C–H bending (1500-1350 cm^{-1}), and (O=)C–O stretching (1300-1150 cm^{-1}). The high incorporation of pendant cyclohexyl rings from the monomer indicates that iCVD is a nondestructive process and is able to retain the functionality.
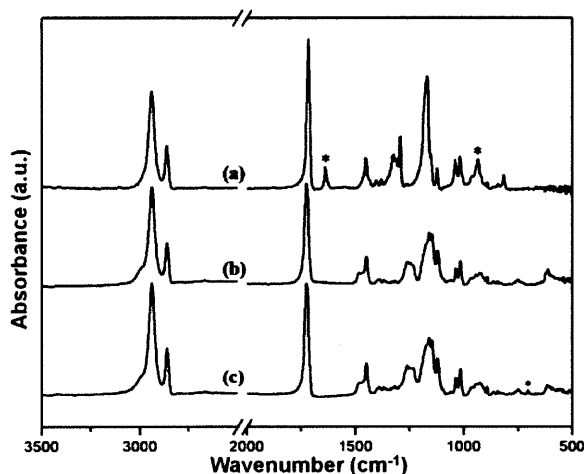
Figure 5-4. Fourier transform IR (FTIR) spectra of (a) cyclohexyl methacrylate (CHMA) monomer, (b) iCVD poly(cyclohexyl methacrylate) (pCHMA) using TBPO as an initiator, and (c) iCVD deposited pCHMA using TBPOB as an initiator. Asterisks (*) represent signature vinyl bonds in (a), and the out-of-plane C–H bending vibrations for benzene derivatives at 700 cm-1 in (c).

105

As seen by comparing Figure 5-4b and Figure 5-4c, the majority of the peak locations and areas of the TBPOB initiated polymer spectrum match well with the TBPO initiated one. However, there is a small absorption peak at ~700 cm^{-1} observed only in Figure 5-4c, which confirms incorporation of TBPOB into the polymer chain. Indeed, most of monosubstituted benzenes adsorb at 697 ± 11 cm^{-1}, which is due to out-of-plane ring bending by sextants. A closer look of this region is shown in Figure 5-5. Clearly TBPO initiated films lack adsorption at ~700 cm^{-1} but for TBPOB initiated films, the peaks are observed in each film and their intensity increases with increasing filament temperature. At higher filament temperature, more initiator radicals are formed and permit higher degree of end group incorporation. The ability to detect aromatic endgroups via FTIR is an advantage of the TBPOB initiator. In contrast, the aliphatic chain ends produced using TBPO do not produce easily resolvable FTIR signatures.
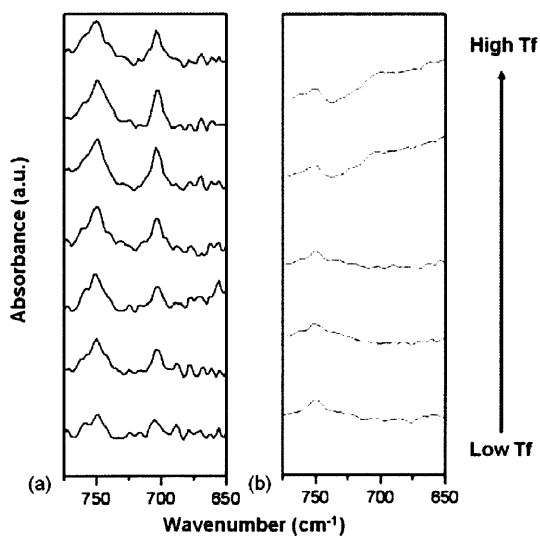
Figure 5-5. Fourier transform IR (FTIR) spectra of (a) iCVD deposited poly(cyclohexyl methacrylate) (pCHMA) using TBPOB as an initiator at filament temperatures of 150, 206, 228, 238, 257, 280 and 350 °C, and (b) iCVD deposited

106

pCHMA using TBPO as an initiator at filament temperatures of 257, 271, 292, 307 and 331 °C.

5.3.3. Compositional Analysis by XPS

Figure 5-6 shows the carbon C 1s high-resolution XPS scans for both TBPO and TBPOB initiated pCHMA polymer films. The spectra can be described using four bonding environment expected solely due to vinyl polymerization of the monomer (Table 5-1). The fitted curves reproduce the observed spectra very well and show excellent agreement of both the binding energies and peak area ratios of iCVD films with the theoretical values.[31] The XPS spectra of the films initiated by TBPOB and TBPO are similar, indicating that the initiator does not change the chemical composition or the degree of polymerization in the film.

Table 5-1. Atomic percentage of carbon enviroment from C 1s XPS spectra.

		theoretical[31]		Experimental (TBPO initiated)		Experimental (TBPOB initiated)	
		binding energy (eV)	area (%)	binding energy (eV)	area (%)	binding energy (eV)	area (%)
1	–C–C*H$_2$–C–	285.0	70.0	285.0	69.2	285.0	68.3
2	–C*H–CO–	285.7	10.0	285.8	10.4	285.7	12.6
3	–CH$_2$–C*H–O–	286.6	10.0	286.7	10.4	286.6	11.0
4	–C*=O	289.2	10.0	288.8	10.0	288.9	8.1

Figure 5-6. Least-squares regressions of the high-resolution scans of C1s using components with Gaussian lineshapes of pCHMA samples initiated by (a) TBPO and (b) TBPOB. Flow rates of monomer and initiator precursors, substrate temperature, filament temperature, and monomer partial pressure are held same between the two sets of experiments.
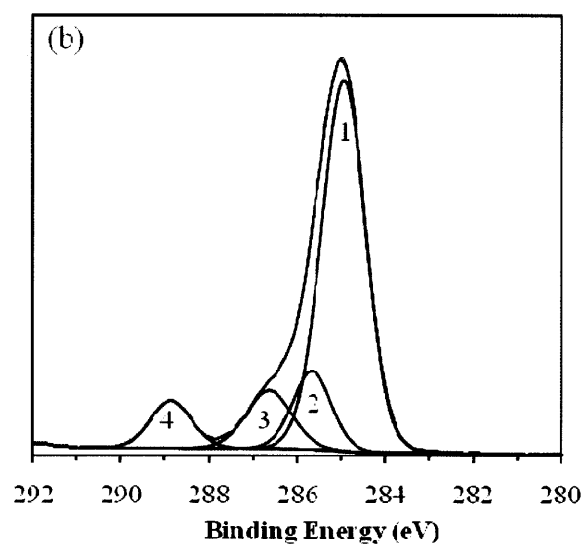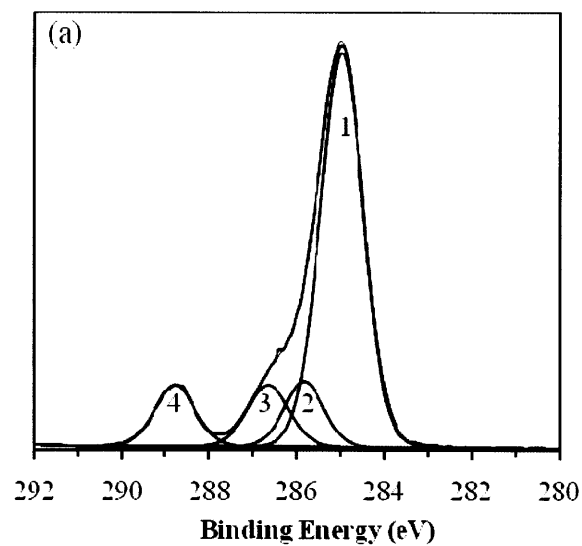
Both FTIR and XPS data support the hypothesis that iCVD produces linear polymeric structure and retains essentially all the pendant cyclohexyl ring functional groups. We expect that TBPOB can be used to initiate iCVD from most, if not all, of the monomers that deposit under TBPO initiation. TBPOB initiated polymer films have similar FTIR and XPS spectrum as TBPO initiated films and show a signature benzene adsorption peak in FTIR. This is the first time that TBPOB has successfully been used in the iCVD system. It not only broadens the iCVD initiator library, but also enables a faster deposition rate and the applications where temperature sensitive substrates and monomers are desired.

5.3.4. Conformality Analysis by SEM

For applications including microfluidics, medical devices, and membranes, good step coverage over non-planar or porous substrates is desired. Step coverage is defined as the ratio of the coating thickness at the bottom to that at the top of the trench. Figure 5-7 shows the step coverage for TBPO and TBPOB initiated iCVD pCHMA films on trenches with different aspect ratios. All the experimental conditions including filament temperature, flow rates of initiator and monomer precursors, and substrate temperature were held same between the two experiments. The dashed line shows the linear best-fit between logarithm of step coverage and the square of the aspect ratio. For TBPO initiated depositions, the radical sticking coefficient, Γ_{TBPO}, is found from the slope as 0.0413, at P_m/P_{sat} of 0.45 and $T_{filament}$ of 257 °C. This value agrees well with Baxamusa's results for the same polymer at a similar P_m/P_{sat}.[11] Performing a similar analysis for the data of TBPOB initiated depositions, a sticking coefficient value of 0.1188 is obtained, which is ~ three times as high as Γ_{TBPO}. Since the pCHMA is the identical precursor, the difference in

conformality between TBPO- and TBPOB-initiated depositions confirms the earlier hypothesis[11] that the sticking probability of the initiator radical controls the observed conformality.
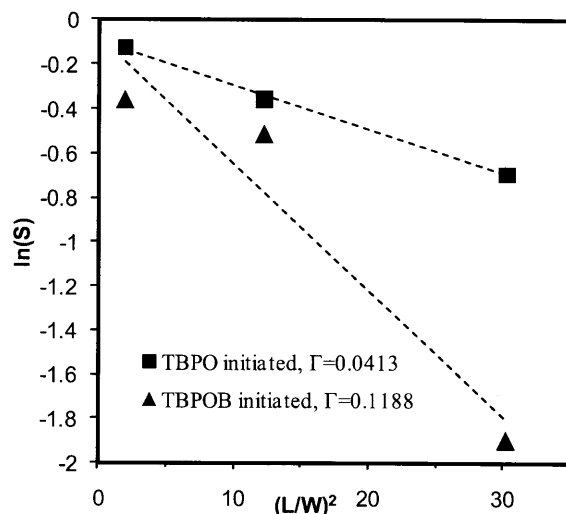
Figure 5-7. Step coverage as a function of aspect ratio square. The dashed lines represent the linear best-fit lines for the data and the slopes are proportional to the sticking probability of the initiating radicals. Here the three different aspect ratios for the trenches are 8.7, 5.5, and 3.4 respectively. Flow rates of monomer and initiator precursors, substrate temperature, filament temperature, and monomer partial pressure are held same between the two sets of experiments.

Cross-sectional SEM micrographs (Figure 5-8a and Figure 5-8b) demonstrate the overall profiles for polymer films growing inside trenches with the aspect ratio of 1.4 by iCVD. Both of them show good thickness uniformity over the entire trench feature, however, the conformality of the TBPO initiated iCVD film is superior to that of TBPOB initiated layer, which is due to its lower sticking coefficient. The thermal decomposition of TBPOB results in the production of both *tert*-butoxy and oxybenzoate radicals, which can then adsorb on the substrate surface. *tert*-butoxy radicals have a higher probability to desorb back into the vapor phase and

110

benzoate radicals are more likely to react with a monomer to form a polymer chain. With more light *tert*-butoxy radicals continuing down the trench to initiate polymerization, TBPO-initiated films are expected to have a better conformality than TBPOB-initiated films.

Figure 5-8. Cross-sectional SEM images of (a) iCVD deposited poly(cyclohexyl methacrylate) (pCHMA) using TBPOB as an initiator, (b) iCVD deposited pCHMA using T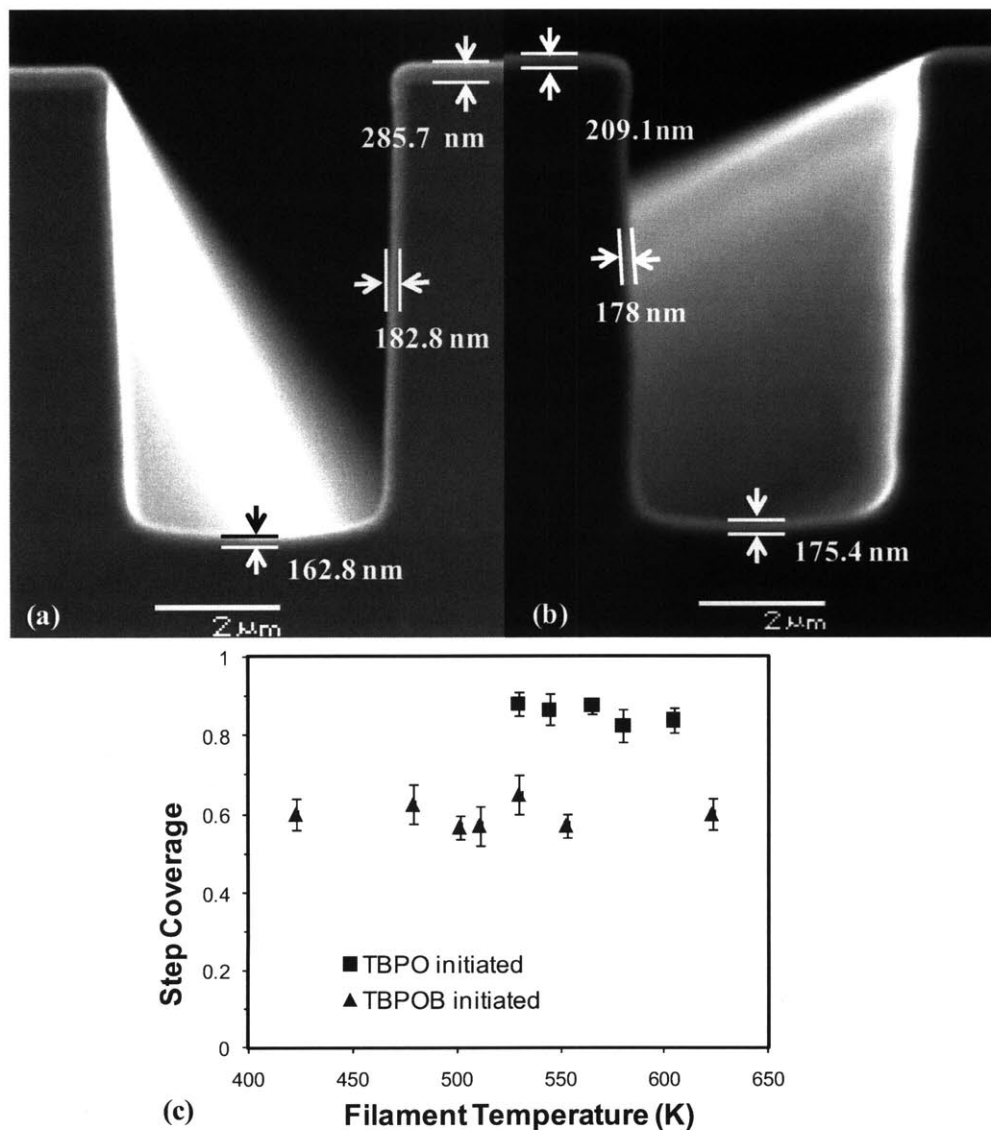BPO as an initiator, and (c) the step coverage as a function of filament temperature. The error bar represents the uncertainty in the measurement of step

coverage. Flow rates of monomer and initiator precursors, substrate temperature and monomer partial pressure are held same between the two sets of experiments.

The dependence of the step coverage on the radical concentration is studied by varying the filament temperature while keeping the monomer surface concentration constant. Substrate cooling can be made difficult by the insulating nature of the vacuum environment and when substrates of low conductivity are used, such as polymers, textiles, and porous materials. More traditional substrates like silicon and metal have higher thermal conductivity and more readily spread heat to counteract the development of temperature gradients. It has been previously found that substrate temperature (T_s) is a function of the chiller temperature (T_c) and filament temperature because of this imperfect heating.[29] The substrate temperature in this study was kept constant by adjusting T_c at different filament temperatures using the equation:[29]

$$T_s = 0.88 \times T_c + 0.04 \times T_f + 0.4006$$

As the filament temperature increases, the concentration of the free radicals, formed by thermal dissociation of the initiator, increases as well. Figure 5-8c shows the effect of filament temperature on the step coverage of trenches with the aspect ratio of 1.4 and P_m/P_{sat}=0.45. In this work, the Thiele modulus $<<1$ for both TBPO- and TBPOB-initiated depositions, indicating that the diffusion is fast enough to prevent the build-up of gas phase concentration gradients of the monomer and therefore the conformality is only determined by sticking probability of the initiator. Independence of the step coverage from the filament temperature when using either initiator shows that the radical concentration does not affect the sticking coefficients of the initiating radicals. The results agree well with previous study on the effect of

radical initiator concentration on step coverage by varying the initiator flow rates.[32] The data further confirmed that TBPO initiated films exhibit a better conformality than TBPOB initiated ones at all different filament temperatures when the monomer surface concentration is fixed.

5.4. Conclusion

We have successfully delivered TBPOB into the reactor and used it as an initiator in the iCVD system for the first time. It permitted the TBPOB-initiated thin film deposition occurs at ~80 °C lower than TBPO at a similar deposition rate. Low filament temperature is advantageous for polymeric substrates which are temperature sensitive or have low glass transition temperature and additionally for monomers that decompose at high temperatures. Under the exactly same experimental conditions, TBPOB-initiated polymerization has a deposition rate 8 times higher than TBPO-initiated polymerization, which makes TBPOB a desired choice where high deposition rates are required.

FTIR and XPS results showed the similarity of the chain structure of TBPOB- to the TBPO-initiated films. The only detectable difference is in endgroups, with the aromatic group in TBPOB providing a unique spectral signature in the FTIR. This peak intensity increased with increase of filament temperature, corresponding to a decrease in number average molecular weight of the TBPOB-initiated pCHMA.

The conformality achieved in the trenches is governed by their aspect ratio and the sticking coefficient of the initiators. The larger oxybenzyl radical produced thus has a higher sticking coefficient than the t-butoxy, which resulted in slightly lower step coverage of TBPOB versus TBPO initiated iCVD pCHMA films over non-planar structures. A higher filament temperature provided a higher initiator radical

concentrations and more FTIR-observable endgroups in the layers grown using TBPOB. At constant surface monomer concentration, increasing the concentration of initiator radicals does not affect the step coverage of the trenches, which indicates that surface monomer concentration is the species determining step coverage.

Acknowledgements

References

(1)   Wilson, J. T.; Cui, W. X.; Chaikof, E. L. *Nano Letters* **2008**, *8*, 1940-1948.

(2)   Stoldt, C. R.; Carraro, C.; Ashurst, W. R.; Gao, D.; Howe, R. T.; Maboudian, R. *Sensors and Actuators a-Physical* **2002**, *97-8*, 410-415.

(3)   Asatekin, A.; Gleason, K. K. *Nano Letters* **2011**, *11*, 677-686.

(4)   Ozaydin-Ince, G.; Dubach, J. M.; Gleason, K. K.; Clark, H. A. *PNAS* **2011**, *108*, 2656-2661.

(5)   Elam, J. W.; Routkevitch, D.; Mardilovich, P. P.; George, S. M. *Chemistry of Materials* **2003**, *15*, 3507-3517.

(6)   Alf, M. E.; Asatekin, A.; Barr, M. C.; Baxamusa, S. H.; Chelawat, H.; Ozaydin-Ince, G.; Petruczok, C. D.; Sreenivasan, R.; Tenhaeff, W. E.; Trujillo, N. J.; Vaddiraju, S.; Xu, J. J.; Gleason, K. K. *Advanced Materials* **2010**, *22*, 1993-2027.

(7)   Dameron, A. A.; Seghete, D.; Burton, B. B.; Davidson, S. D.; Cavanagh, A. S.; Bertrand, J. A.; George, S. M. *Chemistry of Materials* **2008**, *20*, 3315-3326.

(8)   Xu, J. J.; Gleason, K. K. *Chemistry of Materials* **2010**, *22*, 1732-1738.

(9)   Tenhaeff, W. E.; McIntosh, L. D.; Gleason, K. K. *Advanced Functional Materials* **2010**, *20*, 1144-1151.

(10)   Yang, R.; Xu, J. J.; Ozaydin-Ince, G.; Wong, S. Y.; Gleason, K. K. *Chemistry of Materials* **2011**, *23*, 1263-1272.

(11)   Baxamusa, S. H.; Gleason, K. K. *Chemical Vapor Deposition* **2008**, *14*, 313-318.

(12)   Ozaydin-Ince, G.; Gleason, K. K. *Journal of Vacuum Science & Technology A* **2009**, *27*, 1135-1143.

(13)   Lau, K. K. S.; Gleason, K. K. *Advanced Materials* **2006**, *18*, 1972-+.

(14)   Im, S. G.; Bong, K. W.; Kim, B. S.; Baxamusa, S. H.; Hammond, P. T.; Doyle, P. S.; Gleason, K. K. *Journal of the American Chemical Society* **2008**, *130*, 14424-+.

(15)   Denisova, E. T.; Denisova, T. G.; Pokidova, T. S. *Handbook of Free Radical Initiators*; Wiley: New York, 2003.

(16)   Yasutake, M.; Hiki, S.; Andou, Y.; Nishida, H.; Endo, T. *Macromolecules* **2003**, *36*, 5974-5981.

(17)   Lau, K. K. S.; Gleason, K. K. *Macromolecules* **2006**, *39*, 3688-3694.

(18)   Kramer, N. J.; Sachteleben, E.; Ozaydin-Ince, G.; van de Sanden, R.; Gleason, K. K. *Macromolecules* **2010**, *43*, 8344-8347.

(19)   Trujillo, N. J.; Wu, Q. G.; Gleason, K. K. *Advanced Functional Materials* **2010**, *20*, 607-616.

(20)   Martin, T. P.; Kooi, S. E.; Chang, S. H.; Sedransk, K. L.; Gleason, K. K. *Biomaterials* **2007**, *28*, 909-915.

(21)   Lewis, H. G. P.; Caulfield, J. A.; Gleason, K. K. *Langmuir* **2001**, *17*, 7652-7655.

(22)   Chan, K.; Gleason, K. K. *Chemical Vapor Deposition* **2005**, *11*, 437-443.

(23)   Chan, K.; Gleason, K. K. *Langmuir* **2005**, *21*, 11773-11779.

(24)   O'Shaughnessy, W. S.; Baxamusa, S.; Gleason, K. K. *Chemistry of Materials* **2007**, *19*, 5836-5838.

(25)   Nozaki, K.; Bartlett, P. D. *Journal of the American Chemical Society* **1946**, *68*, 1686-1692.

(26)   Nakata, T.; Tokumaru, K.; Simamura, O. *Tetrahedron Letters* **1967**, 3303-&.

(27)   Sacak, M.; Oflaz, F. *Journal of Applied Polymer Science* **1993**, *50*, 1909-1916.

(28)   Cheng, S. Y.; Tseng, J. M.; Lin, S. Y.; Gupta, J. P.; Shu, C. M. *Journal of Thermal Analysis and Calorimetry* **2008**, *93*, 121-126.

(29)   Gupta, M.; Gleason, K. K. *Thin Solid Films* **2006**, *515*, 1579-1584.

(30)   *Polymer Handbook*; 4th ed.; edited by Brandrup, J.; Immergut, E. H.; Grulke, E. A., Eds.; Wiley-Interscience: New York, 1999.

(31)   Beamson, G.; Briggs, D. *High Resolution XPS of Organic Polymers: The Scienta ESCA300 Database*; John Wiley & Sons Ltd: Chichester, UK, 1992.

(32)   Ozaydin-Ince, G.; Gleason, K. K. *Chemical Vapor Deposition*, *16*, 100-105.

CHAPTER SIX

Conclusions

Initiated chemical vapor deposition has been shown to be an attractive process in depositing thin polymer films on solid substrates via free-radical mechanism. The iCVD method is advantageous over other CVD or solution based techniques for producing conformal coatings within complex and for retaining chemical functionality. This thesis has demonstrated the utility of iCVD in synthesizing functional polymer thin films and their applications in interfacial adhesion and film cohesion. CHAPTER TWO described that amine functional thin films were successfully synthesized for the first time via iCVD. The accessible amine sites on the poly(4-aminostyrene) (PAS) surface can be served as a scaffold for further functionalization or as sites capable of nanoadhesive bonding, which was then introduced in CHAPTER THREE. The nanoadhesive bonding technique was developed using the low-temperature (50 °C) and zero-outgassing reaction between the amine groups in iCVD PAS and the epoxy groups in iCVD poly(glycidyl methacrylate) (PGMA). A variety of polymeric substrates, including Si wafers, PC, glass, PET, PE, PA, and COC, were successfully bonded to PDMS and the fabricated devices were able to withstand pressure >150 psi, which is sufficient for microfluidic devices. The devices have conformal NH_2-functionalized coatings inside the microchannels, which prevent channel clogging and also enable the immobilization of biomolecules. The ability to covalently bond carbon-based polymeric substrates at low temperature makes it attractive for applications to the microfluidic devices. Two applications utilizing this nanoadhesive bonding technique were described in CHAPTER THREE. One application is for the growth of E. coli in an iCVD-bonded bioreactor, made of rigid polycarbonate plastics. The bonded device was hydrolytically stable for >1 week and E. coli grew over the entire period. Another application is to synthesize complex microparticles in gas impermeable channels from

118

organic solvents. Homogeneous NOA81 gas impermeable channels were fabricated and showed great organic solvent resistance and high bond strength. Microparticles with controllable height have successfully been synthesized from monomers dissolved in organic solvents. The ability to synthesis particles in gas impermeable microchannels is of great importance because it expands the applicability of flow lithography to new types of monomers that can only be dissolved in organic solvents.
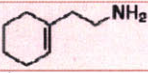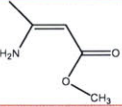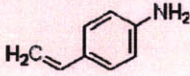
Another amine-functional polymer thin film, poly(aminostyrene-*alt*-maleic anhydride) (PASMa), was introduced in CHAPTER FOUR. The retention of the pendant amine and anhydride chemical functionalities was confirmed. The amine-rich alternating copolymer extensively self-crosslinks after gentle heating and this dramatically increases the mechanical properties of the copolymer. The annealed nanocoatings display an elastic modulus exceeding 20 GPa, far greater than typical polymers (0.5~5 GPa). Additionally, the cross-linked films maintain their flexibility, neither cracking nor delaminating with repeated flexing. Furthermore, the highly crosslinked coating material has oxygen permeability lower than commercially available permeation barrier coatings, making it an attractive material for electronics or food industries. The discovery of PASMa copolymer as hard, yet flexible organic coating materials is particularly intriguing. Owing to the structural constraints imposed by their covalent bonding networks, inorganic materials are typically hard and impermeable, but relatively brittle. On the other hand, organic materials are often flexible, but are relatively soft and permeable. This achievement represents a significant advance in the fabrication of hard, impermeable, yet flexible organic coatings.

This thesis work has been focused on the amine functionalization via iCVD and its applications, using tert-butyl peroxide (TBPO) as the initiating specie. To date,

iCVD polymerization has mainly utilized tert-butyl peroxide (TBPO), tert-amyl peroxide, perfluorooctane sulfonyl fluoride, and triethylamine. In CHAPTER FIVE, tert-butyl peroxybenzoate (TBPOB) has been tested in the iCVD system for the first time and used as an initiator to deposit conformal poly(cyclohexyl methacrylate) (pCHMA) thin films on non-planar substrates. TBPOB, a peroxyester, is a strong free radical source. To use TBPOB as an initiator for iCVD system has been challenging because its vapor pressure is only 0.00337 Torr at room temperature, which is much lower than TBPO (27.3 Torr at 25 °C). In this work, a bubbler was used to deliver the TBPOB into the iCVD reactor. With much lower volatility, TBPOB permitted the thin film deposition occurs at ~80 °C lower than TBPO at a similar deposition rate. Low filament temperature is advantageous for polymeric substrates which are temperature sensitive or have low glass transition temperature and additionally for monomers that decompose at high temperatures. Under the exactly same experimental conditions, TBPOB-initiated polymerization has a deposition rate 8 times higher than TBPO-initiated polymerization, which makes TBPOB a desired choice where high deposition rates are required. The TBPO initiated chains have endgroups derived from the t-butoxy radical. While t-butoxy derived endgroups are also present in the TBPOB initiated films, additionally there are endgroups derived from the oxybenzoate radical. The aromatic group in TBPOB provides a unique spectral signature peak in the FTIR. This peak intensity increased with increase of filament temperature, corresponding to a decrease in number average molecular weight of the TBPOB-initiated pCHMA. The conformality achieved in the trenches is governed by their aspect ratio and the sticking coefficient of the initiators. The larger oxybenzyl radical produced thus has a higher sticking coefficient than the t-butoxy, which resulted in slightly lower step coverage of TBPOB versus TBPO initiated iCVD pCHMA films over non-planar

structures. A higher filament temperature provided a higher initiator radical concentrations and more FTIR-observable endgroups in the layers grown using TBPOB. At constant surface monomer concentration, increasing the concentration of initiator radicals does not affect the step coverage of the trenches, which indicates that surface monomer concentration is the species determining step coverage.

Table 6-1. Amine-containing candidates.

Name	Structure	Vapor Pressure at 25 °C (Torr)	Price
Vinylamine	$H_2C{=}CH{-}NH_2$	1060	N/A
Ethylamine	$H_3C{-}\overset{\overset{CH_2}{\|\|}}{C}{-}NH_2$	304	N/A
Allylamine	$H_2C{=}CH{-}CH_2{-}NH_2$	247	$42.30 (50ml)
Acrylamide	$H_2N{-}\overset{O}{\overset{\|\|}{C}}{-}CH_2$	0.0614	$18.60 (25g)
3-Butenylamine	$H_2C{=}CH{-}CH_2{-}CH_2{-}NH_2$	78.5	$283 (5g)
2-Propen-1-amine	$H_3C{-}\overset{\overset{CH_2}{\|\|}}{C}{-}CH_2{-}NH_2$	75.3	$40 (10g)
2-Buten-1-amine	$H_3C{-}HC{=}CH{-}CH_2{-}NH_2$	61	$167 (1g)
1-Amino-5-hexene	$H_2C{=}CH{-}(CH_2)_4{-}NH_2$	6.36	N/A
2-(1-Cyclohexenyl) ethylamine	(cyclohexenyl-CH₂-CH₂-NH₂ structure)	0.378	$32.50 (5g)
Methyl 3-aminocrotonate	(methyl 3-aminocrotonate structure)	0.449	$17.30 (5g)
4-Aminostyrene	(4-aminostyrene structure)	0.0415	$185.50 (5g)

From this thesis work, two interesting amine functional polymers have been identified. Table 6-1 lists some commercially available amine-containing vinyl monomers which have the potential to be utilized in the iCVD process. Some of them were tried, such as ethylamine and allylamine, but with no success due to their high vapor pressures. Deposition of Methyl 3-aminocrotonate via iCVD was also carried out but the deposited films had low molecular weight due to the side reaction of this

monomer. Some candidates could be interesting and worth trying, such as acrylamide, 3-butenylamine, 2-propen-1-amine, and 2-(1-Cyclohexenyl) ethylamine.

Several applications for the amine functional polymers were indicated. The nanoadhesive bonding technique has a potential for wide applications in the microfluidic devices. Recently, prof. Ram's group are using PMMA substrates to make chips but bonding is challenging and previous bonding chemistry for PC substrates cannot be used. There could be potential collaborations. The hydrolytic resistance is studied and the bonded devices are hydrolytically stable for > 2 weeks. Other resistance, such as to organic solvents, gamma radiation, or high temperatures, could be interesting. This is because for applications in cell growth, device sterilization is normally performed. Moreover, the leftover functionalities on the inside wall of the channel can be used to further immobilize biomolecules. In the thesis, the functional groups inside the microchannel are amine and epoxy groups, however, incorporation of an additional functional group into the channel was not studied in detail. This could be performed by applying a mask or to deposit copolymers that have both the additional functionality and the amine/epoxy groups. An example integration scheme is shown in Figure 6-1. Functional groups A and B can undergo ring-opening curing reaction while C is a third functionality that might have other favored application.
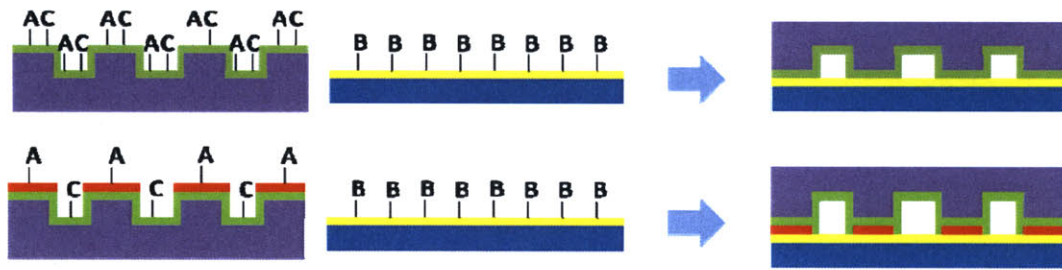
Figure 6-1. Tri-materials integration scheme.

A variety of polymer films have been successfully deposited by iCVD (Figure 6-2). These polymers could serve as candidates for the functional group labeled C in Figure 6-1. Incorporation of a third functionality in the microfluidic device broadens the field of applications for this novel fabrication method. In addition to this, by controlling the thickness of the nano-adhesive layers, nanofluidic devices fabrication could be feasible, which have been impossible in the solution-based techniques.

- **Functionalizable**

PGMA PPMA PPFM PFMA P(MA-alt-St)
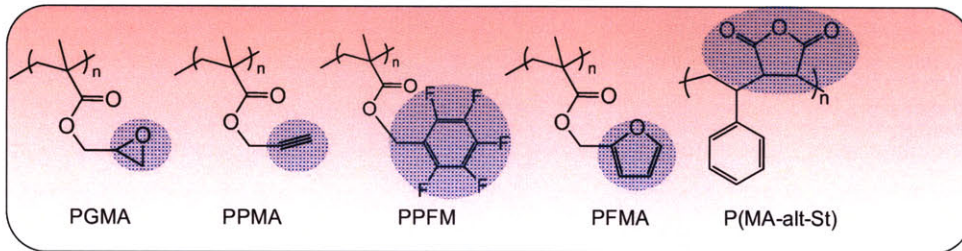
- **Biocompatible** - **iCVD crosslinkers**

PHEMA PVP EGDA DEGDVE DVB
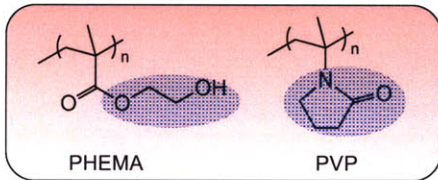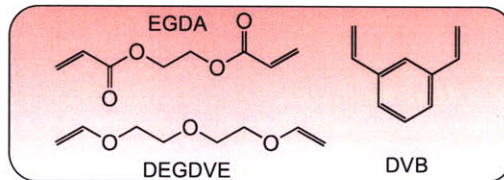
- **PH-responsive** - **Hydrophobic** - **Dielectric** - **Anti-microbial**

P(MAA-co-EA) PPFA PCHMA PDMAMS

Figure 6-2. Some functional monomers polymerized by iCVD.

APPENDIX A

Integration of Amplified Fluorescent
Polymer (AFP) Detection Schemes into
Microfluidic Systems

For microfluidic and sensor applications, good step coverage over non-planar substrates is desired. As introduced in CHAPTER THREE, the conformal, amine-functional iCVD films enable the formation of a robust nanoadhesive with complementary epoxy functional groups. The comparison between this nanoadhesive and other traditional bonding processes is shown in Figure A-1. While the traditional plasma sealing methods are specific for sealing glass or Si wafers to polydimethylsiloxane (PDMS), this new bonding method is compatible with a wide variety of polymeric materials, including polycarbonate (PC), polyethylene terephthalate (PET), polyethylene (PE), polystyrene (PS), polyacrylate (PA), and cyclic olefin copolymer (COC). Bonded devices are able to withstand high pressure and the all-iCVD nanoadhesive bonding process displays high resistance against hydrolytic degradation. Within the channels of the bonded devices, the epoxy and amine groups remain available for subsequent functionalization. This bonding method enables sealing and functionalzation of the microfluidic channels in a single step.

	Fusion Bonding	Hot-press Bonding	Oxygen Plasma Bonding	Nano-adhesive Bonding
Bond Strength	High	Low	High	High
Process Temperature	High	Low	Low	Low
Carbon-based Polymeric Substrates?	×	√	×	√
Cell-cultured or Surface-Functionalized substrates?	×	×	×	√
Functionality inside channels	×	×	×	√
Well-controlled thin conformal coating inside microchannels	–	–	×	√
Stable after surface treatment?	–	–	×	√

Figure A-1. Bonding process comparison.

Successful synthesis of poly(1H,1H,2H,2H-perfluorodecyl acrylate) (PPFDA) via iCVD (Figure A-2b) has already been reported.[1] It is expected that the fluorous effects can be used to deposit fluorous amplifying fluorescent polymer (AFP) (Figure A-2a) on surfaces[2] and also to localize the fluorous-tagged ligands provided by Swager's group. This process will make use of the novel surface functionalization schemes and nanoadhesive bonding technique developed previously.
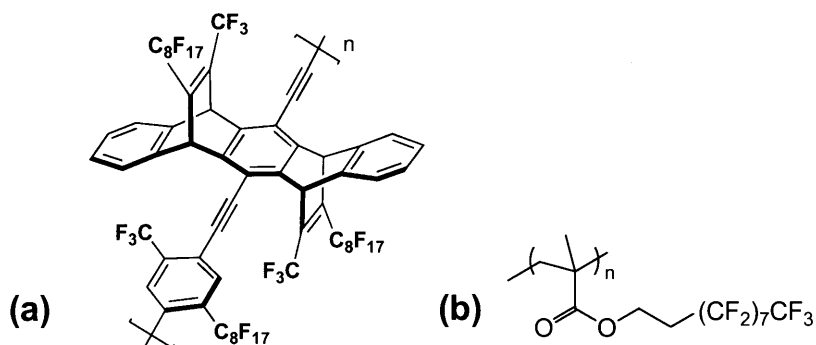

Figure A-2. (a) Amplifying fluorescent polymer (AFP) provided by Swager's group. (b) Poly(1H,1H,2H,2H-perfluorodecyl acrylate) (PPFDA) polymer. AFP has a high degree of fluorination and is selectively soluble in perfluorinated alkanes. It can be attached to PPFDA films via fluorous effects.

The device fabrication process is shown in Figure A-3. Linear microfluidic channels of 500 μm wide and 150 μm deep were prepared on PC substrates. Oxygen plasma was applied to the substrates (0.5-1 min), both for cleaning and surface activation to enhance surface energy for better adhesion. PGMA and PAS films were deposited on flat PDMS and patterned PC substrates via iCVD, respectively. A mask was then placed on the patterned surface and deposited with PPFDA. After removal of the mask, a dual-functionality with amine and fluorous groups can be achieved. After the two substrates were placed face-to-face and ring-opening curing reaction between epoxy and amine groups occurred, microfluidic devices with good sealing could be

fabricated. Within the channel, epoxy and fluorous groups can be used for further functionalization.
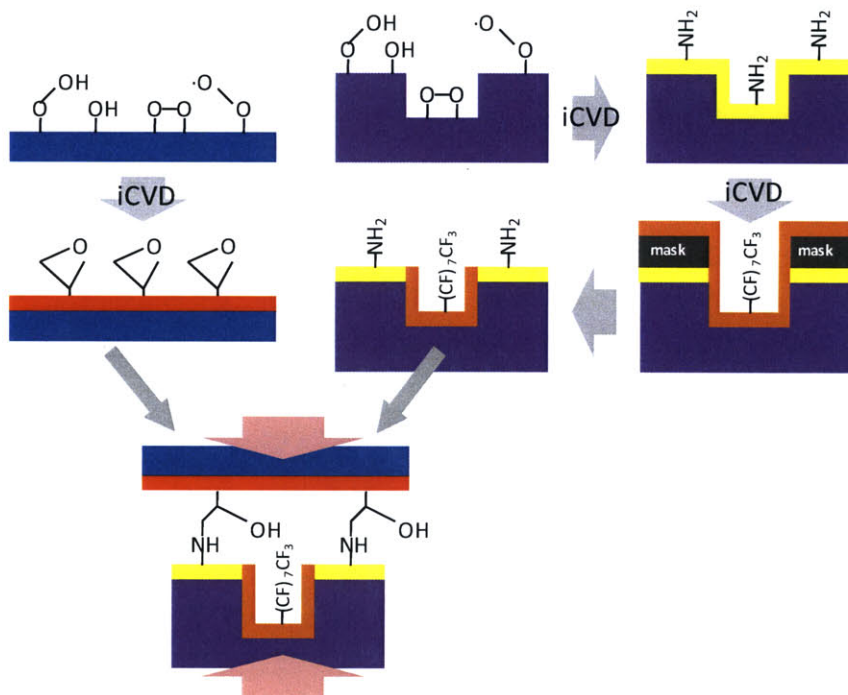

Figure A-3. Scheme of the nano-adhesive bonding process.

AFP solution was then continuously infused through the fabricated microfluidic devices, at a flow rate of 1mL/min. Figure A-4b and Figure A-4d show successful incorporation of AFP onto the PPFDA functionalized microchannel. It supports the hypothesis that iCVD deposited PPFDA can be used to localize fluorous AFP. Bonded device with PPFDA coatings showed a much stronger fluorescent signal than the one without PPFDA coatings, confirmed by both photographs taken under UV lighting and fluorescence micrographs (Figure A-4). This fluorous AFP has unique solubility, high degrees of fluorination, and excellent photophysical properties.
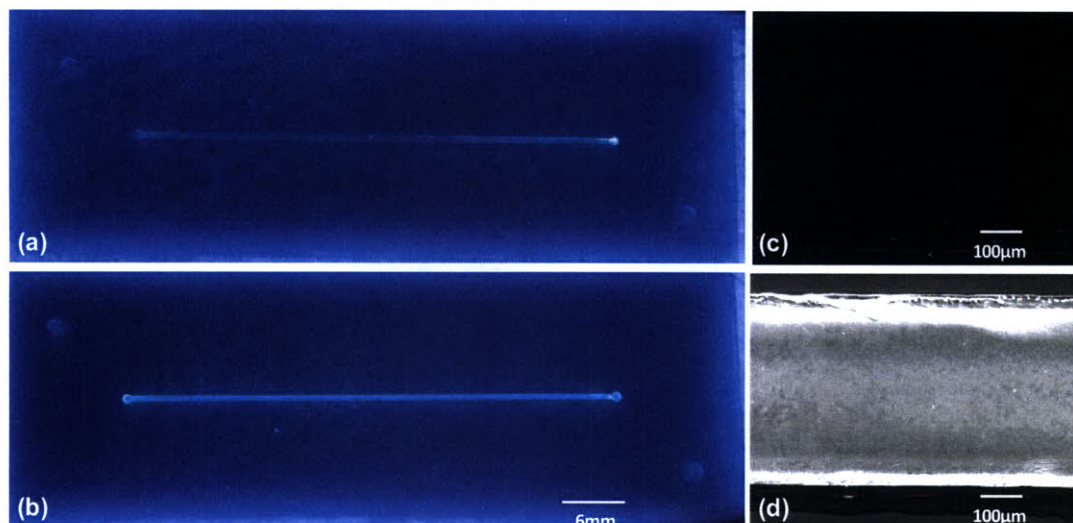
Figure A-4. Photographs of bonded microfluidic devices (a) without iCVD PPFDA and (b) with PPFDA coatings, after infusion of AFP solution and under UV lighting. Fluorescence micrographs of microchannels (c) without PPFDA and (d) with PPFDA coatings.

The next steps will be to further collaborate with Swager's group for analytes detection as well as incorporation of alternate AFPs. AFPs with functional groups that can react with either amine or epoxy groups can be covalently attach to the microchannels. We expect this will increase the stability and also surface density of attached AFPs.

References

(1)   Gupta, M.; Gleason, K. K. *Langmuir* **2006**, *22*, 10047-10052.
(2)   Wang, D.; Oleschuk, R. D.; Horton, J. H. *Langmuir* **2008**, *24*, 1080-1086.